
# *ADDIS ABABA UNIVERSITY*
# *FACULTY OF TECHNOLOGY*
# *SCHOOL OF GRADUATE STUDIES*

## *STRESS AND DEFLECTION ANALYSIS OF CRACKED COMPOSITE PRESSURE VESSEL BY FINITE ELEMENT METHOD*

***A thesis submitted to the School of Graduate Studies of Addis Ababa University in partial fulfillment of the requirement of the Degree of Masters of Science in Mechanical Engineering***
***(Applied Mechanics Stream)***

***Thesis by***

***Tekeliye Tasachew***

***Advisor:***
***Dr. Daniel. Tilahun***

**October, 2015**

# Addis Ababa University

# Addis Ababa Institute of Technology

# School of Mechanical and Industrial Engineering

## *Stress and Deflection Analysis of Cracked Composite Pressure Vessel by Finite Element Method*


**By**

*Tekeliye Tasachew*


**Submitted in accordance with the requirements for the degree**

**MASTER OF SCIENCE(M.Sc.)**

Approved By Board of Directors

| | | |
|---|---|---|
| Daniel Tilahun (Dr.) | _____ | _____ |
| Advisor | Signature | Date |
| _____ | _____ | _____ |
| Internal Examiner | Signature | Date |
| _____ | _____ | _____ |
| External Examiner | Signature | Date |
| Daniel Tilahun (Dr.) | _____ | _____ |
| Chairman of the School | Signature | Date |

DECLARATION

# Addis Ababa University

# School of Graduates

I hereby declare that the research entitled: Stress and Deflection Analysis of Cracked Composite Pressure Vessel by Finite Element Method**.** This thesis is my own independent work, and has no previously been submitted to any other University in order to obtain a degree.

*Signature:* _____

*Date:*_____

Advisor: Daniel Tilahun (Dr.) Signature:_____Date:_____

Head of School: Daniel Tilahun (Dr.) Signature: _____Date:_____

## Acknowledgment

First of all, I would like to thank the almighty God; all things are happened because of him.

I would like to express my warmest thank-you to my Advisor Dr. Daniel Tilahun for his continual guidance and supportive encouragement during the research and for all of his help starting from giving an idea of different areas on his expertise while selecting the title of the thesis at the beginning and continues guidance till the completion.

Last, but not least, I would like to thank my parents, my wife Habtam, and brother Kinfu, my sisters Medhanit, Fetlu and shine for supporting and encouraging during my stay in postgraduate study.

## Abstract

The aim of this thesis is to develop crack and investigate techniques and parameters that could be used to identify crack if it exist in a composite pressure vessel. Many researchers discovered formation or propagation of a crack in a composite pressure vessel will cause a catastrophic failure. Thus, health monitoring for a pressure vessel due to crack using crack detection techniques will minimize or reduce the failure that probably to occur.

This research first focused on mathematical and numerical relation which, represent the governing equation of composite material winding on in a pressure vessel. For modeling different crack size in the composite overwrapped pressure vessel fracture stress theories applied.

Different surface Crack size are considering according to the literature standard values. Model actual size of composite pressure vessel with varied crack size "a" develops on the surface of composite pressure vessel. This research thoroughly analysis the effect of crack on the surface of composite pressure vessel. Those parameters are considered to see the variation of result due to presence of crack. The main parameters are considering stress, principal stress, von mises stress, deflection and fracture stress. According to the parameters it shows that as crack size increase, the average stress will be increase with the given pressure in composite pressure vessel. In contradict; the fracture stress will be decrease as the crack size increase.

In this study, optimal angle-ply orientations of symmetric [$55^0$, $-55^0$] shells designed for maximum burst pressure with allowable crack size were investigated. It is shown that all the strength characteristics of carbon fiber relevant to structural engineering can be explained by the cracks present in the carbon fiber and can be analyzed using fracture mechanics. The stress and deformation are affected due to the presence of crack in composite pressure vessel. These parameter are takes a design crack as the basis for design. Rather than an allowable stress as in current approaches, with which it is compared cracked composite pressure vessel. A full size cylindrical shell of composite pressure vessels is conducted. A mathematical method, A finite element method and compare experimental test are studied to verify a maximum allowable crack size in composite overwrapped pressure vessel with a given optimum winding angles. The roll of crack size design within the wider philosophy of limit state design is discussed.

## Contents

## List of figure

## List of table

## Nomenclature

COPV = composite overwrapped pressure vessel

CFRP = carbon fiber reinforced polymer

LBB = leak before break

MDP = maximum design pressure

MEOP = maximum explosive operational pressure

a = surface crack depth

p = pressure

c = half surface crack length

R = ratio of minimum cyclic stress to maximum cyclic stress

S = applied stress

So = yield stress

NDI= Non Destructive Inspection,

$\sigma_1$ = $principal\ stress$;

$\sigma_{ys}$ = Von Mises Yielding Criterion

$\sigma 2$ = $principal\ stress$

$K_{IC}$ = Fracture Toughness (mpa.$m^{1/2}$)

Y = Shape Factor

Ux = displacement along x- axis

$\sigma_f$ = fracture stress

$\sigma_{local}$ = local average stress

$\sigma_{xx}$ = hoop or circummfertial stress

$\sigma_{yy}$ = axial or longutidnal stress

$\varepsilon_1$ = principal strain

$\sigma_a$ = axial stress

$\sigma_h$ = hoop stress

# CHAPTER ONE

## 1 INTRODUCTION

### 1.1. BACKGRAUND

In today's aerospace and aircraft industries, structural efficiency is the main concern. Due to their high specific strength and light weight, fiber reinforced composites find a wide range of applications. Light weight compression load carrying structures form part of all aircraft, and space vehicle fuel tanks, air cylinders are some of the many applications. In the present work, design analysis of fiber reinforced multi layered composite shell, with optimum fiber orientations; minimum mass under strength constraints for a cylinder with or without stiffeners under axial loading for static condition [2].

There are existing three types of composites. Fibrous Composites**:** It consists of fibers of one material in a matrix material of another material. Particulate Composites**:** These are composed of particles of one material in a matrix of another material. Laminate Composites**:** These are made of layers in which fibers and matrix are made of different materials, including the composites. The purpose of matrix is to transfer loads and protect them against environmental attack and damage due to handling. Based upon the properties required, the matrix and fiber materials are selected [2].

The development of composite overwrapped pressure vessels (COPV) has greatly reduced the mass of aerospace pressure vessels compared to those made of monolithic metals such as titanium, aluminum and nickel-base alloys, the Pressure vessel with a composite shell fully or partially encapsulating a metallic liner". The metallic liner may be either elastically responding or plastically responding depending on the strain in the liner at the proof pressure. Plastically responding liners offer the advantages of Lower mass and potentially lower manufacturing cost. Requires that two different fracture control conditions be met in the liner and be verified during COPV qualification. These are 1) Damage-Tolerance Life (Safe-Life) and 2) Leak-Before-Burst (LBB). Safe-Life means that the largest crack that can escape detection to 90% probability with 95 % confidence by a non-destructive examination (NDE) shall not grow to liner fracture or leakage in before service lives [9].

The father of fracture mechanics is A.A Grifties. His principal contribution is an analysis of crack stability based on energy equilibrium, the decreasing of strain energy U must be equal to the increase of surface energy S due to crack extension. And Irwin extended his theory during at the beginning of $19^{th}$ century [6].

Defects can adevertlly been produced in compoite materials,either during the manficturing process or in the course of the normal service life of the component. The manufacture process has the potential for causing a wide range of defects, the most common of which is "porosity", the presense of small voids in the matrix. Porosity can be caused by in correct, or non-optimal, cure parametres such as duration,temprature, pressure and vacume bleeding of resin. Pororsity levels can be critical, as they will affect mechanical performanse, such as inter -laminar shear stress. Preparation of resin-imprignated fiber layers(pre-preg), prior to curing, can be by hand or machine. In either case there is the potential for the iclussion of forign bodies ranging from backing film to just greasy marks from fingers. More recent low – cost manifucturing techniques , involving the infusion of resin in to pre per-formed dry fibers in moulds, have introduced other potential defects such as fiber misalignment , or waveness, bothe in the plane of maerial and out-of - plane. Stitching of fiber tows (bunche of fiber ) to hold them in place and prevent misallignment during cure, can itself introduce numerous regularly- spaced sites for void formation. In servise damage is most often caused by impacts. In monolithic composites this results in matrix cracking and delimitations of the ply layers. In some case despite, the internal delimitation damage is being extensive [18].

Cracks are developed in the plies. These cracks are lies along the fibers in the plies and are known as ply cracks, matrix cracks, or transverse cracks. In presence of these cracks, laminates responds differently than in its original state and also failure is caused because of these cracks directly, they can lead to de-lamination and laminate failure. For structural integrity it is necessary to perform deformational and failure analysis of laminates with ply cracks. Given laminates these cracks can form in a given ply and grow along the thickness of ply and running parallel small to the fibers in that ply. Such cracks are found because of tensile loading, fatigue loading, as well as by changing in temperature or by thermal cycling. They can generated from fiber-matrix de-bonds or because of manufacturing defects like voids and inclusions. Matrix cracking does not cause structural failure by itself, but it results in significant degradation in

material stiffness and can also develop more severe forms of damage such as de-lamination, and fiber breakage [4].


Fig 1 Acoustical Resonance System Schematic

In general, crack initiation and growth must be correlated with the governing stress intensity factors in a complex state of stress. Changes in crack path are normally induced by 1) Multiracial far field stresses 2) Interaction of the crack tip with micro structural defects 3) Sudden changes in load 4) The embrittlement effect of an aggressive environment. A variety of methods are used to compute the strain energy release rate based on results obtained from finite element analysis. The virtual crack extension method requires only one complete analysis of the structure to obtain the deformations. The total energy release rate or J integral is computed locally at the crack front and the calculation only involves an additional computation of the stiffness matrix of the elements affected by the virtual crack extension. A crack in a body may be subjected to three different types of loading, which involve displacements of the crack surfaces. The mechanical behavior of a solid containing a crack of a specific geometry and size can be predicted by evaluating the stress intensity factors [25].

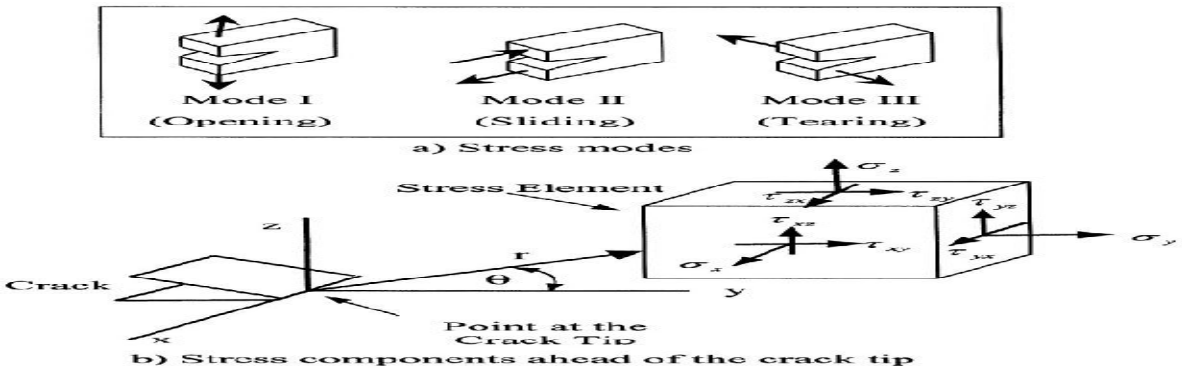


Fig-2 stress loading and mode crack cordinate system.

COD models compare well to the results of the finite element (FE) analyses it is possible that one of them, or a modified version, could be used in conjunction with a flow analysis to determine an approximate leak rate during the actual damage tolerance analysis. Although an FE analysis should be the most accurate method, the time and effort required to create it might not be necessary if a simple analytical model can provide reasonable results. For the COD models to provide a reasonable alternative to a full FE analysis correlation between the two should be within 10%.

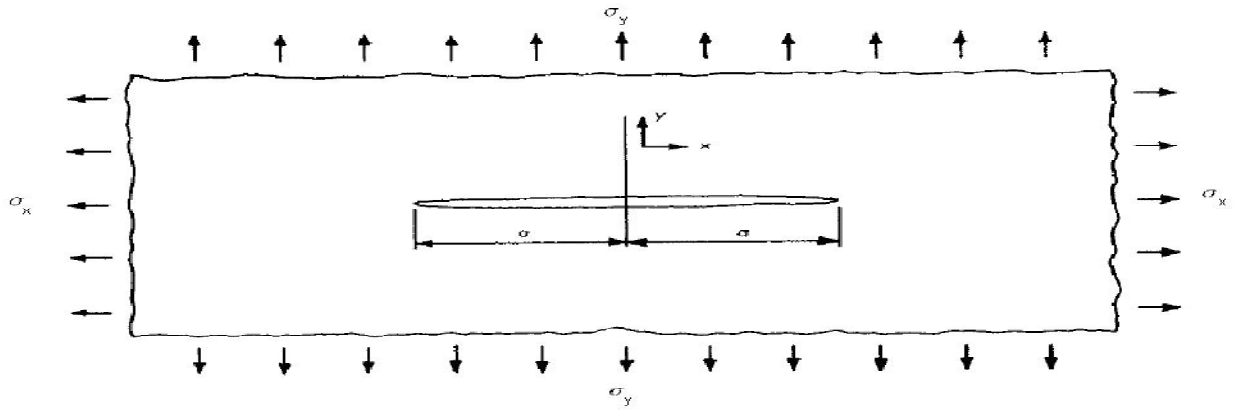

Fig 3. Crack geometry and coordinate system

In all cases, the crack geometries used in this study will resemble that of the generalized crack illustrated in Figure 2, where $\sigma_x$ and $\sigma_y$ represent the far field stresses in the x and y directions, respectively, and a is the half-crack length. All cracks have been assumed to be circumferential in nature, as illustrated in Figure 3, where the y-direction follows along the axis of the pressure vessel and the x-direction represents the hoop direction [29].

Several different non-destructive evaluation (NDE) techniques were evaluated for the potential to be used as a damage detection system. These techniques included: acoustic emission, fiber-optics, and ultrasonic's (resonance, guided waves, and bulk waves). Consideration was given to each of the techniques based on technical complexity, cost, reliability, difficulty to work with, sensitivity, and sensor range. The notable difference in the methods includes the frequency band (acoustic: 0 – 20 kHz; ultrasonic: 20 kHz and up) and the transmission medium. As it is shown in fig .1 [13].

Carbon fiber: Filaments of polyacrylonitrile or pitch (obtained from residues of the petroleum products) are oxidized at high temperatures (300°C) and then heated further to 1500°C in a nitrogen atmosphere. Only the black and bright filaments of hexagonal carbon chains remain, as shown in Figure .4. The high modulus of elasticity is obtained by stretching at high temperature.

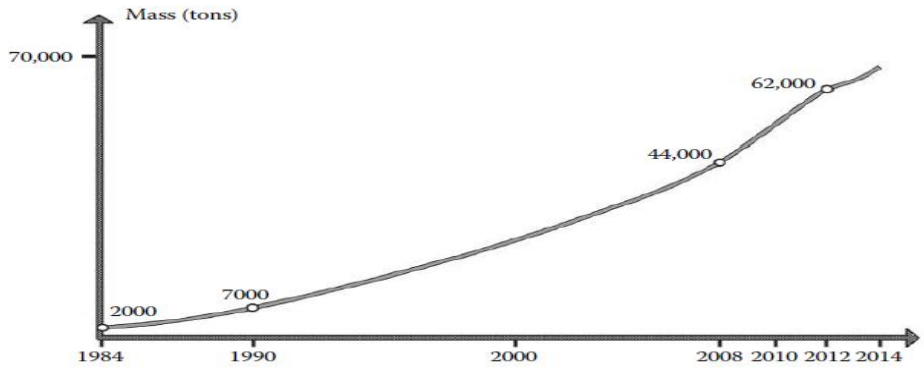


Fig -4 Annual Production Capacities of Carbon Fibers

Fibers consist of several hundreds or thousands of filaments, each of them having a diameter of between 5 and 15 μm, allowing them to be process able on textile machines; for example, in the case of glass fiber, two semi finished fiber products are obtained as shown in Figure 5. These fibers are marketed in the following forms: Short fibers, with lengths of the order of a fraction of a millimeter to a few centimeters. These are felts, mats, and short fibers used in injection molding. Long fibers, which are cut during the time of fabrication of the composite material, are used as is or woven [7].

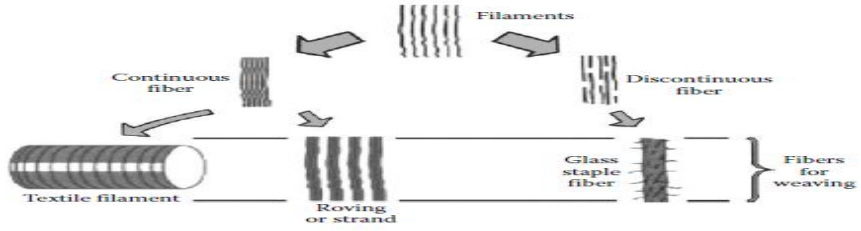


Fig-5 Different fiber forms.

Resins (or matrix) are an important part of any composite. It's basically the glue that keeps the composite together. A resin must have good mechanical properties, good adhesive properties, good toughness properties and good environmental properties. For the mechanical properties this means that an ideal resin must be initially stiff but may not suffer brittle failure. And in order to achieve the full mechanical properties of the fiber, the resin must deform at least the same extend as the fiber. Good adhesion between resin and reinforcement fibers ensures that the loads will be transferred efficiently and cracks and fiber/resin deboning will be prevented. The resistance to crack propagation is a measure for the material's toughness [16].

Cylindrical composite pressure vessels constitute a metallic internal liner and a filament wound and a composite outer shell as shown in Fig. 6. The metal liner is necessary to prevent leaking, while some of the metal liners also provide strength to share internal pressure load. For composite pressure `vessels, most of the applied load is carried by the strong outer layers made from filament wound composite material. Figure 6 Example of filament wound composite pressure vessels.

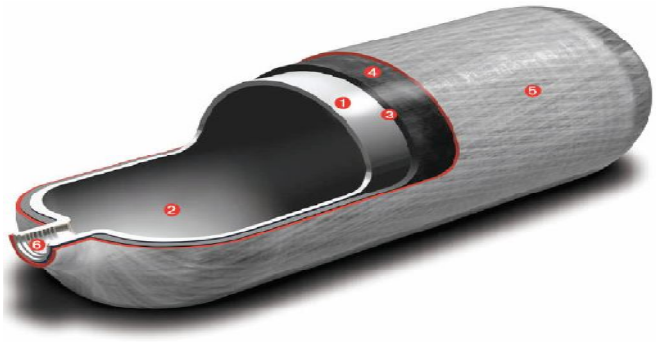


Fig-6 Example of filament wound composite pressure vessels.

1.Ultra thin-walled aluminium liner 2- Protexal smooth, inert, corrosion resistant internal finish 3- Insulating layer 4- High - performance carbon - fiber overwrap in epoxy resin matrix 5- High - strength fibreglass-reinforced plastic (FRP) protective layer with smooth gel coat 6- Precision – machined thread.

The main concept of a composite is that it contains matrix materials. Typically, composite material is formed by reinforcing fibers in a matrix resin as shown in Figure7. The temperature

resistance of composite parts depends on the temperature resistance of the matrix materials. Because a large proportion of composites use polymer-based matrices, temperature resistance is limited by the plastics' properties. Average composites work in the temperature range –40 to +100°C. The upper temperature limit can range between +150 and +200°C for high temperature plastics such as epoxies and Peek [16].

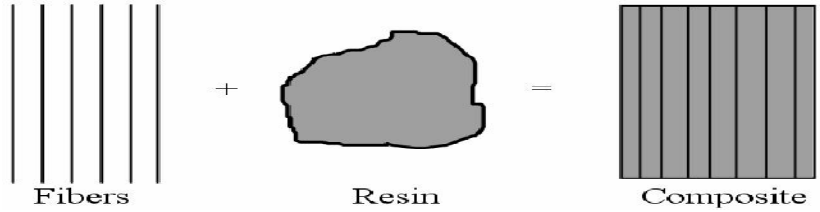


Fig-7 Composite material using fibers and resin

Composite pressure vessel has many application .One of the most difficult issues in the development of alternative energy is in the storage of the gaseous fuel. Most often, the use of gaseous fuels, such as hydrogen and natural gas, can provide outstanding operating benefits and efficiency improvements over conventional fuels. However, the most expensive and complex component of the fuelling system is in the storage of these gaseous fuels. To minimize those tangible problems is finding in today technology. From many applications it can use optimum energy with small size on space shuttle, vehicles and industries [13].

There are shallow researches on this title in Ethiopia. Because of this the research has vital role for further study to solve the problems mentioned above.

### 1.2. Purposes

The purpose of this thesis is to determine the maximum crack formation in the surface of composite pressure vessel with in maximum stored gas or liquid pressure and explore the impact of an oversight crack before burst process.

### 1.3. Objective

#### 1.3.1. Main Objective

The general objective of this thesis is Stress and Deflection Analysis of Cracked Composite Pressure Vessel by Finite Element Method**.** Due to the presence of maximum pressure with a given material in a vessel, there will be maximum stress and deformation on the surface of

cracked composite material. By using analytical solution and finite element method it can be determine the optimum surface crack on the composite pressure vessel. And maximum value of crack length or tolerable crack size determine before a composite pressure vessel fail.

### 1.3.2 Specific Objectives

- To model a composite pressure vessel within a given internal pressure and its crack propagation.
- To find qualitative change of parameters those manifest themselves for surface Crack formation on the composite pressure vessel
- To model the crack on the composite pressure vessel in terms of the type of crack on position where crack propagate on the real physical components.
- To apply finite element analysis to describe the crack influence on the selected modal parameters and component physical properties.

## 1.4. Statement of the Problem

The most difficult damage mechanism to identify is the presence of fatigue damage, which, in turn makes it most difficult to design the pressure vessel to relevant standards. Typical fatigue loading on a composite pressure vessel goes through the following stages throughout its life span: 1. Crack nucleation, 2. Crack initialization, 3. Crack growth, and 4. Crack failure. When examining fatigue loading and failure of these composite pressure vessels, it is paramount to identify the crack presence in the initialization or growth stages of fatigue. The presence of a crack in the aluminum liner will not cause a catastrophic failure of the composite overwrapped pressure vessel (as all standards require a Leak before Burst (LBB) criterion in the design and testing of the pressure vessels. However, the leakage of fluid like liquid and gas in an enclosed space will produce an undesirable critical condition that could result in catastrophic failure of the fuelling system. At the current state of the research, the threshold of the crack growth is unknown, and the ability to, with certainty, predict a specific failure mode is difficult due to the interaction between the liner and the composite. Composite pressure vessel has different testing method to know defected or not such as delimitation, gauge, creep and crack. But, for this research on its specific material, there is no study about crack propagation and crack control up to what value the crack formed without failure. And, also identify crack behavior or failure

mode should be more thoroughly investigate and analysis mixed mode or single mode failure. Therefore, analytical solution result comparing with engineering soft ware (ANSYS) result and it can limit the crack size created on composite pressure vessel and put the value of tolerable surface crack size beside destructive and non distractive inspection.

### 1.5 Scope and limitation of the research

The scope of this research is to perform parametric study to investigate the effect of maximum pressure with a developing crack in composite pressure vessel. FEM is used to simulation a composite pressure vessel in Ansys software and determine the effect of crack inside composite pressure vessel and fracture toughness of the composite pressure vessel. Also give a tolerable surface crack size with a given maximum pressure vessel. The analysis will be done in mathematical and ordinary computers software. Power full Ansys version 16 software is using to get the exact result with mathematical model and experimental result getting from literature. In this research there is no actual lab experiment did. Because, lack of lab equipment facilities and its material expensive.

### 1.6. Organization of the research

Chapter one, background about stress and deflection analysis cracked composite overwrapped pressure vessel, main causes for failure of COPV (crack) and methods which are familiar with different parameter of the considerable failure cause is crack are discussed. The review of literatures will be summarized on the second chapter. The analytical and finite element modeling for the COPV with basic consideration and assumption of crack discussed in the third chapter. The derivation and solution techniques are presented in chapter three. The results obtained and their discussions are included in fourth chapter. Finally conclusion and recommendations for future research are mentioned in the last chapter.

# CHAPTER TWO

## LITERATURE REVIW

Houston ,March 2011[19] explain, Pressure vessels have historically been classified as failing due to either burst or leak-before burst (LBB). These designations have been misleading in the past, suggesting that a vessel that is designated as LBB does not require further monitoring or vigilance. However, it is not recognized that the pressure vessel failure modes must be addressed during all phases (design, qualification, and use) to ensure safety. Because of the additional composite failure modes for COPVs, determination of appropriate ways to address failure modes is usually more complex than for metallic vessels.

Hyun-Sup Jee and Jong-O Lee, [17] Studied on Composite pressure vessels (CPVs) fabricated using a metal or plastic liner under a composite structural skin is commonly used for natural gas storage on road vehicles. The composite skin, which is usually made of high strength carbon (or glass) fiber-epoxy composite, is the primary structural component of the vessel. In the past decade, accidents due to catastrophic rupture and explosive failure of CPVs have occurred, which is attributed to a lack of knowledge about the damage tolerance and useful life of these vessels.

Danai Abhijeet R, Feb-2015, [4] He analyzed composite material in presence of cracks and fatigue life prediction under variable amplitude loads has been attempted by various investigators in the past. Different types of analytical models have been employed by the several authors to predict fatigue life. However, accuracy of predictions has been observed to vary significantly. Although micro-mechanics based models have yielded good results. The fatigue failure mechanisms matrix cracks, dis-bonding, de-laminations and fiber break, are the main causes for progressive failure of composites under fatigue loads. We need proposed to systematically model and analyze the defects to estimate the stiffness degradation of composites by considering failure mechanisms.

S. Borazjani and S. H Tang, 2013, [9] stated that, filament winding is the usual considered process for fabricating composite structures. It is the process in which continuous filaments of fiber are wound on a supporting mandrel. The mandrel rotates with the spinning wheel on a

horizontal axis then carriage begins to move linearly so fibers are laid down in the predetermined path. The most conventional uses of filament winding process are in high-pressure storage tanks, rocket motor cases, launch tubes, and for commercial applications.

Hyun-Sup Jee and Jong-O Lee, [17] the third pressure vessel design (Type III) consists of a metal liner, usually aluminum for prevention of oxidation corrosion, and a composite wrap overlay on the cylinder. The composite overlay, different than the Type II cylinder, consists of both hoop and transverse wraps on the cylinder. This results in complete coverage of composite material over the surface of the cylinder. The composite can be composed of different materials, typically carbon fiber or fiberglass, with blends of the materials also used. The advantage of this type of design is a reduction in weight of the cylinder, as the metal liner thickness can be reduced. The metal liner of the cylinder serves primarily as a membrane to contain the pressurized gases, as the composite wrap is not leak-tight. The composite overlay only retains the stress of the compressed gases. This system works primarily because the composite has a very high modulus of elasticity in comparison to the metal liner, resulting in the composite overlay taking the bulk of the load in the structure.

Stephen W. Tsai 2008 **[**14**]** the rapidly expanding applications of composites in the recent past have provided much optimism for the future of our technology. Although man-made composites have existed for thousands of years, the high technology of composites has evolved in the aerospace industry only in the last twenty years. Filament-wound pressure vessels using glass fibers were the first strength critical application for modern composites. After these, boron filaments were developed in the 1960's, which started many US Air Force programs to promote aircraft structures made of composites. The F-111 horizontal stabilizer was the first flight-worthy composite component.

Yoneda. M April 17, 2008[16] the service load level is increased to 140 MPa, a value within the rank of the plastic behavior of the material, the existence of an unquestionable superficial cracking can be observed. As a result of the capillary effect, a greater amount of water can penetrate and be distributed through these cracks until it reaches the zones of interfacial micro-cracking, thereby intensifying the attack on the interface at this point. The result is an rise in the losses of the strength properties E and R. The increase in the density of cracks in areas where fibers oriented to $90^0$ are present causes the alteration of the fiber–matrix interface after long

exposure periods. The loss suffered in the BSE fracture energy provides indirect evidence of the deterioration of the interface between the fiber and the matrix. This is of a greater extent to the losses which occurred in the resistance and the modulus, and agree with that observed by the researchers.

M.P.F Sutcliffe, February 1992[19] Despite their excellent material characteristics, structural composite materials are susceptible to fatigue fracture phenomena when subjected to certain cyclic loads (static or dynamic) and/or environmental factors (temperature and corrosive media). Failure processes may actually begin during fabrication or at a low applied stress level. In consequence, the thermal and chemical shrinkage of laminate constituents, low velocity surface impact as well as localised damage during service, holes, notches or joints are potential sources of crack-like defects such as debondings and delaminations. Hence, an understanding and prediction of further propagation of such defects is of paramount importance for predicting the service (or fatigue) life of composite materials subjected to long-term cyclic loads.

Csir-Cmeri March 2014[16] the fatigue life till crack nucleation for a steel-lined hoop wrapped composite pressure vessel containing a surface flaw (notch) using strain-life approach. Firstly, static stress analysis taking into account the non-linear material behavior of steel liner was performed using finite element method to provide input for the fatigue analysis. Then fatigue analysis was carried out by applying a cyclic pressure inside the pre-stressed cylinder using strain-life approach, and the results obtained by the numerical simulations are discussed. The approach associated with these calculations can be used to study the effect of various material and geometry parameters on the fatigue life of the pressure vessel.

S.Borazjani and S H Tang 2013[9] Finite element analysis was employed for investigating the structural behavior of pressure vessels. Aluminum alloy was utilized as the inside layer covered with Carbon/Epoxy fiber which was roving at different winding angles. FEA employed failure criteria such as Tsai-Wu, Tsai-Hill and maximum stress to predict the burst pressure, maximum shell displacement and determine the optimum winding angle. Results and discussions were resulted in the following findings: Based on Tsai-Wu and Tsai-Hill failure criteria, $55^0$ winding angle was approved as the optimum winding angle due to its maximum burst pressure and minimum shell displacement. This optimum angle was in good correlation with the experimental results trend and the netting analysis. Determining burst pressure using maximum stress failure

theory was lead to less conservative results and higher burst pressure due to estimating the burst pressure based on ultimate strength of Carbon/Epoxy fiber.

In 1964, the authors, Rosato D.V and Grove C.S. in their book titled, [8] Filament winding: Its Development, Manufacture, Applications and Design defined it as a technique which "produces high-strength and lightweight products; consists basically of two ingredients; namely, a filament or tape type reinforcement and a matrix or resin". The unique characteristics of these materials made great revolutions for many years .The concept of filament winding process had been introduced in early 40's and the first attempt was made to develop filament-winding equipment. The equipment that was designed in 1950's was very basic; performing the simplest tasks using only two axes of motion (spindle rotation and horizontal carriage). Machine design consisted of a beam, a few legs and cam rollers for support. The simplistic design was sufficient to create the first filament wound parts: rocket motor cases. Initial advancements came in the form of mechanical systems that allowed an operator to program a machine by the use of gears, belts, pulleys and chains. These machines had limited capabilities and capacities, but were accurate.

Bryan C. Lung**,** [13] Identify, Several different non-destructive evaluation (NDE) techniques were evaluated for the potential to be used as a damage detection system. These techniques included: acoustic emission, fiber-optics, and ultrasonics (resonance, guided waves, and bulk waves). Consideration was given to each of the techniques based on technical complexity, cost, reliability, difficulty to work with, sensitivity, and sensor range. The notable difference in the methods includes the frequency band (acoustic: 0 – 20 kHz; ultrasonic: 20 kHz and up) and the transmission medium.

W. K. Ahmed, A-H. I. Mourad,[22] explain Fracture mechanics generally is based on two types of analysis, namely residual strength analysis to determine the maximum crack size that can be tolerated, and fatigue crack growth analysis to calculate the time for crack growth from a certain initial crack size until the maximum tolerable crack size in order to determine the safe life. These analyses are usually based on the SIF intensity factor. Therefore, knowing the SIF is important for the fracture mechanics. Energy release rate, GI, at the center of the crack front was examined by the finite elements method using the virtual crack closure method (VCCM). The model of a carbon monofilament which has a straight edge crack from the surface located at its center. The model was analyzed as both isotropic and orthotropic materials. In the case of the

isotropic material, Young's modulus (E) is set to be 285GPa, Poison's ratio (ν) 0.3. In the case of the orthotropic material, the energy release rate (GI) is converted to the stress intensity factor (KI).

Sayman (2005)[3] studied analysis of multi-layered composite cylinders under hydrothermal loading. Mackerle (2002) gives a bibliographical review of finite element methods applied for the analysis of pressure vessel structures and piping from the theoretical as well as practical points of view. Xia et al. (2001) studied multi-layered filament-wound composite pipes under internal pressure. Xia et al. (2001) presented an exact solution for multi-layered filament-wound composite pipes with resin core under pure bending. Rao and Sinha (2004) studied the effects of temperature and moisture on the free vibration and transient response of multidirectional composites. A three-dimensional finite element analysis developed for the solution. The effect of surface cracks on strength has been investigated theoretically and experimentally for glass/epoxy filament wound pipes, by Tarakçioglu et al. (2000). They were investigated theoretically and experimentally the effect of surface cracks on strength in glass/epoxy filament wound pipes which were exposed to open ended internal pressure.

**Literature reveals that:**

- Most of the finite element analyses of composite pressure vessels are based on elastic constitutive relations and traditional thin- walled laminated shell theory
- Optimization of composite pressure vessels is done by changing the parameters of the composite materials including filament winding angle, lamination sequence, and material
- In the past decade, accidents due to catastrophic rupture and explosive failure of CPVs have occurred, which is attributed to a lack of knowledge about the damage tolerance and useful life of these vessels.
- Hole and notches are the potential source of crack. And matrix cracks, dis-bonding, de-laminations and fiber break, are the main causes for progressive failure.
- Determining burst pressure using maximum stress failure theory was lead to less conservative results and higher burst pressure due to estimating the burst pressure based on ultimate strength of Carbon/Epoxy fiber.
- Several different non-destructive evaluation (NDE) techniques were evaluated for the potential to be used as a damage detection system.

- Filament winding: Its Development, Manufacture, Applications and Design.

**The present research focuses on:**

- Determination of tolerable surface crack size with a given maximum pressure and optimum fiber winding angle.
- Identify the behavior of stress and deformation cracked composite pressure vessel material.
- Comparison of results among theoretical, experimental and software.

# CHAPTER THREE

## MATERIAL, METHODS AND CONDITION

### 3.1. Materials

Carbon fibers are very common in high-modulus and high-strength applications. The advantages of carbon fibers include high specific strength and modulus, low coefficient of thermal expansion and high fatigue strength. The material of this cylindrical vessel consists of the aluminum alloy inside layer reinforced with six layers of Carbon/Epoxy T300/LY5052 fiber. The application of this material is used light weight construction material like composite pressure vessel on vehicles and aeronautical industries. To store liquid and gas energy, such as hydraulic oil, hydrogen gas and helium gas etc….

#### 3.1.1. Properties of Composites

Table 1 Mechanical properties carbon fiber reinforced polymer "CFRP"

| | **Density( kg/m$^3$ )** | **$E_1$ (Gpa)** | **$E_2$ (GPa)** | **$u_{12}$** | **$G_{12}$ (GPa)** | **t(MPa )** |
|---|---|---|---|---|---|---|
| **CFRP** | **1570** | **135** | **8** | **0.27** | **3.8** | **-** |

Table 2 Strength parameters for cfrp composite.

| $X_T$ (MPa) | $X_C$ ((MPa)) | $Y_T$ (MPa) | $Y_C$ (MPa) | S (MPa) |
|---|---|---|---|---|
| 1860 | 1470 | 76 | 85 | 98 |

Where:-

$E_1$= Longitudinal Modulus $E_2$= Transverse Modulus

u =Poisson's Ratio

$G_{12}$ =Shear Modulus S = in-plane shear strength

$x_t$= longitudinal tensile strength $y_t$ = transverse tensile strength

$x_c$= longitudinal compressive strength $y_c$ = transverse compressive strength

Source: [9]

### 3.1.2 Filament winding

Angle-Ply Laminates: Angle-ply laminates have an arbitrary number of layers (n). Each ply has the same thickness and is the same material. The plies halt can be either symmetric (see fig 8)

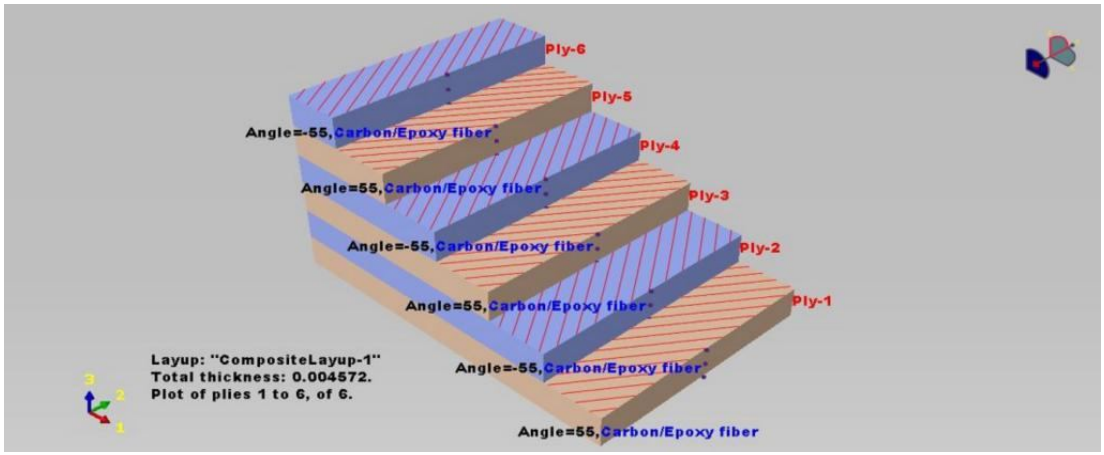


Fig-8 Layer stacking

As shown in fig 9 fibers are impregnated with a resin by drawing them through an in-line resin bath, Depending on the desired properties of the product; winding patterns such as hoop, helical can be developed. The product is then cured with or without heat & pressure. Each ply is pressed to remove any entrapped air & wrinkles; the lay-up is sealed at the edges to form a vacuum seal, [16].

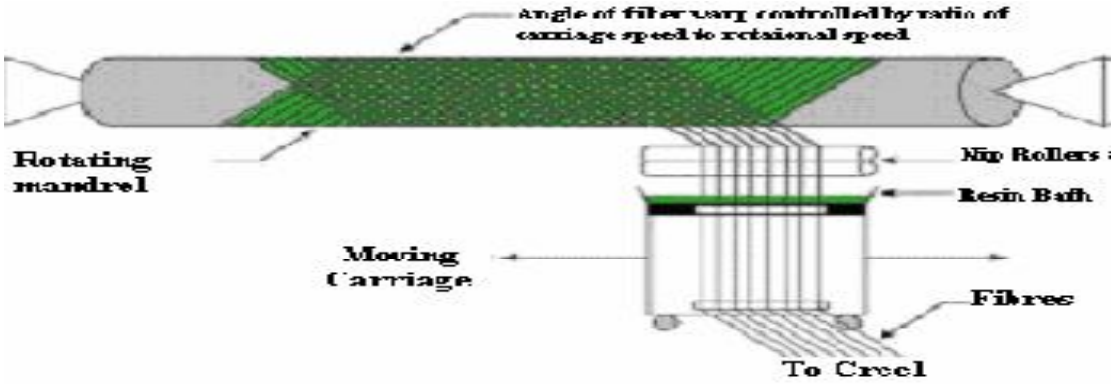


Fig-9 Arrangement of layer Filament winding

### 3.2 Dimension

The vessel is sketched with 1200 mm length, 300 mm diameter at the center point and the wall thickness of (0.3-4) mm based on the geometry. The wall thickness of vessel in center section of the vessel is 0.3 mm and each lamina thickness is 0.762. The inner radius of the vessel is 150 mm, considering six composite layers (4.572 mm); the outer radius of the vessel becomes 154.872 mm. All dimension taken from previously what they did maximum stress failure without the presence of crack by finite element method. For light weight and compact space select this dimension, [9].

Table 3 Dimensions of composite pressure vessel

| Length(mm) | Internal Diameter (mm) | each lamina thickness (mm) | composite layers | composite layers thickness (mm) | outer radius of the vessel (mm) | initial crack (mm) | Crack Angel |
|---|---|---|---|---|---|---|---|
| 1200 | 300 | 0.762 | 6 | 4.572 | 154.872 | | |

### 3.3. Methods and Methodology

**Method**

The methods which are used for this research are mathematical modeling /Analytical solution. And using ANSYS version 16 soft ware, to determine or analysis the given model output and Interpretation of results.

**Methodology**

- Model, a given composite pressure vessel and develop surface crack size “a” by FEM and analyze the result and see the effect of crack on COPV.
- Compare the result which develops analytical solution and engineering soft ware (ANSYS 16) result.

- And comparing the developed crack its stress and stress fracture, and put the value of tolerable surface crack size developed in a given material.

### 3.4. Condition and Mechanics of Composite Materials

Linear elastic theories of fiber reinforced composite are developed and are widely used in engineering. In this chapter, elastic constitutive equations and Micromechanical behaviors of composites are presented. The spatial position of the ellipsoid relative to the directions of principal stress enables to determine whether the material under study is isotropic or anisotropic. Figure 10 illustrates this phenomenon. An easy way to see the effects of anisotropy on the deformation of a sample consists in loading a plate of anisotropic material in its own plane. Figure 11 illustrates the deformations under load, respectively, of an isotropic and anisotropic plate. In the latter case, the oblique lines on Figure 11 represent the reinforcement fibers. It should be recalled that a longitudinal loading applied to the isotropic plate creates an extension in the longitudinal direction and a contraction in the transverse direction. As seen on Figure 12, the same loading applied to an anisotropic plate creates an angular distortion, in addition to the classical longitudinal extension and transversal contraction.

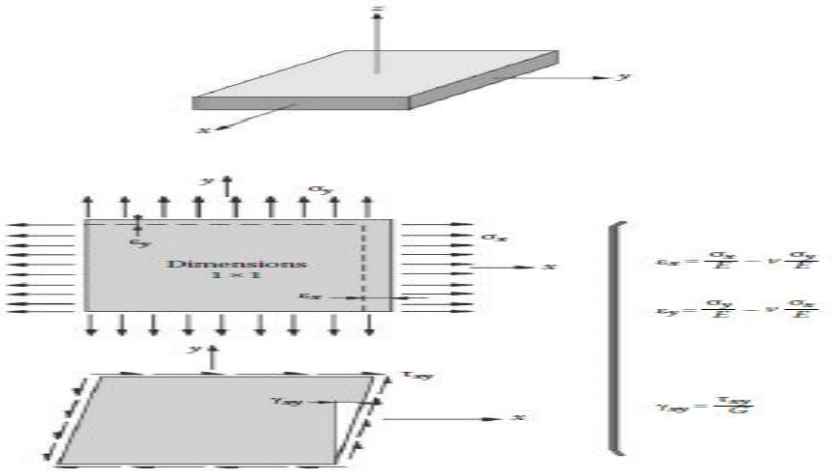


Fig-10 Isotropic plate

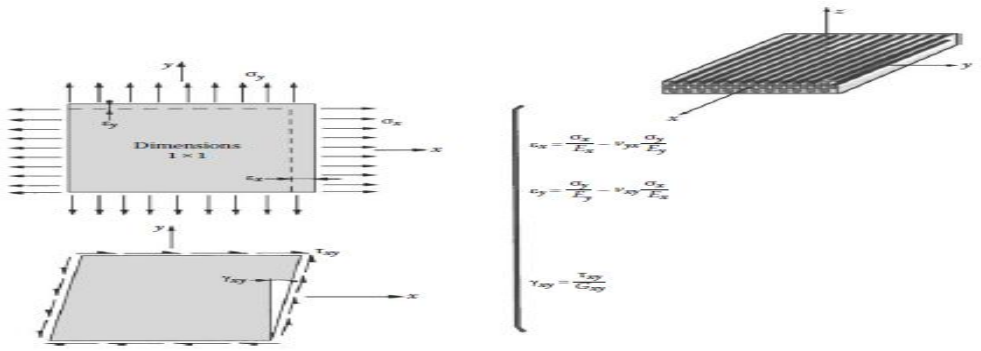


Fig-11 anisotropic plate

### 3.4.1. Elastic Constitutive Equation of Orthotropic

The constitutive equations for a general linear elastic solid relates the stress and Strain tensors through the expression,

$$\sigma_{ij} = C_{ijkl}\,\varepsilon_{kl} \qquad (3, 4.1)$$

Where;

$\sigma_{ij}$ ,$\varepsilon_{kl}$ = Stress tensor and strain tensor respectively

$C_{ijkl}$ = The fourth order tensor of elastic constants

Fiber reinforced composite materials are considered to have orthotropic elasticity because these materials posses three mutually perpendicular planes of the elastic symmetry. Constitutive equation orthotropic elasticity can be defined by giving nine individual elastic stiffness parameters. In this case the stress-strain relations are of the forms. [6]

$$\begin{Bmatrix}\sigma_1\\ \sigma_2\\ \sigma_3\\ \tau_{12}\\ \tau_{13}\\ \tau_{23}\end{Bmatrix} = \begin{bmatrix} C_{1111} & C_{1122} & C_{1133} & 0 & 0 & 0\\ & C_{2222} & C_{2233} & 0 & 0 & 0\\ & & C_{3333} & 0 & 0 & 0\\ & & & C_{1212} & 0 & 0\\ & sym & & & C_{1313} & 0\\ & & & & 0 & C_{2323}\end{bmatrix} \begin{Bmatrix}\varepsilon_{11}\\ \varepsilon_{22}\\ \varepsilon_{33}\\ \gamma_{12}\\ \gamma_{13}\\ \gamma_{23}\end{Bmatrix} \qquad (3.4.2)$$

Where, material stiffness parameters $C_{ijkl}$ are defined by engineering constant:

$$
\begin{aligned}
C_{1111} &= \frac{1-\nu_{23}\nu_{32}}{E_2E_3\Delta} \\
C_{2222} &= \frac{1-\nu_{13}\nu_{31}}{E_1E_3\Delta} \\
C_{3333} &= \frac{1-\nu_{12}\nu_{21}}{E_1E_2\Delta} \\
C_{1122} &= \frac{\nu_{21}+\nu_{31}\nu_{23}}{E_2E_3\Delta} = \frac{\nu_{12}+\nu_{32}\nu_{13}}{E_1E_3\Delta} \\
C_{1133} &= \frac{\nu_{31}+\nu_{21}\nu_{32}}{E_2E_3\Delta} = \frac{\nu_{13}+\nu_{12}\nu_{23}}{E_1E_2\Delta} \\
C_{2233} &= \frac{\nu_{32}+\nu_{12}\nu_{31}}{E_1E_3\Delta} = \frac{\nu_{23}+\nu_{21}\nu_{13}}{E_1E_2\Delta} \\
C_{1212} &= G_{12} \\
C_{1313} &= G_{13} \\
C_{2323} &= G_{23}
\end{aligned}
\tag{3.4.3}
$$

Where;

$$
\Delta = \frac{1-\nu_{12}\nu_{21}-\nu_{23}\nu_{32}-\nu_{31}\nu_{13}-2\nu_{21}\nu_{32}\nu_{13}}{E_1E_2E_3} \tag{3.4.4}
$$

Due to composite material's stability there are restrictions on the elastic constants as follow

$$
\begin{aligned}
&C_{ijkl} > 0 \\
&|C_{1122}| < \sqrt{C_{1111}C_{2222}} \\
&|C_{1133}| < \sqrt{C_{1111}C_{3333}} \\
&|C_{2233}| < \sqrt{C_{2222}C_{3333}}
\end{aligned}
\tag{3.4.5}
$$

Composite materials are compressible. There for, the determinant of the stiffness b/n fiber and Matrix should be positive,

$$\det(C_{ijkl}) > 0$$

or

$$C_{1111}C_{2222}C_{3333} + 2C_{1122}C_{1133}C_{2233} - C_{2222}C_{1133}^2 - C_{1111}C_{2233}^2 - C_{3333}C_{1122}^2 > 0 \quad (3.4.6)$$

It is obvious that elastic constants $C_{ijkl}$ depend on the elastic modulus, shear modulus and Poisson's ratio. However, these material parameters are difficult to obtain by experimental investigation. The alternative choice is to evaluate these material parameters by a micro mechanics approach.

### 3.4.2 Micromechanical Behavior of Composites

Fiber reinforced composite materials (FRC) are built from fibers and a resin matrix. Mechanical properties of FRC materials not only depend on properties fibers and resin used but also depend on the organization and the envelopment of fibers in the resin matrix. The interfacial bonding strength between fiber and resin is another factor that affects the strength of the composite. Filament wound composite pressure vessels maybe regarded as assemblies of unidirectional FRC are the focus of this work.

Currently, there are several models to describe and evaluate the properties of composites, as found from literature review. The rule of mixtures based on a simple one-dimensional model is the simplest. In terms of longitudinal modulus and in plane Poisson's ratio the results match the experimental data very well and are written as follows. [6]

$$E_1 = {}_f E_f + (1 - {}_f)E_m \quad (3.4.7)$$

$$\nu_1 = {}_f \nu_f + (1 - {}_f)\nu_m \quad (3.4.8)$$

Where: $_f$ = Fiber volume fraction, Carbone fiber = 0.55

$E_f$= Elastic module of fiber

$E_m$ = Elastic module of matrix

$E_1$= Elastic longidunal module

$\boldsymbol{\nu}_{12}$=Major Poisson ratio

The most advanced theory to evaluate the transverse modulus of the unidirectional laminates was derived by Hashin. The equations are complex, and some of material constants are difficult to establish. Highly sophisticated mathematical models are not useful when if the required data are not available. When Chamis's formula is compared Hashin's theory, it is found that the results are similar, though Chamis's formula is very simple. Thus it is recommended to employ Chamis's formula for transverse elastic modulus as follows:-

$$E_{22} = \frac{E_m}{1-(1-\frac{E_m}{E_{22}{}^f})\sqrt{\varphi}} \qquad (3.4.9)$$

Where $E_{22}{}^f$ = Fiber transversal elastic modulus For similar reasons, the shear modulus Proposed by Chamis is also recommended

$$|G_{12} = \frac{G_m}{1-(1-\frac{G_m}{G_{12}{}^f})\sqrt{\varphi}} \qquad (3.4.10)$$

The in-plain Poisson's ratio $\upsilon_{21}$ can be derived by the reciprocity relationship

$$\nu_{21} = \frac{\nu_{12}E_{11}}{E_{22}} \qquad (3.4.11)$$

The out of plane shear modulus transverse to the fiber direction $G_{23}$ is proposed by Hashin wit upper and lower bound values. Tsai also presented equations (3.4.6, 3.4.7) for $G_{23}$ which agrees quite well with Hashin's upper bound and is relatively simple.

$$G_{23} = \frac{\varphi+\delta(1-\varphi)}{\frac{\varphi}{G_{23}{}^f}+\frac{\delta(1-\varphi)}{G_m}} \qquad (3.4.12)$$

and

$$\delta = \frac{3 - 4\nu_m + \frac{G_m}{G_{23}{}^f}}{4(1-\nu_m)} \tag{3.4.13}$$

Equations (3, 4.1) to (3.4.13) are based on the assumption that both fiber and resin form elastically and there are no voids within the resin. In fact void content has a significant effect on Mechanical properties and is discussed here.

### 3.4.3. Macro Mechanical Behavior Of A Lamina

#### 3.4.3.1. Stress-Strain Relations for Plane Stress in an Orthotropic Material

A unidirectional reinforced lamina in the 1-2 planes as shown in Figure 15, a Plane stress state is defined by setting

$\sigma_3 = 0, \sigma_{23} = 0, \tau_{13} = 0$ (3.4.14)

So that

$\sigma_1 \neq 0, \sigma_2 \neq 0, \quad \tau_{12} \neq 0$ (3.4.15)

Plane stress on a lamina is not merely an idealization of reality, but instead is a Practical and achievable objective of how we must use a lamina with fibers in its plane. After all, the lamina cannot withstand high stresses in any direction other than that of the fibers, so why would we subject it to unnatural stresses such as $\sigma_3$? That is, we except to load a lamina only in plane stress because carrying in-plane stresses is its fundamental capability. A unidirectional reinforced lamina need 'help' carrying in-plane stress perpendicular to its fibers, but that help can be provided by other (parallel) layers that have their fibers in the direction of the stress. Thus, a Laminate is needed, but we concentrate on the characteristics of a lamina in this section.

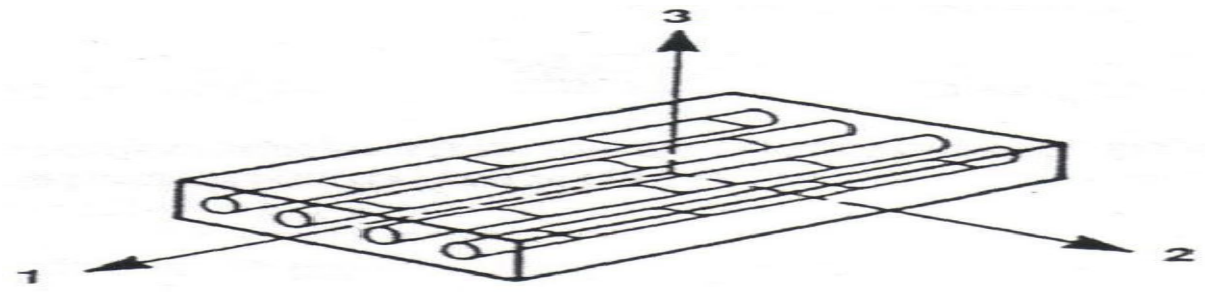


Fig 12 Unidirectional reinforced lamina.

For orthotropic materials, imposing a state of plane stress results in implied out of-Plane strains of

$$\varepsilon_3 = S_{13}\sigma_1 + S_{23}\,\sigma_2 \qquad \gamma_{23} = 0 \qquad \gamma_{31} = 0 \tag{3.4.16}$$

where

$$S_{13} = -\frac{\nu_{13}}{E_1} = -\frac{\nu_{31}}{E_3} \qquad S_{23} = -\frac{\nu_{23}}{E_2} = -\frac{\nu_{32}}{E_3} \tag{3.4.17}$$

Moreover, the strain-stress relations

$$\begin{bmatrix} \varepsilon_1 \\ \varepsilon_2 \\ \gamma_{12} \end{bmatrix} = \begin{bmatrix} S_{11} & S_{12} & 0 \\ S_{12} & S_{22} & 0 \\ 0 & 0 & S_{66} \end{bmatrix} \begin{bmatrix} \sigma_1 \\ \sigma_2 \\ \tau_{12} \end{bmatrix} \tag{3.4.18}$$

Supplemented by Equation (3.4.16) where

$$S_{11} = \frac{1}{E_1} \qquad S_{12} = -\frac{\nu_{12}}{E_1} = -\frac{\nu_{21}}{E_2} \qquad S_{22} = \frac{1}{E_2} \qquad S_{66} = \frac{1}{G_{12}} \tag{3.4.19}$$

Note that in order to determinate $\varepsilon_3$ in Equation (3.4.16), $\upsilon_{13}$ and $\upsilon_{23}$ must be known in addition to the engineering constants in Equation (3.4.19). That is $S_{13}$ and $S_{13}$ arise from $S_{13}$ and $S_{23}$ in Equation (3.4.16). The strain-stress relations in Equation (3.4.18) can be inverted to obtain the stress strain Relations.

$$\begin{bmatrix}\sigma_1\\ \sigma_2\\ \tau_{12}\end{bmatrix}=\begin{bmatrix}Q_{11} & Q_{12} & 0\\ Q_{12} & Q_{22} & 0\\ 0 & 0 & Q_{66}\end{bmatrix}\begin{bmatrix}\varepsilon_1\\ \varepsilon_2\\ \gamma_{12}\end{bmatrix} \tag{3.4.20}$$

Where the Qij are the so-called reduced stiffness's for a plane stress state in the 1-2 plane which are determined either (1) as the components of the inverted compliance matrix in Equation (3.4.18) or (2) from the $C_{ij}$ directly by applying the condition $\sigma_3 = 0$ to the strain stress relations to get an expression for $\varepsilon_3$ and simplifying the results to get

$$Q_{ij} = C_{ij} - \frac{C_{i3}C_{j3}}{C_{33}} \qquad \text{i,j=1,2,6} \tag{3.4.21}$$

The term $C_{63}$ is zero because no shear-extension coupling exists for an orthotropic lamina in principal material coordinates. For the orthotropic lamina, the $Q_{ij}$ are

$$Q_{11} = \frac{S_{22}}{S_{11}S_{22} - S_{12}^2} \qquad Q_{22} = \frac{S_{11}}{S_{11}S_{22} - S_{12}^2}$$
$$Q_{12} = \frac{S_{12}}{S_{11}S_{22} - S_{12}^2} \qquad Q_{66} = \frac{1}{S_{66}} \tag{3.4.22}$$

Or, in terms of the engineering constants,

$$Q_{11} = \frac{E_1}{1-\nu_{12}\nu_{21}} \qquad Q_{22} = \frac{E_2}{1-\nu_{12}\nu_{21}}$$
$$Q_{12} = \frac{\nu_{12}E_2}{1-\nu_{12}\nu_{21}} = \frac{\nu_{21}E_1}{1-\nu_{12}\nu_{21}} \qquad Q_{66} = G_{12} \tag{3.4.23}$$

Note that there are four independent material properties; $E_1$, $E_2$, and G12, in Equations (3.4.18) and (3.4.20) are considered in addition to the reciprocal relation

$$\frac{\nu_{12}}{E_1} = \frac{\nu_{21}}{E_2} \tag{3.4.24}$$

The preceding stress-stain and strain-stress relations are the basis for stiffness and stress analysis of an individual lamina subjected to forces in its own plane. Thus, the relations are indispensable in laminate analysis.

### 3.4.3 Stress-Strain Relations for a Lamina of Arbitrary Orientation

The stresses and strains were defined in the principal material coordinates for an orthotropic material. However, the principal directions of orthotropic often do not coincide with coordinate directions that are geometrically natural to the solution of the problem. For example, consider the helically wound fiber-reinforced circular cylindrical shell in Figure 13. There, the coordinates natural to the solution of the shell problem are the shell coordinates x', y', z'. The filament-winding angle is defined by cos(y', y) = cos α; also, z' = z. Other examples include laminated plates with different laminate at different orientations. Thus, a relation is needed between the stresses and strains in the principal material coordinates and those in the body coordinates. Then, a method of transforming stress-strain relations from one coordinate system to another is also needed. At this point, we recall from elementary mechanics of materials the transformation equations for expressing stresses in a z-y coordinate system in terms of stresses in 1-2 coordinate systems.

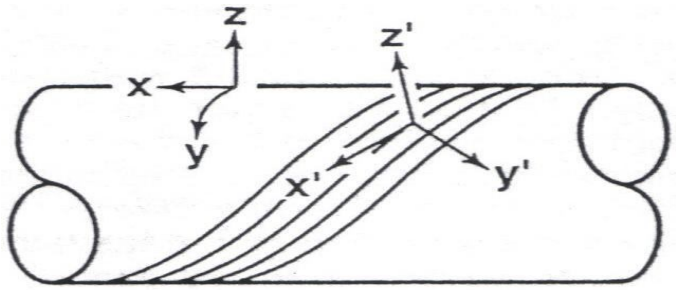


Fig 13 helically wound fiber-reinforced circular cylindrical l shell

$$\begin{bmatrix} \sigma_x \\ \sigma_y \\ \tau_{xy} \end{bmatrix} = \begin{bmatrix} \cos^2\theta & \sin^2\theta & -2\sin\theta\cos\theta \\ \sin^2\theta & \cos^2\theta & 2\sin\theta\cos\theta \\ \sin\theta\cos\theta & -\sin\theta\cos\theta & \cos^2\theta - \sin^2\theta \end{bmatrix} \begin{bmatrix} \sigma_1 \\ \sigma_2 \\ \tau_{12} \end{bmatrix} \tag{3.4.25}$$

Where θ is the angle from the z-axis to the 1-axis (see Figure 13). Note especially that the transformation has nothing to do with the material properties but is merely a rotation of stress directions. Also, the direction of rotation is crucial.

Similarly, the strain-transformation equations are:-

$$\begin{bmatrix} \varepsilon_x \\ \varepsilon_y \\ \frac{\gamma_{xy}}{2} \end{bmatrix} = \begin{bmatrix} \cos^2\theta & \sin^2\theta & -2\sin\theta\cos\theta \\ \sin^2\theta & \cos^2\theta & 2\sin\theta\cos\theta \\ \sin\theta\cos\theta & -\sin\theta\cos\theta & \cos^2\theta - \sin^2\theta \end{bmatrix} \begin{bmatrix} \varepsilon_1 \\ \varepsilon_2 \\ \frac{\gamma_{12}}{2} \end{bmatrix} \quad (3.4.26)$$

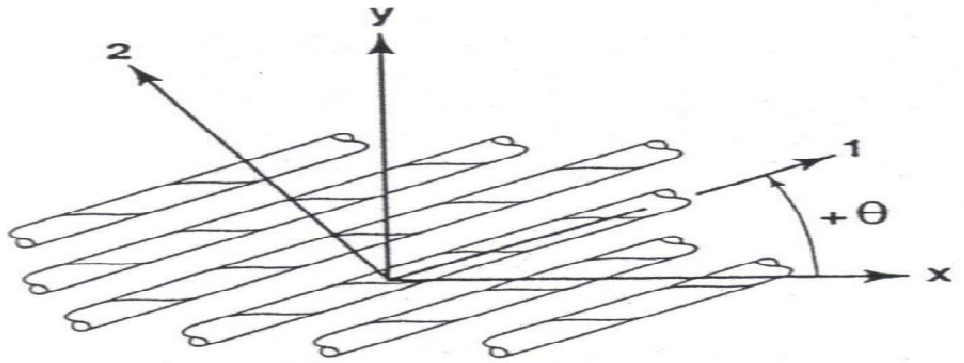


Fig 14 Positive rotation of principal material axes from x-y axes

Where we observe that strains do transform with the same transformation as stresses if the tensor definition of shear strain is used (which is equivalent to dividing the engineering shear strain by two). The transformations are commonly written as:

$$\begin{bmatrix} \sigma_x \\ \sigma_y \\ \tau_{xy} \end{bmatrix} = [T]^{-1} \begin{bmatrix} \sigma_1 \\ \sigma_2 \\ \tau_{12} \end{bmatrix} \quad (3.4.27)$$

$$\begin{bmatrix} \varepsilon_x \\ \varepsilon_y \\ \frac{\gamma_{xy}}{2} \end{bmatrix} = [T]^{-1} \begin{bmatrix} \varepsilon_1 \\ \varepsilon_2 \\ \frac{\gamma_{12}}{2} \end{bmatrix} \quad (3.4.28)$$

Where the superscript -1 denotes the matrix inverse and

$$[T]=\begin{bmatrix} \cos^2\theta & \sin^2\theta & 2\sin\theta\cos\theta \\ \sin^2\theta & \cos^2\theta & -2\sin\theta\cos\theta \\ -\sin\theta\cos\theta & \sin\theta\cos\theta & \cos^2\theta-\sin^2\theta \end{bmatrix} \tag{3.4.29}$$

However, if the simplex matrix

$$[R]=\begin{bmatrix} 1 & 0 & 0 \\ 0 & 1 & 0 \\ 0 & 0 & 2 \end{bmatrix} \tag{3.4.30}$$

Due to Reuter is introduced, then the engineering strain vectors

(3.4.31)

$$\begin{bmatrix} \varepsilon_1 \\ \varepsilon_2 \\ \gamma_{12} \end{bmatrix} = [R]\begin{bmatrix} \varepsilon_1 \\ \varepsilon_2 \\ \frac{\gamma_{12}}{2} \end{bmatrix}$$

$$\begin{bmatrix} \varepsilon_x \\ \varepsilon_y \\ \gamma_{xy} \end{bmatrix} = [R]\begin{bmatrix} \varepsilon_x \\ \varepsilon_y \\ \frac{\gamma_{xy}}{2} \end{bmatrix} \tag{3.4.32}$$

can be used instead of the tensor strain vectors in the strain transformations as well as in stress-strain law transformations, the beauty of Reuter's transformation is that concise matrix notation can then be used. As a result, the ordinary expressions for stiffness and compliance matrices with awkward factors of 1/2 and 2 in various rows and columns are avoided. A so-called especially orthotropic lamina is an orthotropic lamina whose principal material axes are aligned whit the natural body axes:

$$\begin{bmatrix} \sigma_1 \\ \sigma_2 \\ \tau_{12} \end{bmatrix} = \begin{bmatrix} \sigma_x \\ \sigma_y \\ \tau_{xt} \end{bmatrix} = \begin{bmatrix} Q_{11} & Q_{12} & 0 \\ Q_{12} & Q_{22} & 0 \\ 0 & 0 & Q_{66} \end{bmatrix} \begin{bmatrix} \varepsilon_1 \\ \varepsilon_2 \\ \gamma_{12} \end{bmatrix} \tag{3.4.33}$$

Where the principal material axes are shown in Figure 14. These stress-strain relations apply when the principal material directions of an orthotropic lamina are used as coordinates.

However, as mentioned previously, orthotropic lamina are often constructed in such a manner that the principal material coordinates do not to be interpreted as meaning that the principal material coordinates do not coincide with the natural coordinates of the body. This statement is not to be interpreted as meaning that the material itself is no longer orthotropic; instead, we are just looking at an orthotropic material in an unnatural manner, i.e., in a coordinate system that is oriented at some angle to the principal material coordinate system. Then, the basic question is: given the stress-strain relations in the principal material coordinates, what are the stress strain relations in x-y coordinates? Accordingly, we use the stress and strain transformations of Equations (3.4.27) and (3.4.28) along with Reuter's matrix, Equation (3.4.30), after abbreviating Equation (3.4.33) as:-

$$\begin{bmatrix}\sigma_1\\ \sigma_2\\ \tau_{12}\end{bmatrix} = [Q]\begin{bmatrix}\varepsilon_1\\ \varepsilon_2\\ \gamma_{12}\end{bmatrix} \tag{3.4.34}$$

to obtain

$$\begin{bmatrix}\sigma_x\\ \sigma_y\\ \tau_{xy}\end{bmatrix} = [T]^{-1}\begin{bmatrix}\sigma_1\\ \sigma_2\\ \tau_{12}\end{bmatrix} = [T]^{-1}[Q][R][T][R]^{-1}\begin{bmatrix}\varepsilon_x\\ \varepsilon_y\\ \gamma_{xy}\end{bmatrix} \tag{3.4.35}$$

However, [R] [T] $[R]^{-1}$can be shown to be $[R]^{-1}$ where the superscript T denotes the Matrix transpose. Then, if we use the abbreviation

$$[\overline{Q}] = [T]^{-1}[Q][T]^{-T} \tag{3.4.36}$$

The stress-strain relations in x-y coordinates are

$$\begin{bmatrix}\sigma_x\\ \sigma_y\\ \tau_{xy}\end{bmatrix} = [\overline{Q}]\begin{bmatrix}\varepsilon_x\\ \varepsilon_y\\ \gamma_{xy}\end{bmatrix} = \begin{bmatrix}\overline{Q}_{11} & \overline{Q}_{12} & \overline{Q}_{16}\\ \overline{Q}_{12} & \overline{Q}_{22} & \overline{Q}_{26}\\ \overline{Q}_{16} & \overline{Q}_{26} & \overline{Q}_{66}\end{bmatrix}\begin{bmatrix}\varepsilon_x\\ \varepsilon_y\\ \gamma_{xy}\end{bmatrix} \tag{3.4.37}$$

The stress-strain relations in x-y coordinates are in which

$$
\begin{aligned}
\overline{Q}_{11} &= Q_{11}\cos^4\theta + 2(Q_{12}+2Q_{66})\sin^2\theta\cos^2\theta + Q_{22}\sin^4\theta \\
\overline{Q}_{12} &= (Q_{11}+Q_{12}-4Q_{66})\sin^2\theta\cos^2\theta + Q_{12}(\sin^4\theta+\cos^4\theta) \\
\overline{Q}_{22} &= Q_{11}\sin^4\theta + 2(Q_{12}+2Q_{66})\sin^2\theta\cos^2\theta + Q_{22}\cos^4\theta \\
\overline{Q}_{16} &= (Q_{11}-Q_{12}-2Q_{66})\sin\theta\cos^3\theta + (Q_{12}-Q_{22}+2Q_{66})\sin^3\theta\cos\theta \\
\overline{Q}_{26} &= (Q_{11}-Q_{12}-2Q_{66})\sin^3\theta\cos\theta + (Q_{12}-Q_{22}+2Q_{66})\sin\theta\cos^3\theta \\
\overline{Q}_{66} &= (Q_{11}+Q_{22}-2Q_{12}-2Q_{66})\sin^2\theta\cos^2\theta + Q_{66}(\sin^4\theta+\cos^4\theta)
\end{aligned}
\qquad (3.4.38)
$$

Where the bar over the Qij matrix denotes that we are dealing whit the transformed reduced stiffness's instead of the reduced stiffness's, Qij. Note that the transformed reduced stiffness matrix Qij has terms in all nine positions in contrast to the presence of zeros in the reduced stiffness matrix $Q_{ij}$. However, there are still only four independent material constants because the lamina is orthotropic. In the general case with body coordinates x and y, there is coupling between shear strain and normal stresses and between shear stress and normal strains, i.e., shear-extension coupling exists. Thus, in body coordinates, even an orthotropic lamina appears to be anisotropic. However, because such a lamina does have orthotropic characteristics in principal material coordinates, it is called a generally orthotropic lamina because it can be represented by the stress-strain relations in Equation (3.4.37). That is, a generally orthotropic lamina is an orthotropic lamina whose principal material axes are not aligned whit the natural body axes.

The only advantage associated with generally orthotropic lamina as opposed to anisotropic laminae is that generally orthotropic laminae are easier to characterize experimentally. However, if we do not realize that principal material axes exist, then a generally orthotropic lamina is indistinguishable from an anisotropic lamina. That is we cannot take away the inherent orthotropic character of a lamina, but we can orient the lamina in such a manner as to make that character quite difficult to recognize.

As an alternative to the foregoing procedure, we can express the strains in terms of the stresses in body coordinates by inversion of the stress-strain relations in Equation (3.4.37) transformation of the strain-stress relations in principal material coordinates from Equation (3.4.18)

$$
\begin{bmatrix} \varepsilon_1 \\ \varepsilon_2 \\ \gamma_{12} \end{bmatrix} = \begin{bmatrix} S_{11} & S_{12} & 0 \\ S_{12} & S_{22} & 0 \\ 0 & 0 & S_{66} \end{bmatrix} \begin{bmatrix} \sigma_1 \\ \sigma_2 \\ \tau_{12} \end{bmatrix} \qquad (3.4.39)
$$

to body coordinates. We choose the second approach and apply the transformations of Equations (3.4.27) and (3.4.28) along with Reuter's matrix, Equation (3.4.30), to obtain:-

$$\begin{bmatrix}\varepsilon_x\\ \varepsilon_y\\ \gamma_{xy}\end{bmatrix}=[T]^T[S][T]\begin{bmatrix}\sigma_x\\ \sigma_y\\ \tau_{xy}\end{bmatrix}=\begin{bmatrix}\overline{S}_{11} & \overline{S}_{12} & \overline{S}_{16}\\ \overline{S}_{12} & \overline{S}_{22} & \overline{S}_{26}\\ \overline{S}_{16} & \overline{S}_{26} & \overline{S}_{66}\end{bmatrix}\begin{bmatrix}\sigma_x\\ \sigma_y\\ \tau_{xy}\end{bmatrix} \tag{3.4.40}$$

where $[R][T]^{-1}[R]^{-1}$ was found to be $[T]^T$ and

$$\begin{aligned}
\overline{S}_{11} &= S_{11}\cos^4\theta+(2S_{12}+S_{66})\sin^2\theta\cos^2\theta+S_{22}\sin^4\theta\\
\overline{S}_{12} &= S_{12}(\sin^4\theta+\cos^4\theta)+(S_{11}+S_{22}-S_{66})\sin^2\theta\cos^2\theta\\
\overline{S}_{22} &= S_{11}\sin^4\theta+(2S_{12}+S_{66})\sin^2\theta\cos^2\theta+S_{22}\cos^4\theta\\
\overline{S}_{16} &= (2S_{11}-2S_{12}-S_{66})\sin\theta\cos^3\theta-(2S_{22}-2S_{12}-S_{66})\sin^3\theta\cos\theta\\
\overline{S}_{26} &= (2S_{11}-2S_{12}-S_{66})\sin^3\theta\cos\theta-(2S_{22}-2S_{12}-S_{66})\sin\theta\cos^3\theta\\
\overline{S}_{66} &= 2(2S_{11}+2S_{22}-4S_{12}-S_{66})\sin^2\theta\cos^2\theta+S_{66}(\sin^4\theta+\cos^4\theta)
\end{aligned} \tag{3.4.41}$$

Recall that the Sij are defined in terms of the engineering constants in Equation (3.4.19). Because of the presence of Q16 and Q26 in Equation (3.4.37) and of $S_{16}$ and $S_{26}$ in Equation (3.4.40), the solution of problems involving so called generally orthotropic laminae is more difficult than problems with so-called especially orthotropic laminae. That is, shear-extension coupling complicates the solution of practical problems. As a matter of fact, there is no difference between solutions for generally orthotropic laminae and those for anisotropic laminate whose stress-strain relations, under conditions of plane stress, can be written as:-

$$\begin{bmatrix}\sigma_1\\ \sigma_2\\ \tau_{12}\end{bmatrix}=\begin{bmatrix}Q_{11} & Q_{12} & 0\\ Q_{12} & Q_{22} & 0\\ 0 & 0 & Q_{66}\end{bmatrix}\begin{bmatrix}\varepsilon_1\\ \varepsilon_2\\ \gamma_{12}\end{bmatrix} \tag{3.4.42}$$

or in inverted from as

$$\begin{bmatrix}\varepsilon_1\\ \varepsilon_2\\ \gamma_{12}\end{bmatrix}=\begin{bmatrix}S_{11} & S_{12} & S_{16}\\ S_{12} & S_{22} & S_{26}\\ S_{16} & S_{26} & S_{66}\end{bmatrix}\begin{bmatrix}\sigma_1\\ \sigma_2\\ \tau_{12}\end{bmatrix} \tag{3.4.43}$$

where the anisotropic compliances in term of the engineering constants are

$$S_{11} = \frac{1}{E_1} \qquad S_{12} = \frac{1}{E_2} \qquad S_{16} = \frac{\eta_{12,1}}{E_1} = \frac{\eta_{1,12}}{G_{12}}$$
$$S_{12} = -\frac{\nu_{12}}{E_1} = -\frac{\nu_{21}}{E_2} \qquad S_{66} = \frac{1}{G_{12}} \qquad S_{26} = \frac{\eta_{12,1}}{E_2} = \frac{\eta_{2,12}}{G_{12}} \tag{3.4.44}$$

Note that some new engineering constants have been used. The new constants are called coefficients of mutual influence by Lekhnitskii and are defined as Ηi,ij = coefficient of mutual influence of the first kind that characterizes stretching in the i-direction caused by shear stress in the ij-plane.

$$\eta_{i,ij} = \frac{\varepsilon_i}{\gamma_{ij}} \tag{3.4.45}$$

The ij-plane caused by normal stress in the i-direction

$$\eta_{ij,i} = \frac{\gamma_{ij}}{\varepsilon_i}$$

for $\sigma_{ij} = \sigma$ and all other stresses are zero. (3.4.46)

Lekhnitskii defines the coefficients of mutual influence and the Poisson's ratios with subscripts that are reversed from the present notation. The coefficients of mutual influence are not named very effectively because the Poisson's ratios could also be called coefficients of mutual influence. Instead, the ij,i and i,ij are more appropriately called by the functional name shear-extension coupling coefficients. Other anisotropic elasticity relations are used to define Chentsov coefficients that are to shearing strains what Poisson's ratios are to shearing stresses and shearing strains. However, the Chentsov coefficients do not affect the in--plane behaviour of laminae under plane stress. The Chentsov coefficients are defined as μij,kl = Chentsov coefficient that characterizes the shearing strain in the kl-plane due to shearing stress in the ij-plane, i.e.

$$\mu_{ij,kl} = \frac{\gamma_{kl}}{\gamma_{ij}} \tag{3.4.47}$$

For $\tau_{ij} = \tau$ and all other stresses are zero.

The Chentsov coefficients are subject to the reciprocal relations

$$\frac{\mu_{kl,ij}}{G_{kl}} = \frac{\mu_{ij,kl}}{G_{ij}} \tag{3.4.48}$$

Note that the Chentsov coefficients are more effectively called the functional name of shear-shear coupling coefficients. The out-of-plane shearing strains of an anisotropic lamina due to in-plane shearing stress and normal stresses are

$$\gamma_{13} = \frac{\eta_{1,13}\sigma_1 + \eta_{2,13}\sigma_2 + \mu_{12,13}\tau_{12}}{G_{13}}$$
$$\gamma_{23} = \frac{\eta_{1,13}\sigma_1 + \eta_{2,13}\sigma_2 + \mu_{12,13}\tau_{12}}{G_{23}} \tag{3.4.49}$$

Where, in both the shear-shear coupling coefficients and the shear-extension coupling coefficients are required. Note that neither of these shear strains arise in an orthotropic material unless it is stressed in coordinates other than the principal material coordinates. In such cases, the shear-shear coupling coefficients and the shear-extension coupling coefficients are obtained from the transformed compliances as in the following paragraph. Compare the transformed orthotropic compliances in Equation (3.4.41) whit the anisotropic compliances in terms of engineering constants in Equations (3.4.44). Obviously an apparent shear-extension coupling coefficient results when an orthotropic lamina is stressed in non-principal material coordinates. Redesignate the coordinates 1 and 2 in Equation (3.4.43) as x and y because, by definition, an anisotropic material has no principal material directions. Then, substitute the redesignated $S_{ij}$ from Equation (3.4.44) in Equation (3.4.41) along with the orthotropic compliances in Equation (3.4.19). Finally, the apparent engineering constants for an orthotropic lamina that is stressed in non-principal x-y coordinates are:-

$$\frac{1}{E_x}=\frac{1}{E_1}\cos^4\theta+\left[\frac{1}{G_{12}}+\frac{2\nu_{12}}{E_1}\right]\sin^2\theta\cos^2\theta+\frac{1}{E_2}\sin^4\theta$$

$$\nu_{xy}=E_x\left[\frac{\nu_{12}}{E_1}(\sin^4\theta+\cos^4\theta)-\left[\frac{1}{E_1}+\frac{1}{E_2}-\frac{1}{G_{12}}\right]\sin^2\theta\cos^2\theta\right]$$

$$\frac{1}{E_y}=\frac{1}{E_1}\sin^4\theta+\left[\frac{1}{G_{12}}-\frac{2\nu_{12}}{E_1}\right]\sin^2\theta\cos^2\theta+\frac{1}{E_2}\cos^4\theta$$

$$\frac{1}{G_{xy}}=2\left[\frac{2}{E_1}+\frac{2}{E_2}+\frac{4\nu_{12}}{E_1}-\frac{1}{G_{12}}\right]\sin^2\theta\cos^2\theta+\frac{1}{G_{12}}(\sin^4\theta\cos^4\theta)$$

$$\eta_{xy,x}=E_x\left[\left[\frac{2}{E_1}+\frac{2\nu_{12}}{E_1}-\frac{1}{G_{12}}\right]\sin\theta\cos^3\theta-\left[\frac{2}{E_1}+\frac{2\nu_{12}}{E_1}-\frac{1}{G_{12}}\right]\sin^3\theta\cos\theta\right]$$

$$\eta_{xy,y}=E_y\left[\left[\frac{2}{E_1}+\frac{2\nu_{12}}{E_1}-\frac{1}{G_{12}}\right]\sin^3\theta\cos\theta-\left[\frac{2}{E_2}+\frac{2\nu_{12}}{E_1}-\frac{1}{G_{12}}\right]\sin\theta\cos^3\theta\right] \quad (3.4.50)$$

### 3.4.4 Stress in composite pressure vessel

#### 3.4.4.1 Winding Angle

Winding angle has significant effects on the structure of filament-wound vessels; so determining the appropriate angle for each part of the vessel is an important issue. The winding angle is defined for the two types of geodesic and non-geodesic winding based on the need for friction between fibers and the shell as in Eq. (3.4.51) and fig 15. The second part of the following relation relates to the non-geodesic winding method [9]:

$$\alpha(R)=\sin^{-1}\left(\frac{R_0}{R}\right)\mp\delta\left(\frac{R-R_0}{R_{tl}-R_0}\right)^n \quad (3.4.51)$$

Here, R is the radial distance from the center line to a point in the layer, is the radius of the polar axis, and is the radius at the dome-cylinder tangent line. A geodesic winding pattern, as in this research is obtained by choosing δ= 0.

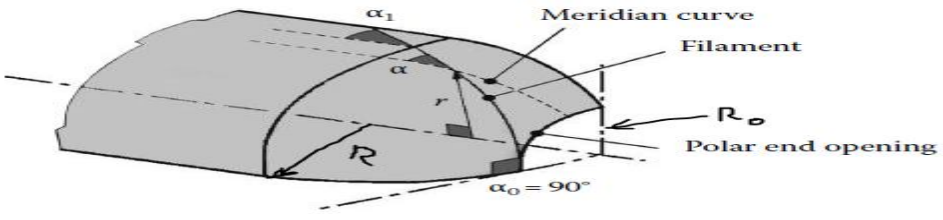


Fig 15 Winding Angle

Filaments wound helically {angle} α1) in the cylindrical part are following geodesic line toward the heads such that r sin α = constant. The circle making up the head is a geodesic line characterized by r = ro.

### 3.4.4.1 Design of Pressure Vessels, Optimum Winding Angle and Displacement.

Netting analysis is one of the most popular analytical techniques used for investigating the behavior of multi-layered composite materials, especially for filament-wound pressure vessels. The main assumption in netting analysis is that all loads are carried by the fibers neglecting the stiffness of the matrix and internal pressure subjected to the vessel produces a hoop-to-axial-stress ratio of 2:1.

A section of such a shell is shown in Figure 17. The hoop (circumferential) stress, hoop s and the longitudinal stress, long s are indicated in the figure. The shell is assumed to be long and thin resulting in hoop s and long s to be uniform through the thickness. Therefore in this case hoop s and long s are also referred to as membrane stress (there are no bending stresses associated with this type. Figure 17 indicates the thin-wall cylindrical vessel with the thickness of "t" and length of "L" which is subjected into the internal pressure of "P". In order to calculate the axial (longitudinal) and hoop stresses at the cylinder with the radius of "R", Eq. (3.4.54) can be utilized

$$N_{\emptyset} = \frac{PR}{2} \quad , \quad N_{\theta} = PR \tag{3.4.52}$$

Axial and hoop stresses can be calculated as in Eq. (3.4.53):

$$\sigma_{axial} = \frac{N_{\emptyset}}{t} = \frac{PR}{2t} \quad , \quad \sigma_{hoop} = \frac{N_{\theta}}{t} = \frac{PR}{t} \tag{3.4.53}$$

Axial and hoop stresses can be calculated according to equilibrium across the cut section too as in Eqs:-

$$PL(2R) = 2\sigma_{hoop}Lt$$

$$P\pi r^2 = 2\sigma_{axial}(2\pi Rt)$$

$$\sigma_{hoop}(\sigma_h) = \frac{PR}{t}$$

$$\sigma_{axial}(\sigma_a) = \frac{PR}{2t} \qquad (3.4.54)$$

$$\tau = \sigma_{hoop} \sin\theta \cos\theta$$

The burst pressure increases with increasing winding angle up to $55^0$ degrees because laminates show more resistance to hoop stress than the axial stress. As the curve reaches to its maximum in $55^0$ degrees, the amount of burst pressure decreases due to fiber higher resistance to axial stressand its lower resistance to hoop stress [9].

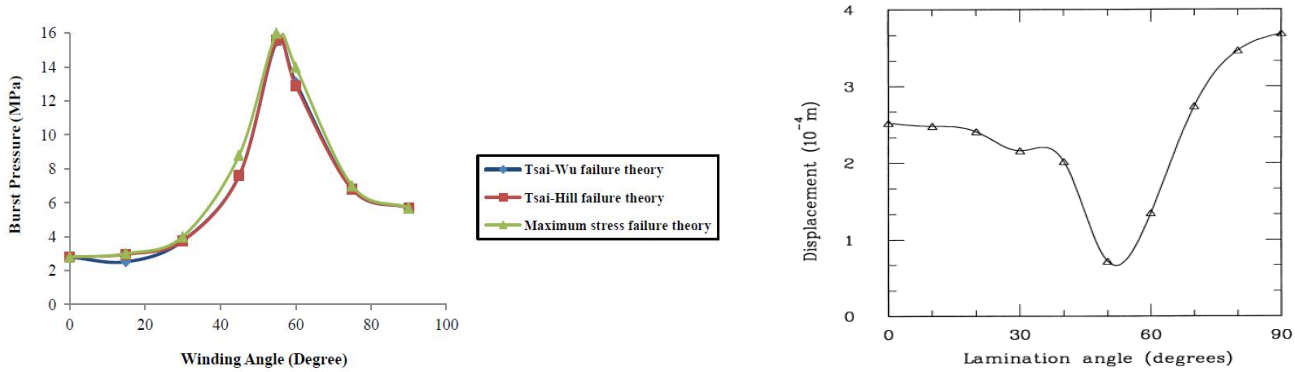


Fig 16 Variation of burst pressure with increasing winding angle and displacement.

The displacement at the central clamped pressure vessel due to the presence of pressure there will be dependence on orientation of fiber as the above fig 16.

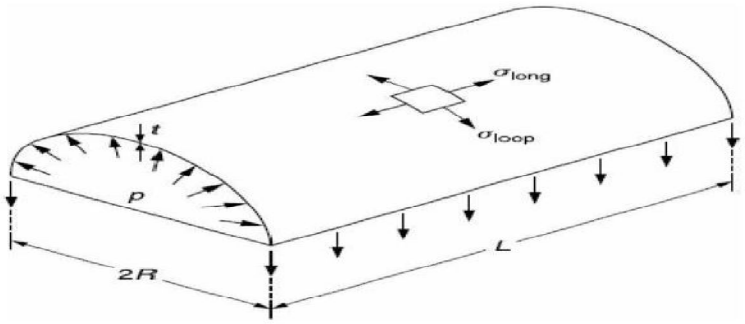


Fig 17 Thin cylindrical shell

Optimum winding angle can be estimated by using ultimate tensile strength along with applying netting analysis respect to 2:1 hoop-to-axial stress ratio as it is shown at Eqs. (3.4.53) and

(3.4.54) as it is shown in figure 17. The body diagram of the cylinder consists of axial and hoop forces wrapped with the fibers at the angle of "α" is indicated at figure 18.

$$N_\theta = \sigma_u t \sin^2 \alpha \qquad N_\phi = \sigma_u t \cos^2 \alpha \tag{3.4.55}$$

$$\frac{N_\theta}{N_\phi} = \tan^2 \alpha = 2 \qquad \alpha = \arctan(\sqrt{2}) = 54.7^0$$

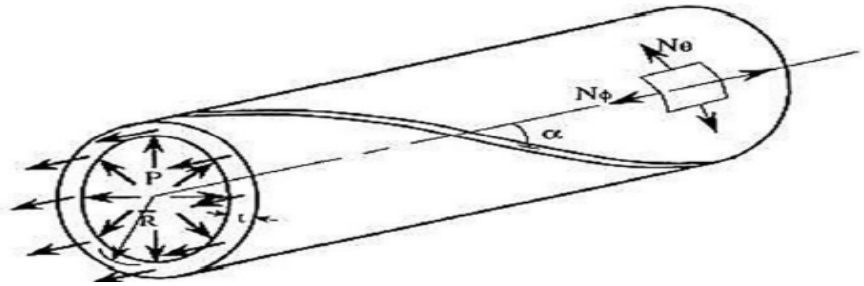


Fig 18 Body diagram of axial and hoop forces and internal pressure

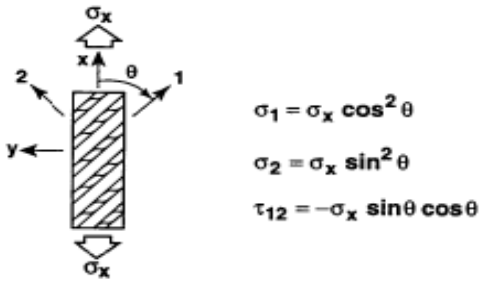


Fig 19 helical winding orientation ($55^0$,$-55^0$)

### 3.4.4. Crack Predicting In Different Orientation and Susceptible Areas in COPV

#### 3.4.5.1 Crack susceptible areas in composite pressure vessel.

The composite material pressure vessel has many damage mechanisms in it. The initial damage mechanism contains the matrix crack due to the stress as well as the crack grown. Fatigue crack growth rate behavior of small cracks in bi-axially loaded COPV liners. The experimental procedure included the use of a laser notch to quickly generate small surface fatigue cracks with the desired size and aspect ratios. An out-of-plane constraint system was designed to allow fully reversed, fully plastic testing of thin sheet uniaxial coupons. Finally, an experimental procedure was developed to initiate small fatigue cracks in COPVs. This initial crack will initiate at joint

part or at middle part of the composite pressure vessel as shown in fig. This initial crack size depends on the amount of energy applied on composite pressure vessel. The size may be notch size or hole size it depend on the profile of tip of piston. The NASA Johnson Space Center White Sands Test Facility (WSTF) has used laser shearography (LS) for several years to inspect and test composite overwrapped pressure vessels (COPVs). Shearography inspection of COPVs for impact damage and other anomalies has been demonstrated to have a lower detection limit than most other NDE methods. This test method is the damage can be taken as circle or hole and take the diameter of hole with related to applied pressure in terms of energy [7]

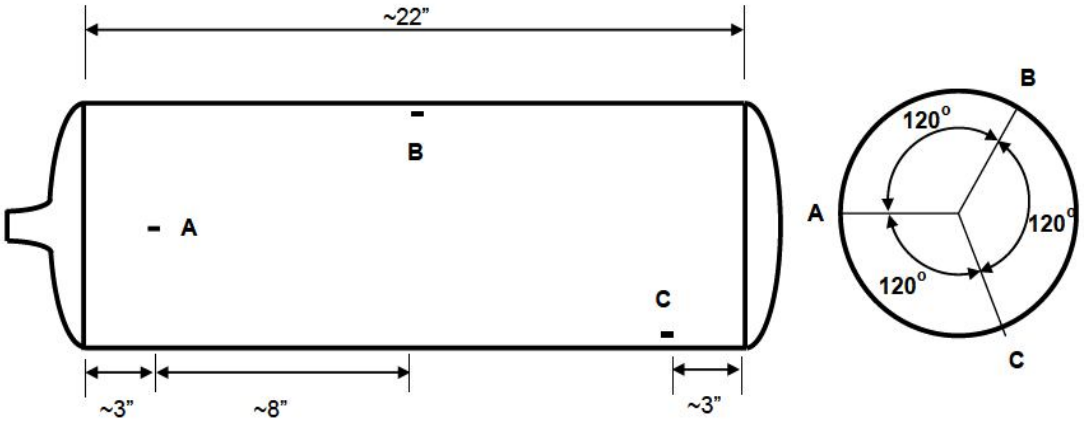


Fig 20 Schematic of the location of crack development in composite pressure vessel

### 3.4.5.2 Crack predicting in composite pressure vessel

All efforts to predicting crack growth and fatigue in a composite laminate are affected by the unique and complex manner in which crack can be grow in the matrix parallel to the fiber. Thus, if a crack is cut parallel to the fibers as shown to the fig, it will grow in direction parallel to itself, i.e. That mines it is self similar manner. However, if a crack cut at some angel to the fiber the crack will be still grow parallel to the fiber and not parallel to itself i.e. Non self similar growth as showmen in the fig. Then, because of a composite laminate results in a crack growth that is locally sometimes not globally. A crack growth a non self similar so predicting the effect of many kinds of a damage growth.[6]

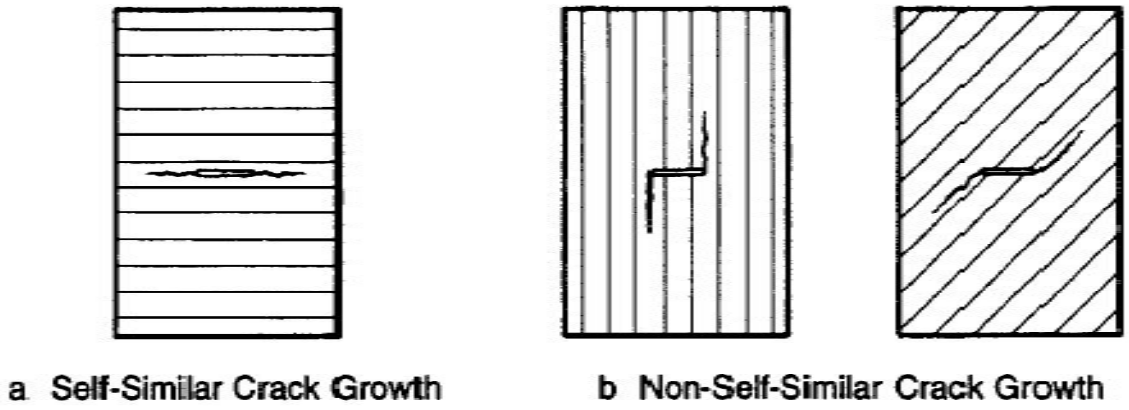


Fig 21 self similar crack growth and non self similar crack growth

According to the thickens of the composite pressure vessel we have different crack size on the following table. 4 [27].

Surface crack width and depth ratios

| *a/c* | *a/t* | *a/c* | *a/t* | *a/c* | *a/t* |
|---|---|---|---|---|---|
| 0.2 | 0.25 | 0.3 | 0.25 | 0.4 | 0.25 |
| 0.2 | 0.38 | 0.3 | 0.38 | 0.4 | 0.38 |
| 0.2 | 0.50 | 0.3 | 0.50 | 0.4 | 0.50 |
| 0.2 | 0.75 | 0.3 | 0.75 | 0.4 | 0.75 |

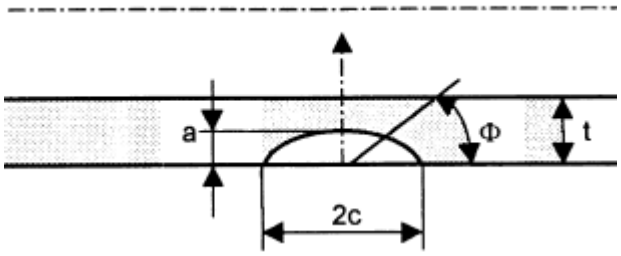


Table 4, surface crack size on composite material

### 3.5 Mathematical Module of Crack Opening Displacement.

#### 3.5.1 Introduction

Fracture mechanics is the study of mechanical behavior of cracked materials subjected to an applied load. In fact, Irwin developed the field of fracture mechanics using the early work of Inglis, Griffith, and Westergaard. Essentially, fracture mechanics deals with the irreversible process of rupture due to nucleation and growth of cracks. The formation of cracks may be a complex fracture process, which strongly depends on the microstructure of a particular crystalline or amorphous solid, applied loading, and environment. **Brittle Fracture** is a low-energy process (low energy dissipation), which may lead to catastrophic failure without warning since the crack velocity is normally high. Therefore, little or no plastic deformation may be

involved before separation of the solid. On the other hand, **Ductile Fracture** is a high-energy process in which a large amount of energy dissipation is associated with a large plastic deformation before crack instability occurs. Consequently, slow crack growth occurs due to strain hardening at the crack tip region. [25]

Crack propagation in composite materials consisting of a matrix material and a set of fiber inclusions. While in [Nee87] and [WRO97] crack paths in a fixed domain of a specimen supplied with defined material properties are considered, we aim to simulate cracks inside different materials of a composite specimen paying attention to various possibilities of cracking phenomena like matrix crack, fiber deboning and fiber breakage [1].

### 3.5.2 Crack Opening Model

A crack may propagate in three different modes: opening mode (called mode I), sliding mode (mode II) or tearing mode (mode III). These three modes form the basis for any crack propagation, that is, the propagation conditions of any crack can always be decomposed as a combination of the three modes. Those propagation modes which are the combination of the three basic modes are called mixed modes [25].

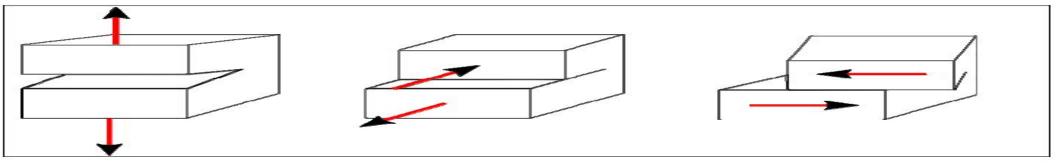

Fig 22 Crack propagation modes, from left to right: mode I (opening), mode II (sliding), mode III (tearing)

### 3.5.3 Crack growth and Fracture Control in composite pressure vessel.

#### 3.5.3.1 Crack growth

Fracture Mechanics allows the analysis of crack propagation in terms of the energy release rate which is the elastic energy which is released when a crack grows divided by the increment of created area. The parameter $K_I$ and $K_{II}$ are called the stress intensity factor which is the crack

driving force and its critical value is a material property known as fracture toughness, which in turn, is the resistance force to crack extension [14] the interpretation of eq. (3.4.58). Suggests that crack extension is brittle solids is completely governed by the critical value of the stress-intensity factor defined by eq. (3.4.56).

In fact $K_I$, $K_{II}$ equation is applicable to a specimen containing other crack geometry subjected to a remotely applied tensile stress. Experimentally, the critical value of, $K_I$, $K_{II}$ known as fracture toughness, can be determined at a fracture stress when the crack length reaches a critical or maximum value prior to rapid crack growth . Thus $K_I \rightarrow K_{IC}$ and $\sigma \rightarrow \sigma s_f$ when $a \rightarrow a_c$. Given a loaded structure, the energy release rates (G) associated to each propagation mode (GI, GII, GIII) can be computed at the crack tip. The critical value of the energy release rate in a given mode (GIc, GIIc, GIIIc) is a property of the material or the adhesive. So, as a first try, a simple propagation criterion may be written:GI < GIc ; GII < GIIc; GIII < GIIIc

$$K_1 = Y\sigma\sqrt{\pi c} \quad \text{= mode 1 stress intensity factor} \qquad (3.4.56)$$

Constant depending on geometry/loading — Average stress (i.e. away from crack) — Crack size

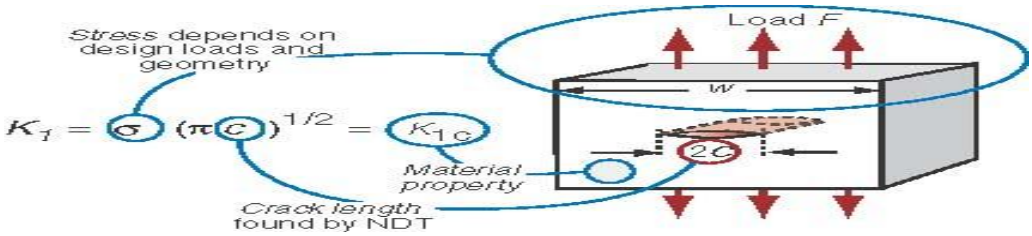


*Fig 23 crack length found by NDT*

### 3.5.3.2 Virtual crack closure technique

The propagation of a crack is possible when the energy released for unit width and length of fracture surface (named Strain Energy Release Rate, G) is equal to a threshold level or fracture toughness, characteristic for each material (Janssen et al., 2004).

According to the Virtual Crack Closure Technique, the evaluation of the Strain Energy Release Rate can be obtained starting from the assumption that for an infinitesimal crack opening, the strain energy released is equal to the amount of the work required to close the crack. Therefore, the work W required to close the crack can be evaluated by performing two analyses. The first analysis is needed to evaluate the stress field at the crack tip for a crack of length "a" and the second one is aimed to obtain displacements in the configuration with the crack front appropriately extended from a to a+Δa (Figure 24).

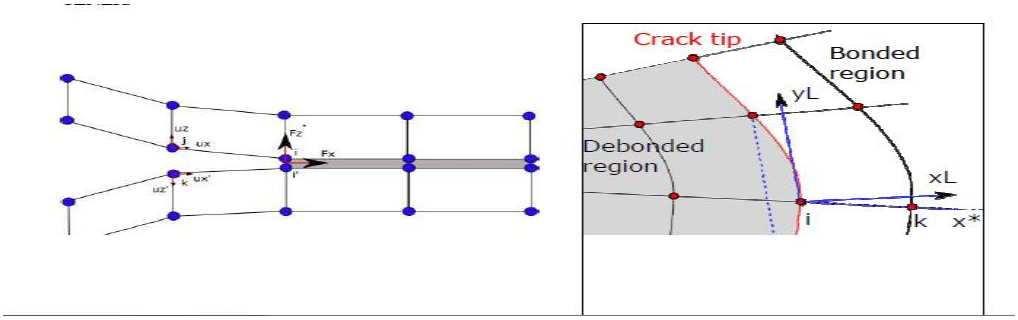


Fig 24 Two-steps virtual crack closure technique: schematization of the two configurations before (a) and after the crack extension (b)

### 3.5.3.3 Fracture Control

Structures usually have inherent flaws or cracks introduced during 1) welding process due to welds, embedded slag, holes, porosity, lack of fusion and 2) service due to fatigue, stress corrosion cracking (SCC), impact damage and shrinkage. A fracture-control practice is vital for design engineers in order to assure the integrity of particular structure. This assurance can be accomplished by a close control of Design constraints, Fabrication, General yielding, Maintenance, Nondestructive evaluation (NDE) and Environmental effects. The pertinent details for the above elements depend on codes and procedures that are required by a particular organization. However, the suitability of a structure to brittle fracture can be evaluated using the concept of fracture mechanics, which is the main subject in this section. For instance, the elapsed time for crack-initiation and crack-propagation determines the useful life of a structure, for which the combination of an existing crack size, applied stress, and loading rate may cause the stress intensity factor reach a critical value.

### 3.5.4 Fracture stress, principal stress, von mises stress and deflection inside cracked COPV.

Consider an orthotropic solid in a plain stress state. Plain strain deformation is not treated here. The coordinate x and y coincide with the principal axis 1 and 2 of the orthotropic material.

Principal stress on composite material and shear stress [7]

$$\sigma_1 = \sigma_x cos^2\theta \ , \quad \sigma_2 = \sigma_x sin^2\theta$$
$$\tau_{12} = \quad -\sigma_x cos\theta sin\theta \qquad (3.\ 4.57)$$

Von Mises Yielding Criterion

This criterion is deduced from the Maximum Distortion Energy Theory in which the state of stress is referred to as the principal stress directions and the principal stresses defined by the following common mathematical equations. [26]

$$(\sigma_1 - \sigma_2)^2 + (\sigma_3 - \sigma_2)^2 + (\sigma_3 - \sigma_1)^2 = 2\sigma^2{}_{ys} \qquad (3.\ 4.58)$$

$\sigma_1, \sigma_2,\ principal\ stress;\ \sigma_{ys}$ =Von Mises Yielding Criterion

Consider a Crack Running in the x direction, which coincides with the principal material axis 1. [24]

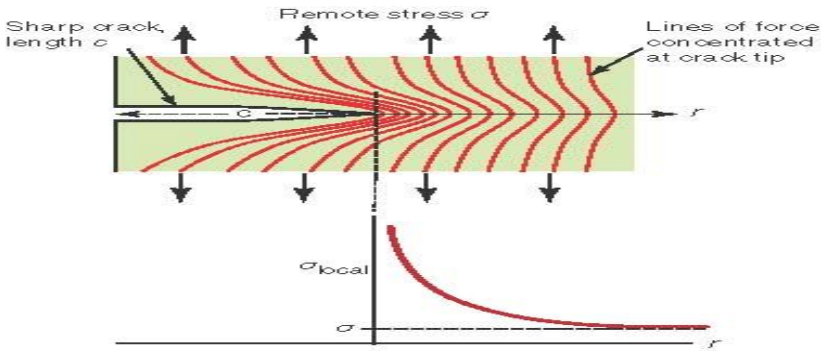


Fig 25 Lines of force in a cracked body under load

$$\sigma_{local} = \sigma\left(1 + Y\sqrt{\frac{\pi c}{2\pi r}}\right) \qquad (3.4.58)$$

Far from the crack where r >> c, the local stress fall s to the value of tip crack . Near the crack r << c, the local stress rises sharply as Fig 25. [26]

$$\sigma_f = \frac{kIC}{(\pi a)^{\frac{1}{2}} .Y} \tag{3.4.59}$$

Where: $K_{IC}$ = Fracture Material Toughness

Y = Shape Factor

$\sigma_f$ = fracture stress

c = a crack size

r = far distance from the crack tip.

$\sigma_{local}$ = Local stress around crack tip.

The model depends on the geometrical shape factor which is found the cracked composite pressure vessel. The shape factor depends on the following formula, [26].

$$Y = (1+\sqrt{2(1+\rho)})\lambda^{\frac{1}{4}}\{1.12 - 0.01(\rho - 1)\} \tag{3.4.60}$$

Where: - $\lambda = \frac{E2}{E1}$ , $\rho = \frac{(E2/E1)2}{2G12} - (\nu_{12} . \nu_{21})^{1/2}$

Deflection

By hooks law, the circumfrectal strain is related by hoop stress and young's modus (E). In turn, by strain displacement relations it can express hoop strain in terms of the radial displacement $u_x$ due to the maximum tangential stress along in the x axis [28]. By considering the bottom of pressure vessel along y axis degree of free dome is zero means the constraint on y axis. And the radial displacement of the junction between the cylinder and bottom remain zero and that the bottom plate is sufficiently flexible that the moment at the junction can be consider being zero.

$$u = \varepsilon_1 * d_m \tag{3.4.61}$$

Where: u = deflection along x axis

$d_m$ = mean diameter

### 3.5.5 A Chart of Fracture Toughness K1c and Yield Strength σy the Contours Show the Transition Crack Size, a or $C_{critor}$.

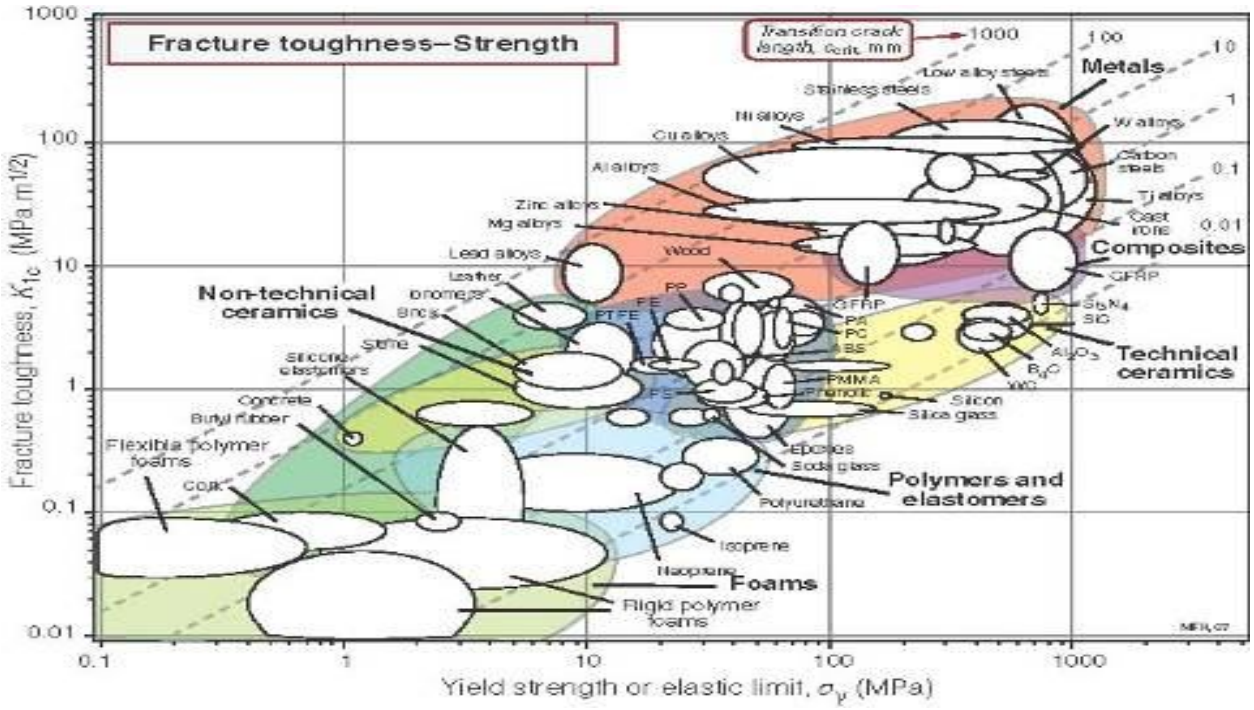


**Fig 26 A Chart of Fracture Toughness $K_{1c}$ and Yield Strength $\sigma_y$**

### 3.5.6 Chart of fracture toughness $K_{lc}$ and modulus E. Contours Show the toughness, $G_c$.

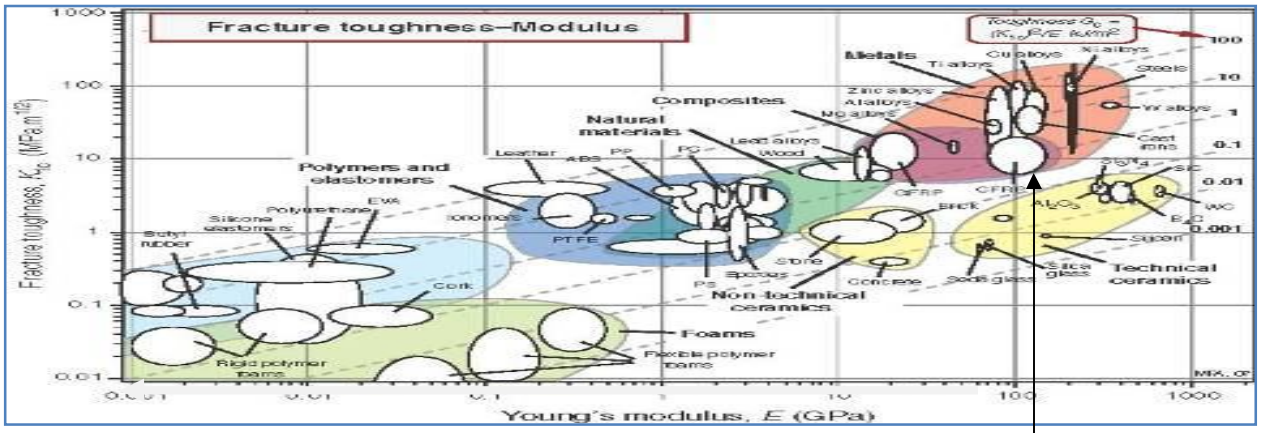


Fig 27 Chart of Fracture Toughness Klc and Modulus E

### 3.5.7 Mathematical model result

Table 5 mathematical result

| Description | Internal pressure | Crack a(mm) | $\sigma_{ys}$ (Mpa) | $\varepsilon_1$ | $K_{IC}$ | $\sigma_f$ mpa | $\sigma_h$ mpa | $\sigma_{hlocal}$ (Mpa) | $\sigma_a$ (Mpa) | $\frac{\sigma_f}{\sigma_{max}}$ | $u_x$ $10^{(-4)}$ (m) |
|---|---|---|---|---|---|---|---|---|---|---|---|
| Composite pressure vessel | 16mpa | 0.1 | 333.4 | 0.06e-2 | 35 | 1458 | 492 | 578 | 246 | 2.6 | 1.94 |
| | | 0.2 | 386.3 | 0.07e-2 | 35 | 1029 | 492 | 665 | 246 | 1.7 | 2.24 |
| | | 0.3 | 411 | 0.08e-2 | 35 | 833 | 492 | 706.3 | 246 | 1.36 | 2.5 |
| | | 0.4 | 432 | .081e-2 | 35 | 730 | 492 | 743 | 246 | 1.15 | 2.6 |
| | | 0.5 | 450 | .084e-2 | 35 | 700 | 492 | 775 | 246 | 1.08 | 2.7 |
| | | 0.6 | 468 | .088e-2 | 35 | 589 | 492 | 805.4 | 246 | 0.8 | 2.8 |

### 3.6. Crack Size in Composite Pressure Vessel by Fem Using ANSYS Version 16 Soft Ware

#### 3.6.1 Finite Element Models.

A 3D Finite Element model was created to simulate fracture test in ANSYS. Solving a fracture mechanics problem involves performing a linear elastic or elastic-plastic static analysis and then using specialized post processing commands or macros to calculate desired fracture parameters ansys manual book. In this section, we will concentrate on two main aspects of this procedure: Modeling the crack region and calculating surface crack parameters. The most important region in a fracture model is the region around the edge center of the crack. In linear elastic problems, it has been shown that the displacements near the crack tip (or crack front)

Vary as a, where "a" is the distance from the crack tip. The stresses and strains are singular at the crack tip, varying as $1/\sqrt{a}$. To pick up the singularity in the strain, the crack faces should be coincident, and the elements around the crack tip (or crack front) should be quadratic.

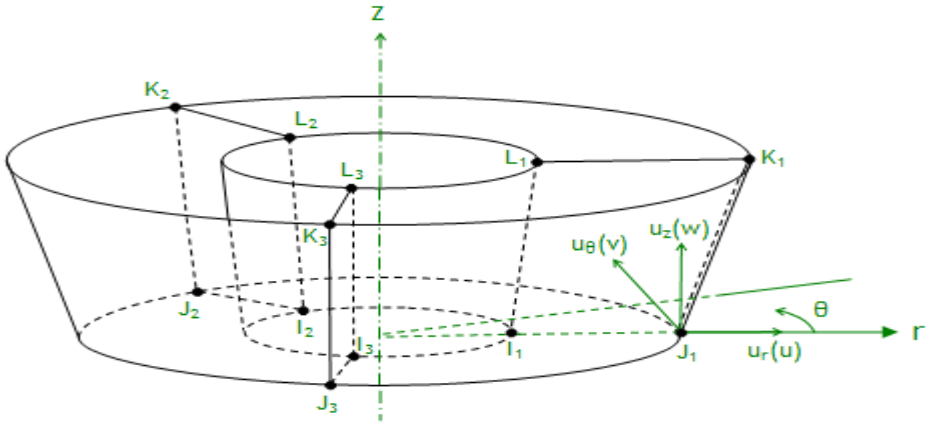


Fig 28 Tet 4 node Solid285 Layered Structure

Use Layered S **Solid285** solid to model layered solids. The layered section definition is given by ANSYS section (SECxxx) commands. A prism degeneration option is also available. After modeling the crack model as per the standard dimensions, a quarter point elements are created at the crack tip. Where, $x_o$ = Element x-axis and x = Element x-axis

In order to assess the accuracy of the analytical models developed by van miss. Fracture stress and the elastic stress field theory, finite element models for MODEL part and crack geometry have been created using ANSYS v16.

Table 6 Finite Element Model Geometries

| Length(mm) | Internal D(mm) | Lamina Thickness (mm) | Layers thickness (mm) | Composite layers | Crack size (mm) | Internal pressure (pa) |
|---|---|---|---|---|---|---|
| 1200 | 300 | 0.762 | 4.872 | six | 0.1-0.5 | 16e6 |

To see the effect of crack on actual composite pressure vessel it use full size and open head of pressure vessel model. Develop different crack size on at the inside surface of composite vessel. Boundary conditions can be enforced on the top and bottom side of vessel.

### 3.6.2 Geometry modeling and Steps FEM Ansys v16

#### I) Define element type

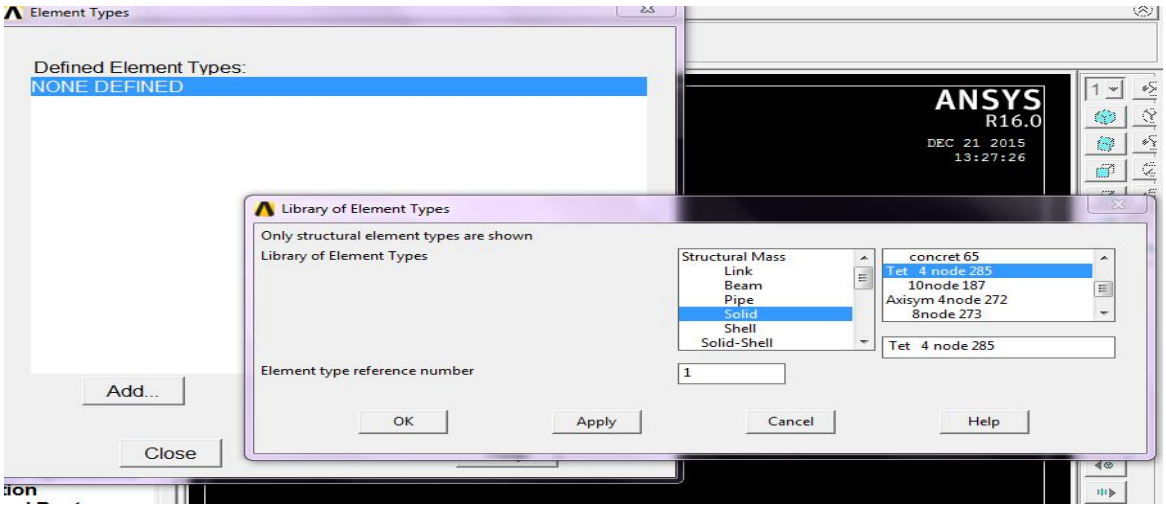


Fig 29 element type

## II) Material selection

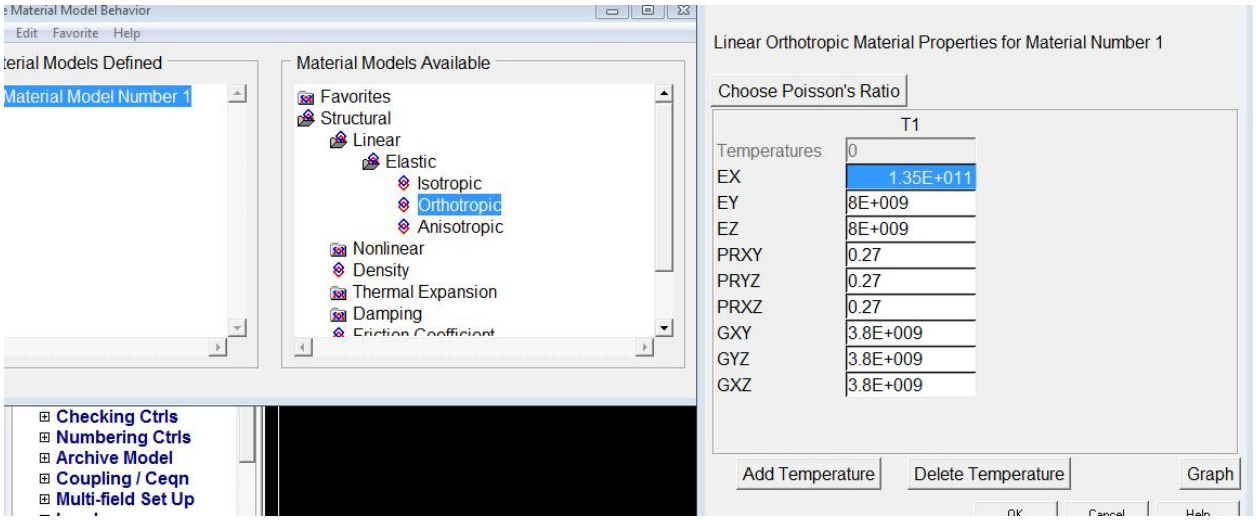


Fig 30 material type

## III) Section different layers at $55^0$ fiber orientatio

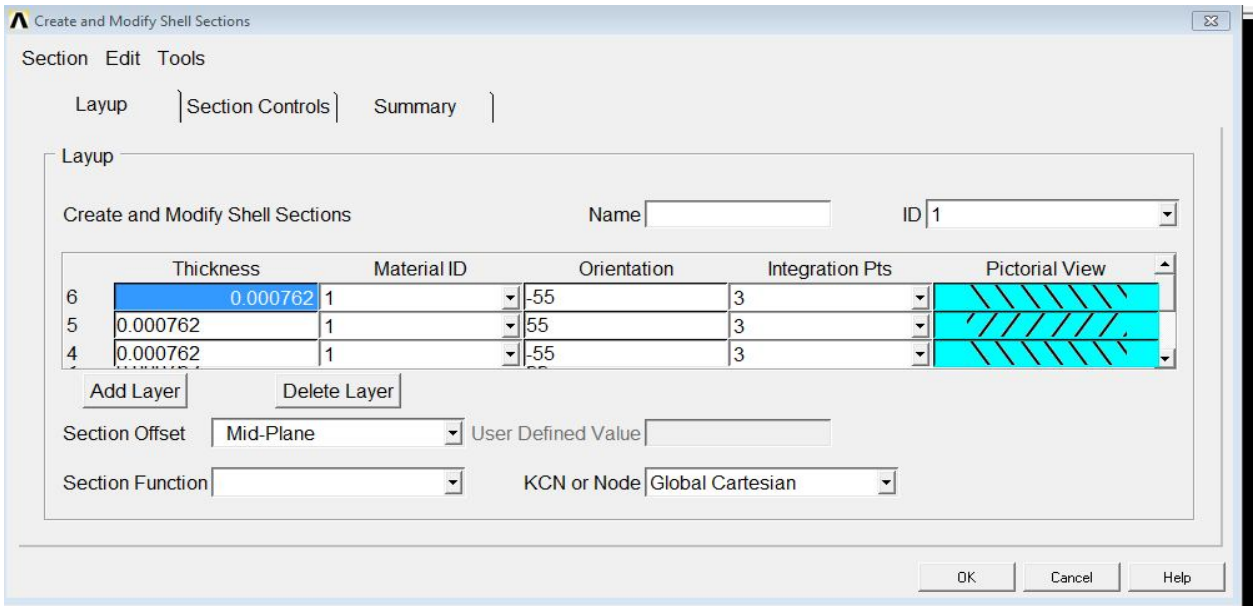


Fig 31 fiber orientation

Summary

| | | |
|---|---|---|
| Shell ID | = | 1 |
| Shell Name | = | |
| Total Thickness | = | 0.004572 |
| Number of Layers | = | 6 |
| Number of Section Pts | = | 18 |
| Section Offset Information | = | Mid-Plane |
| Laminate Density | = | 1570.000000 |

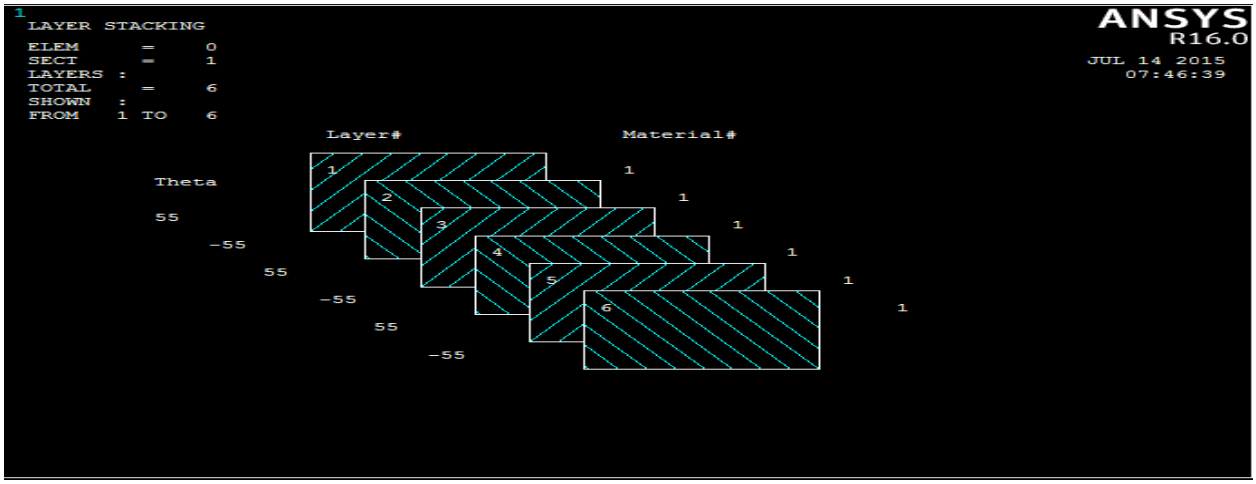


**Fig 32 Symmetrical stacking sequence fiber orientation out put**

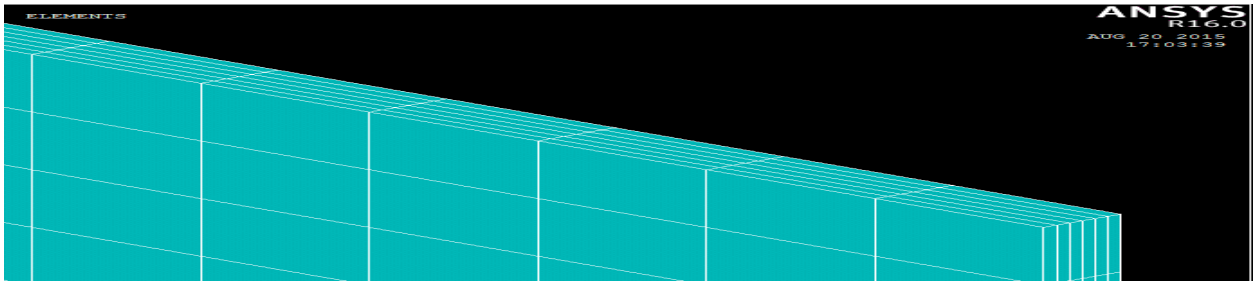


Fig 33 Six layers arranged composite

### Iv) Finite Element Modeling (Mesh Generation)

In this step, previously defined geometric models in ANSYS software is further defined by meshed finite elements and nodes. Thus, the geometric model with finite element will simulate the physical components in more suitable form as well it will be More preferable to obtain

approximate results to the exact result of the solution from the analysis. To get more near value Ansys result from experimental result use fine element edge length and element division as table below.

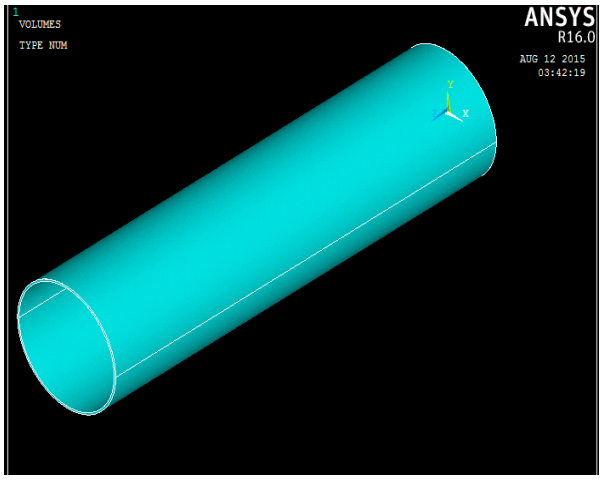


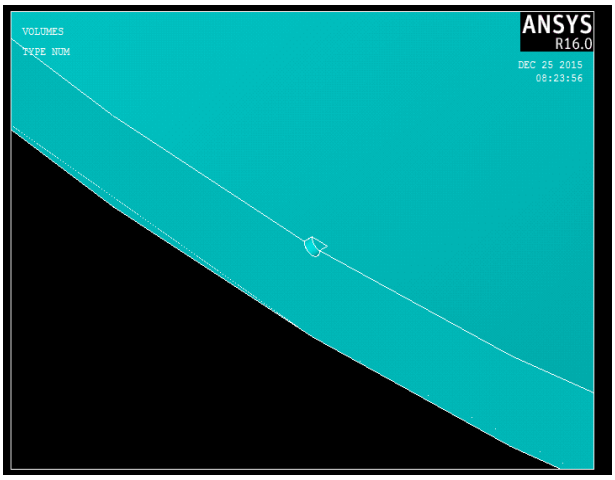


Fig 34 Geometric model without meshing

Fig 35 Geometric model and Enlarge crack size

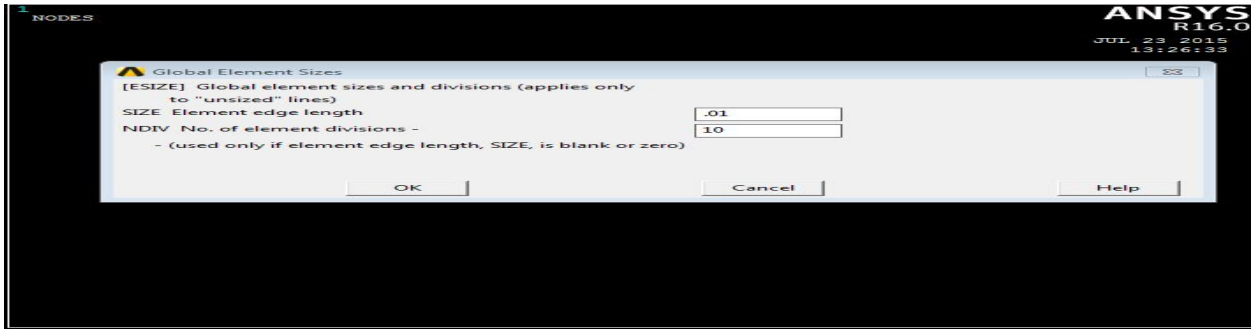


Fig 36 Discrtzination of geometric model with finite elements

Density of the generated meshes is controlled at global and at local level. A default option “smart sizing” for specifying element sizes at global level is applied. And for the benefit of keeping singularities at crack tip “key point sizing” for concentrating the middle nodes of element around crack tip are specified to shift to corner nodes.

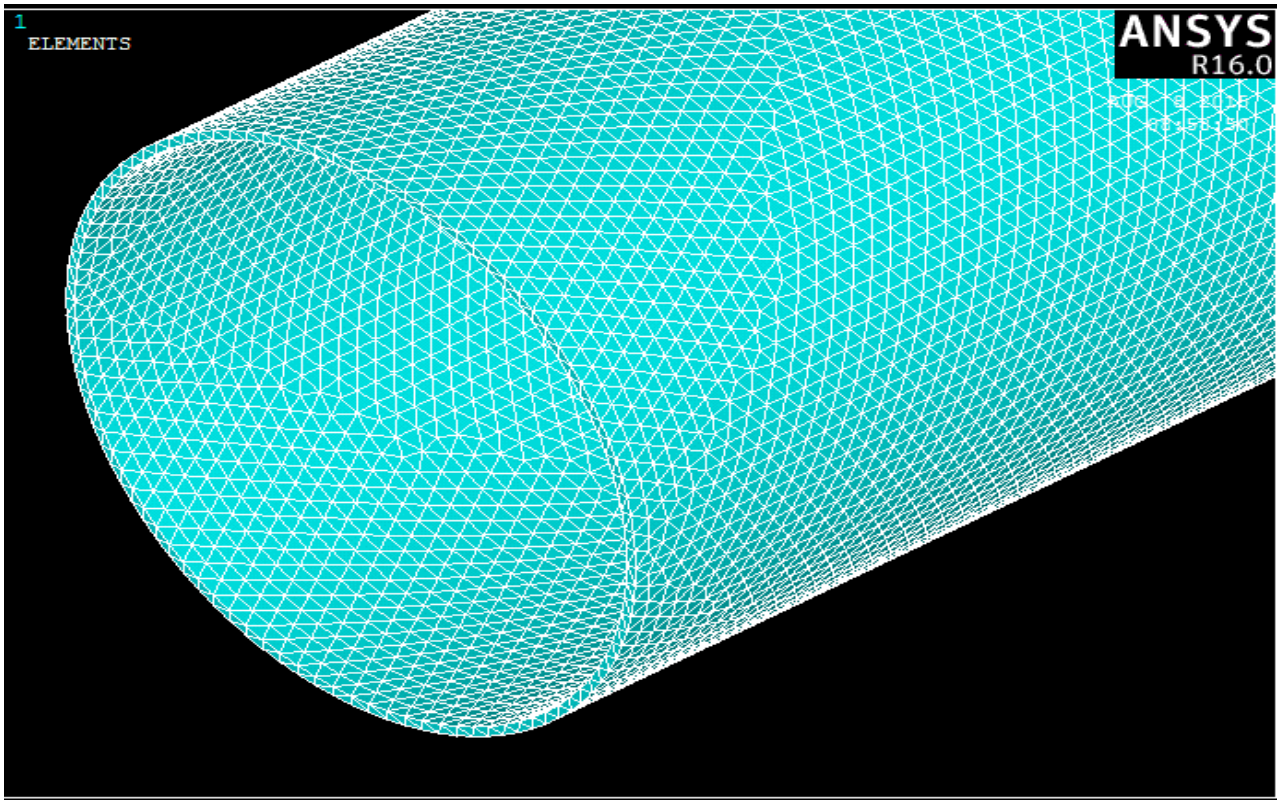


Fig 37 Meshing Composite over warped pressure vessel without crack

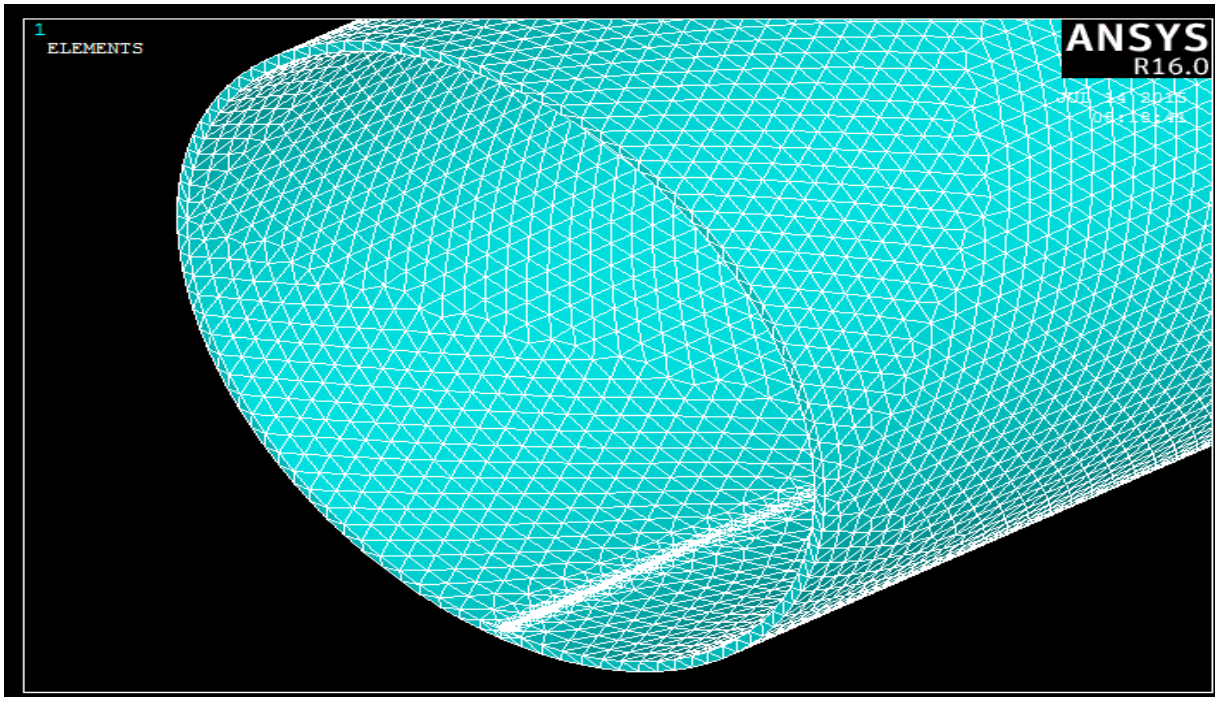


Fig 38 Discritization of geometric model with crack size

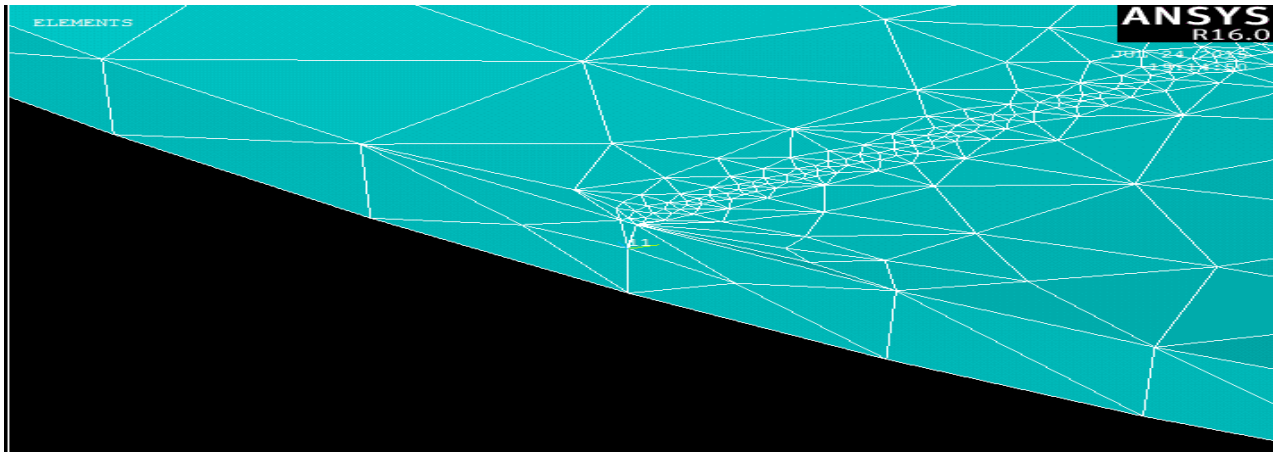


Fig 39 Distribution of elements at crack surface by finite element method

## V) Apply Loads

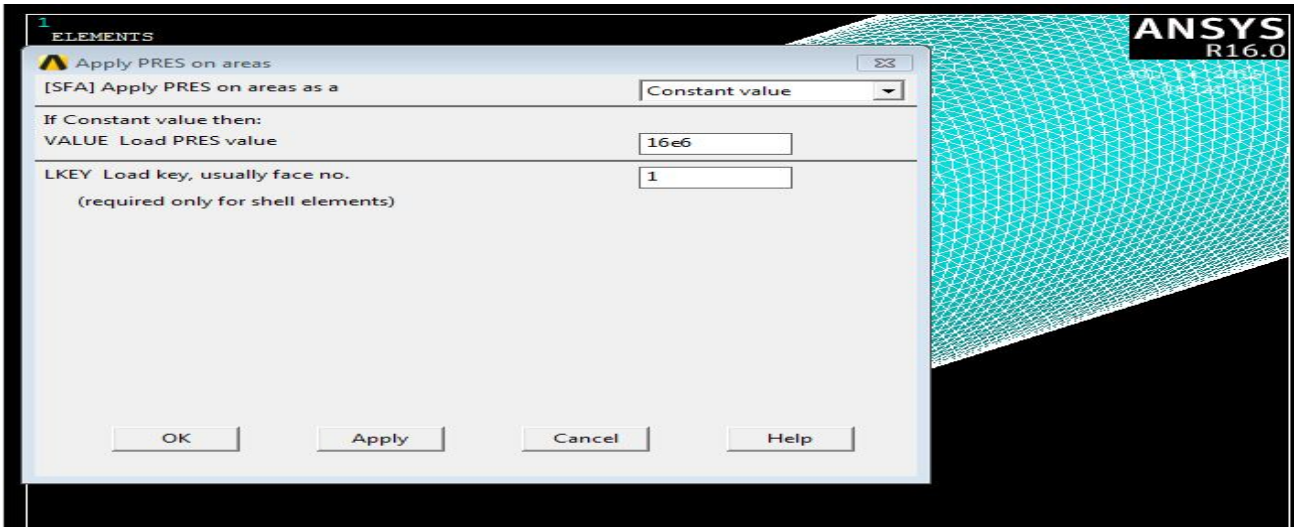


In this step, essential and boundary conditions are specified. Where, the loads are applied at the inner surface of the "copv" and also fix all degree of free dome on both side of end of top and bottom open end surface make zero displacement on x, y , z axis. And apply on inner surface of pressure vessel as shown in fig below.

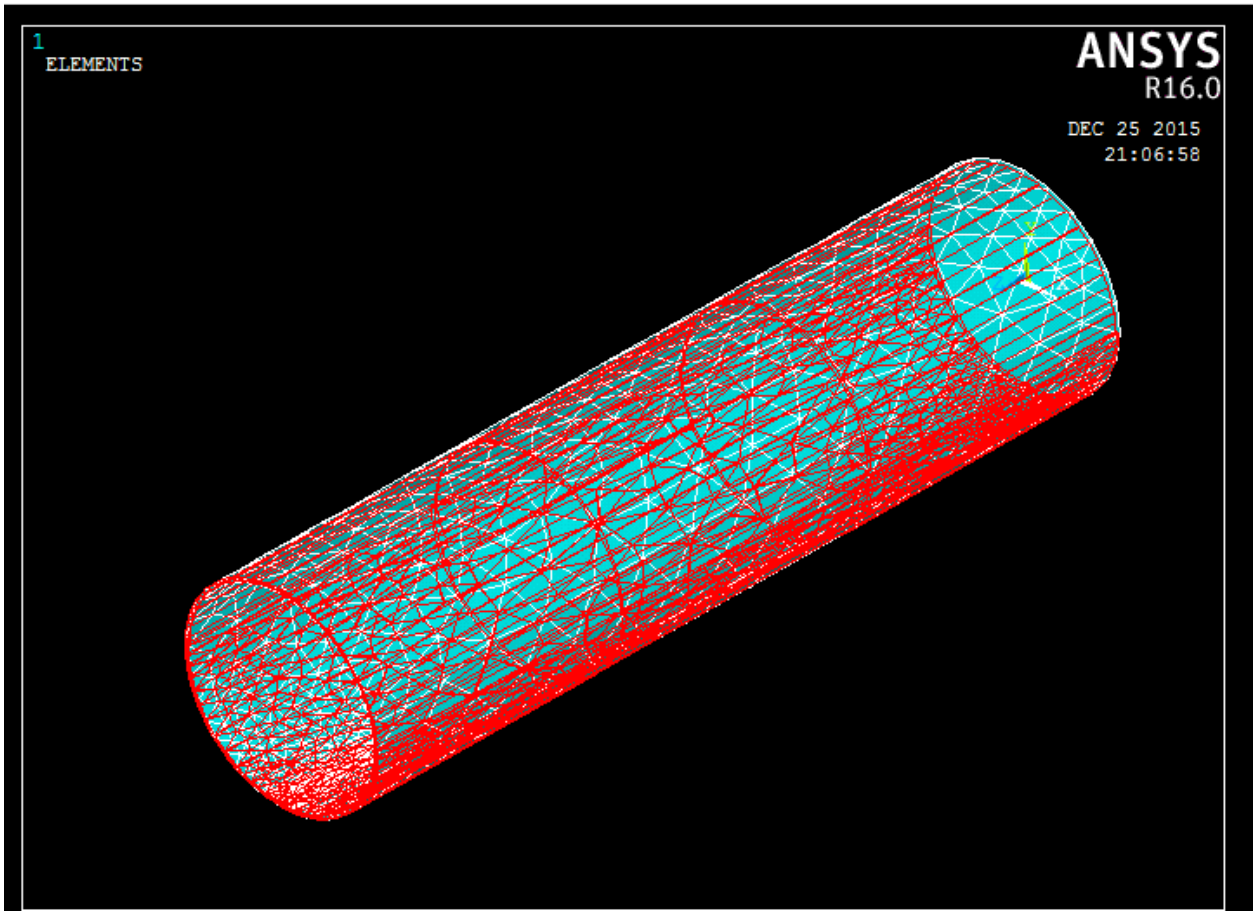


Fig 40 Applied loads

**VI. Defined Analysis Solution Options**

At this step, Analysis types are selected in terms of expected result that could characterize the components from either the components exposed to damage (cracked) or not. Among from few analysis options provided in the finite element analysis software ANSYS, a static analysis are carried out taking into consideration the objective of this thesis. For the solution consider different crack size from 0.1mm up to 0.5mm. And, it analysis different stress value which is related the given developed crack size. The value of stresses are related to the manually mathematical model and experimental result with a given orientation fiber angel. The other thing is the Ansys analysis with the given crack there is a maximum stress concentration created. These stress leads to energy realize to the material structure.

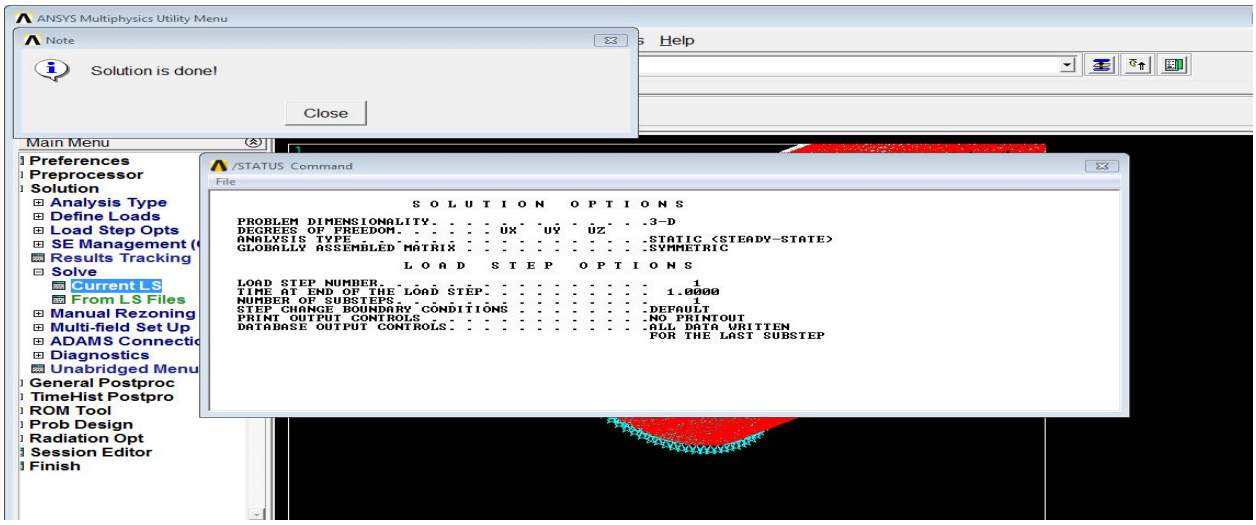


Fig 41 Analysis Solution

## VII. Ansys software Result

Solve the model using the linear static solver options in ANSYS. Then proceed to Post Processing, plot result and make sure the deformed shape is correct (see Fig 41). It will list the stress at this point. The result at the tip of or crack area and observe the maximum stress develop and put as graph in various color. The red color is shows maximum stress occurs. Develop five crack size in composite pressure vessel observe the result in various condition.

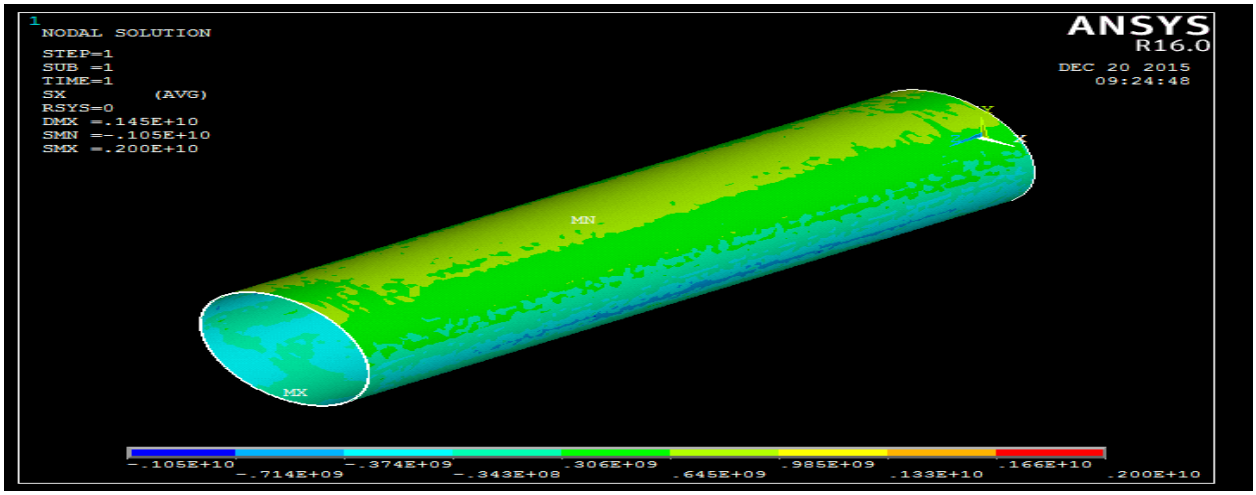


Fig 42 Stress along x axis for crack size 0.0001m

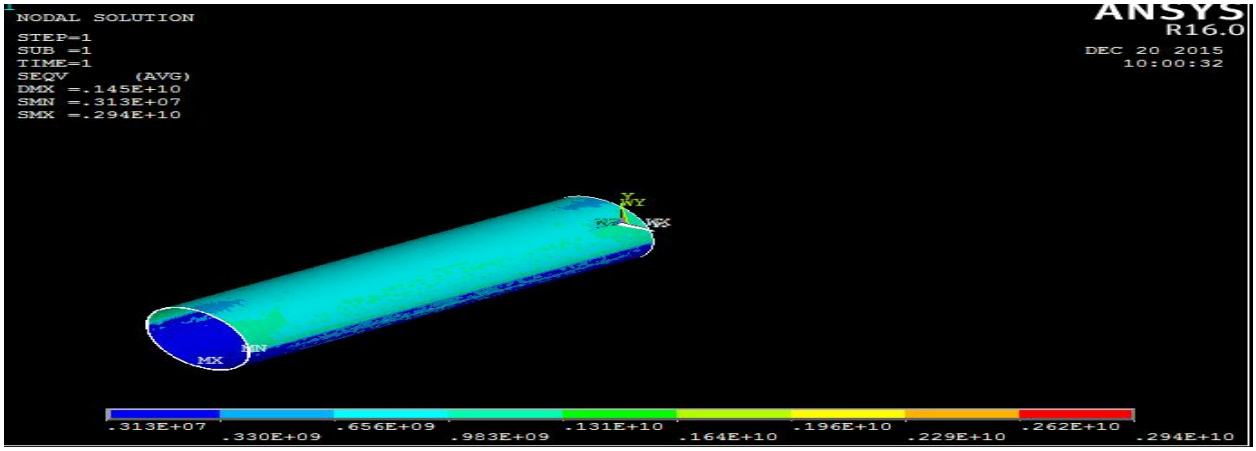


**Fig 43 von mises stress for crack Size 0.0001m**

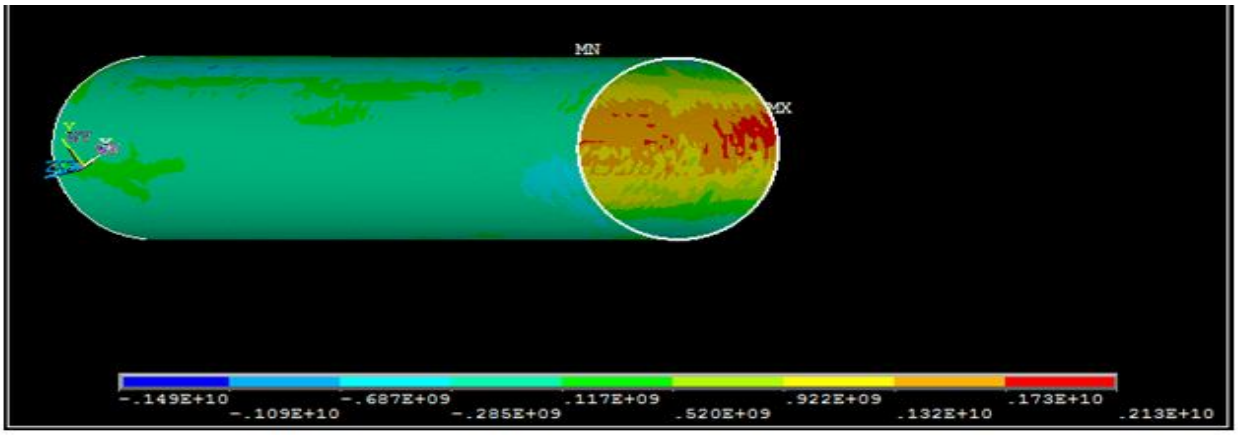


Fig 44 Stress along x axis for crack size 0.0002m

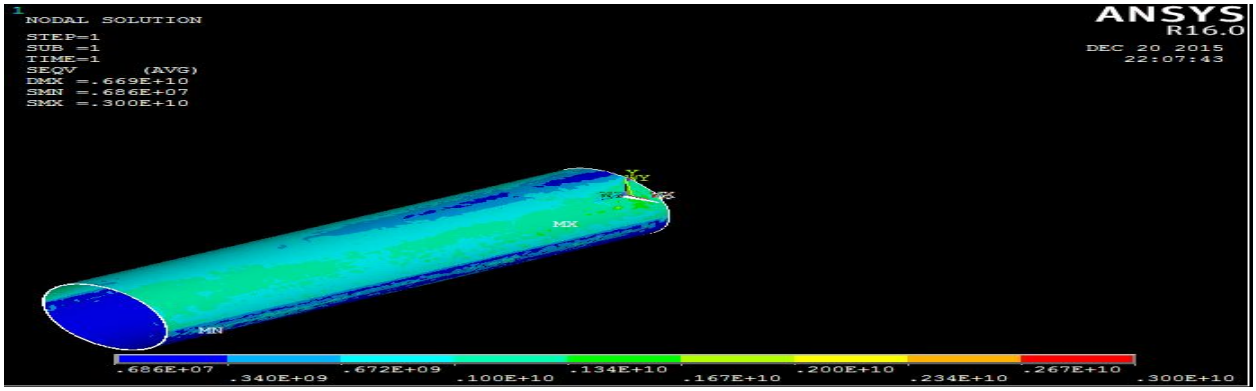


Fig 45 von mises stress along for crack size 0.0002m

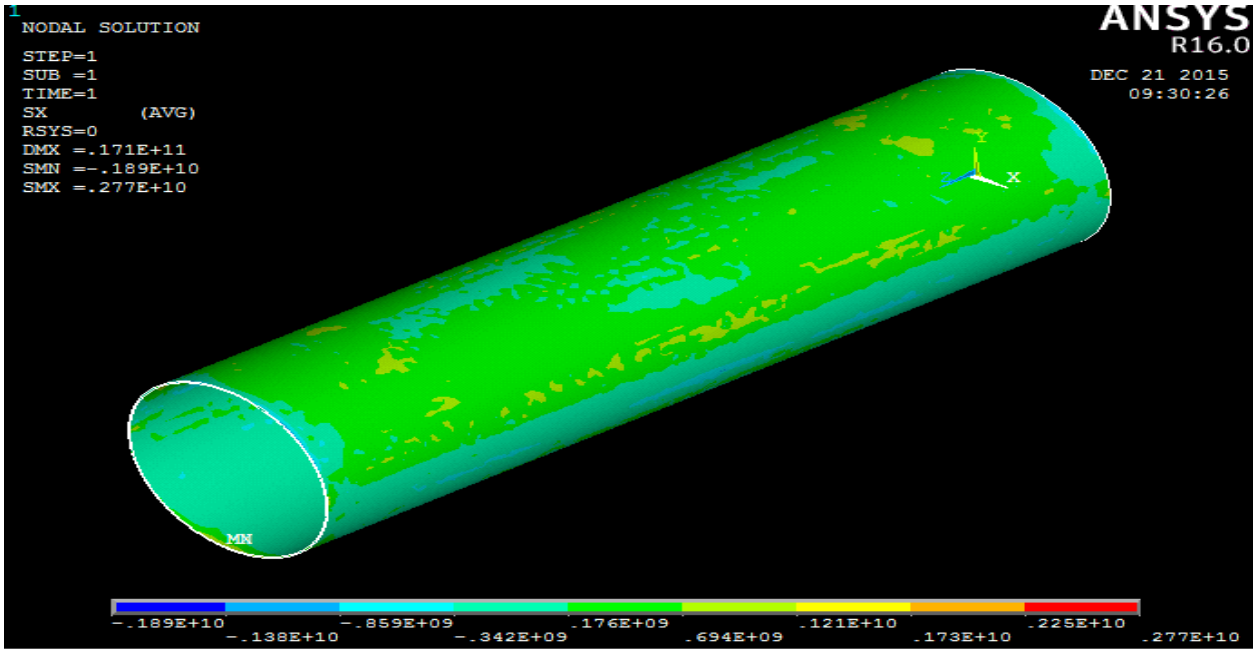


Fig 46 Stress along x axis for crack size 0.0003m

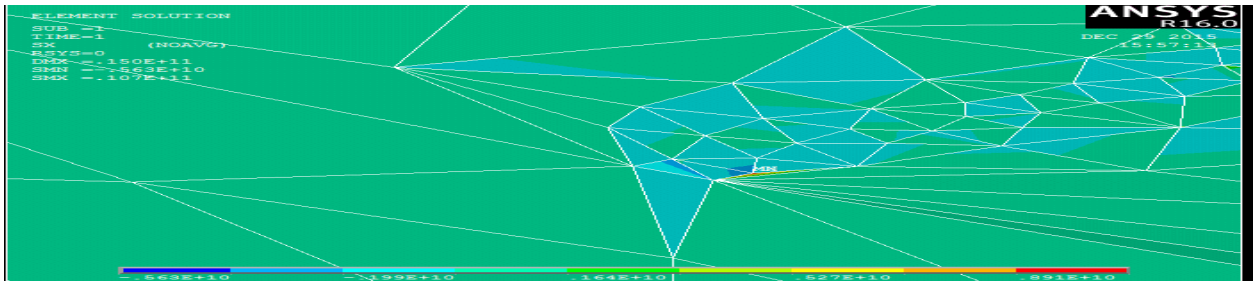


Fig 47 Stress along x axis for crack size 0.0003m

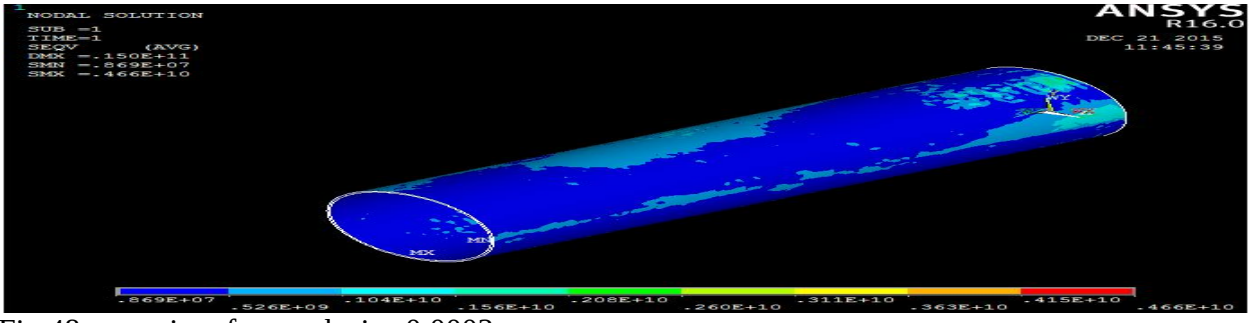


Fig 48 von mises for crack size 0.0003m

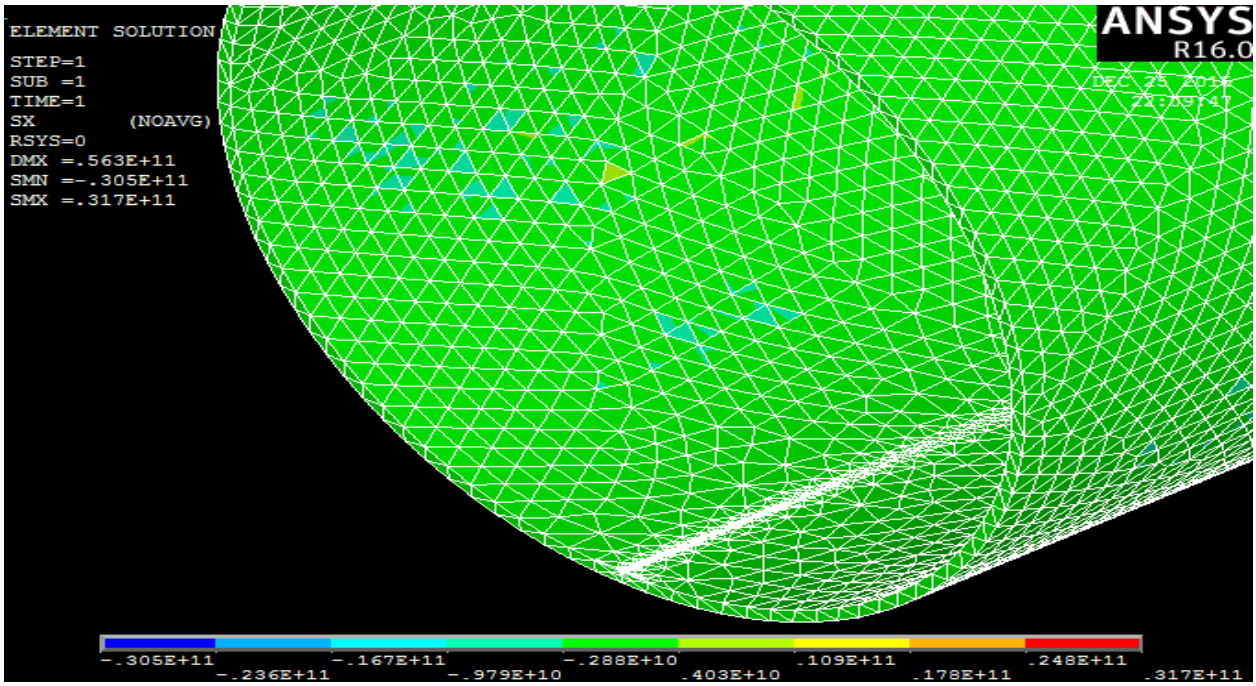


**Fig 49 Stress along x axis for crack size 0.0004m**

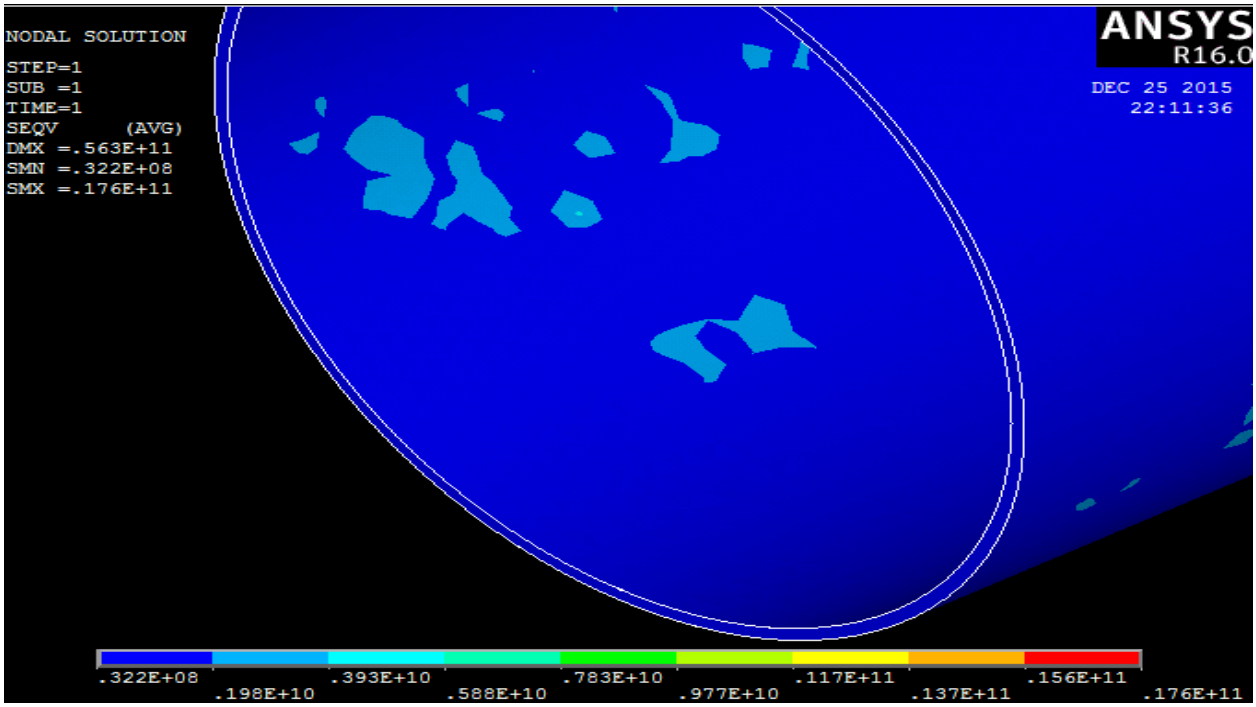


Fig 50 von mises for crack size 0.0004m

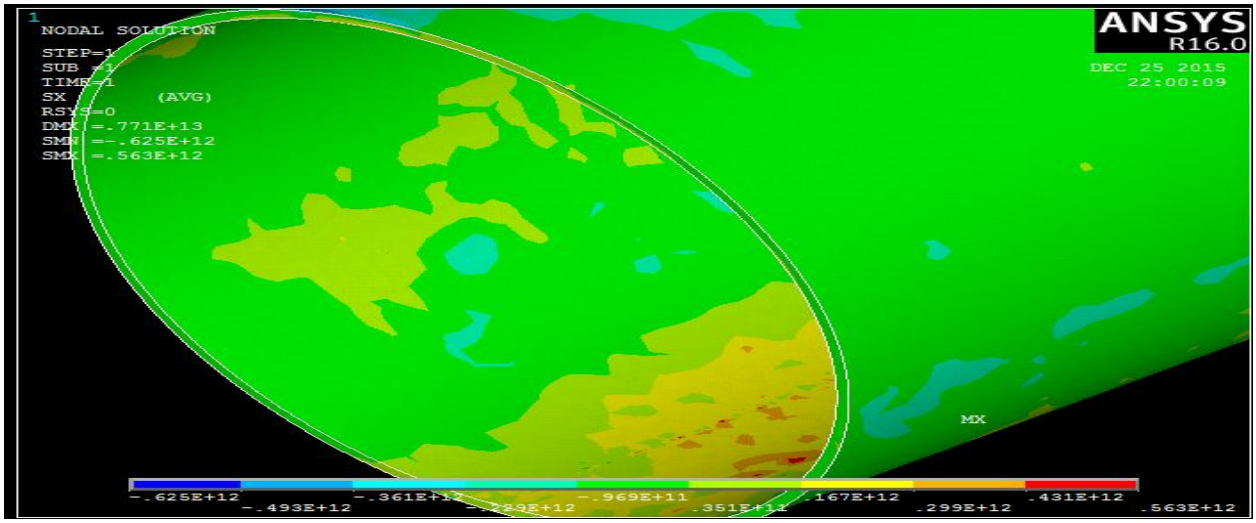


Fig 51 Stress along x axis for crack size 0.0005m

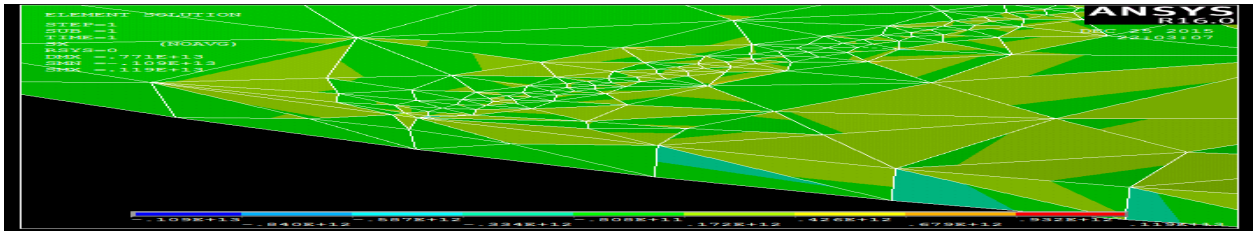


Fig 51 Stress along x axis for crack size 0.0005m.

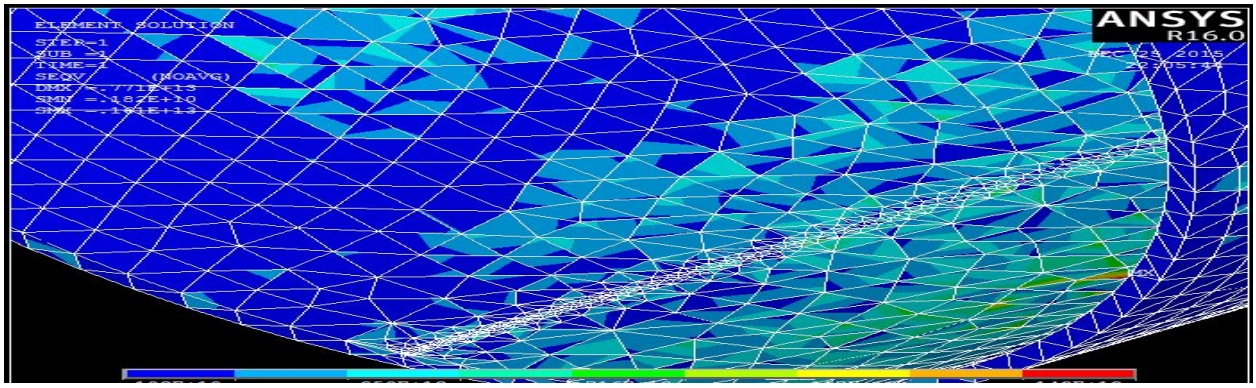


Fig 52 von mises for crack size 0.0005m

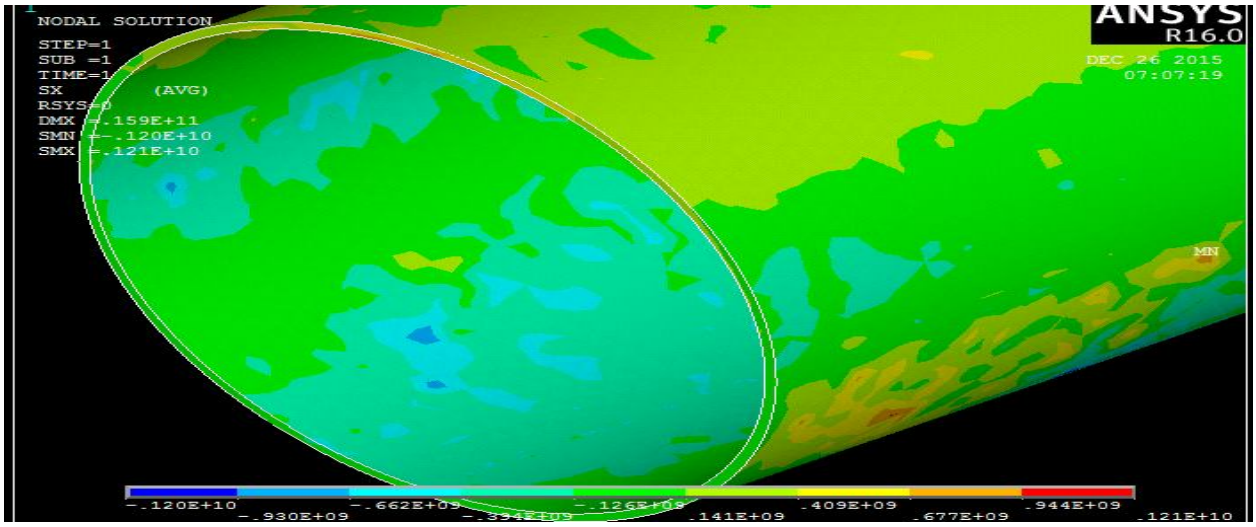


Fig 53 Stress along x axis for crack size 0.0006m

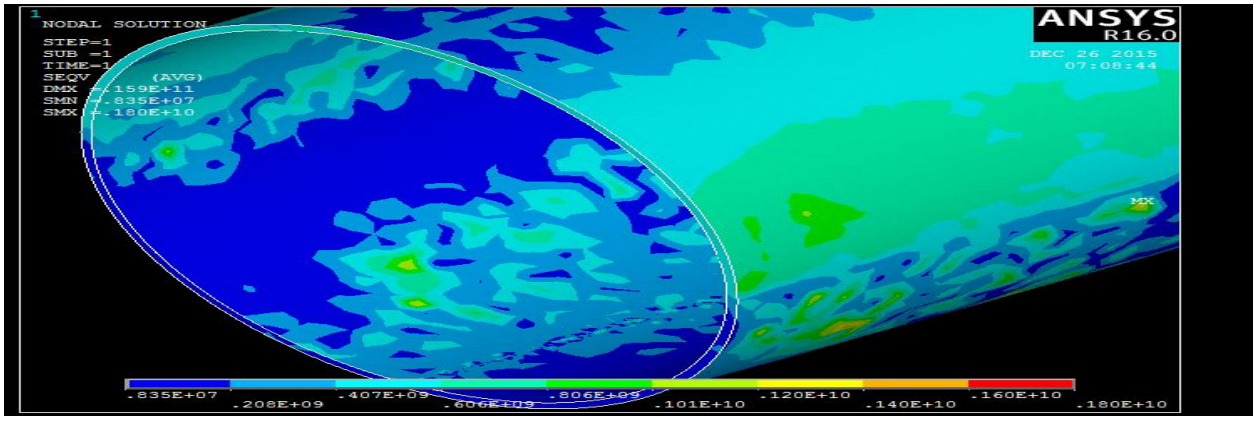


Fig 54 von mises for crack size 0.0006m

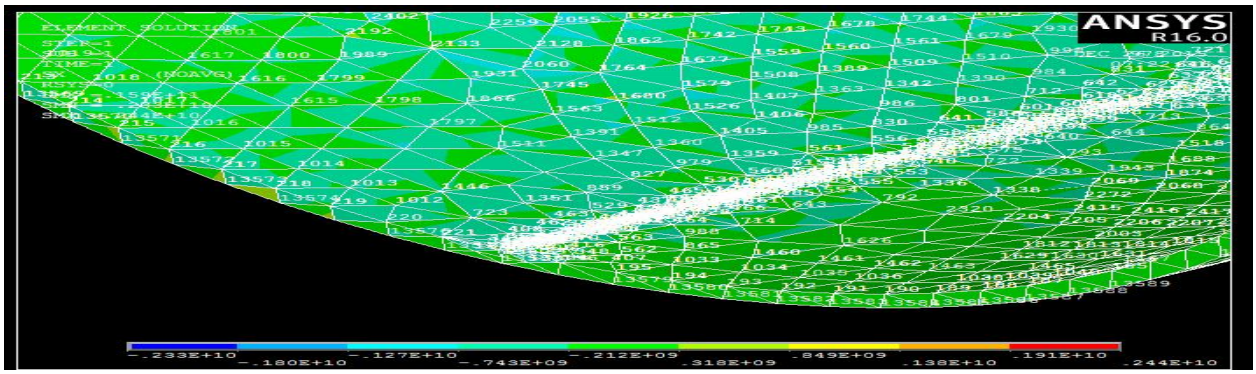


Fig 54 Element and node number distribution


Fig 54 Node and node number distribution

**Ansys soft ware results is summarized as follows**

Table 7 Ansys result

| Describ-tion | Crack a(mm) | $K_{Ic}$ | p | $\sigma_f$ | $\sigma_{avg\ max}$ | $u_x$ $10^{-4}$ (m) | $\varepsilon_1$ ($10^{-2}$) | $\boldsymbol{\sigma_{ys}}$ (mpa) | $\frac{\sigma_f}{\sigma max}$ |
|---|---|---|---|---|---|---|---|---|---|
| Composite pressure vessel | 0.1 | 35 | 16(mpa) | 1458 | 560 | 1.5 | 0.07 | 370 | 2.56 |
| | 0.2 | | | 1029 | 700 | 4.1 | 0.05 | 400 | 1.65 |
| | 0.3 | | | 833 | 725 | 1.8 | 0.19 | 417.8 | 1,14 |
| | 0.4 | | | 730 | 729 | 3.3 | 0.2 | 451 | 0.96 |
| | 0.5 | | | 700 | 790 | 1.54 | 0.29 | 460 | 0.89 |
| | 0.6 | | | 625 | 800 | 1.58 | 0.41 | 461 | 0.46 |

# CHAPTER FOUR

# RESULTS AND DISCUSSION

In chapter three, steps and input parameters that are used in the analysis of composite over warped pressure vessel. Identify and give a condition that is satisfies full assumption value with susceptible crack area. And thoroughly I have seen mechanical behavior of composite material related to pressure vessel and relationship between fiber winding angel and its orientation according to the maximum pressure service. In this portion I have seen on mathematical model and engineering software with related to the given parameter. And the analysis of mathematical model and engineering software are shown in the following result. It put the result in terms of numerical value and graphs. The results are given with the given developed crack size and its effect.

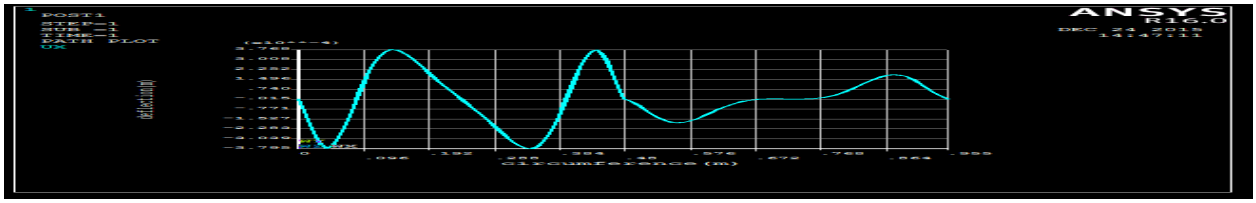


Fig 55 Displacement along x axis "$u_x$" versus circumference for crack size 0.0001m

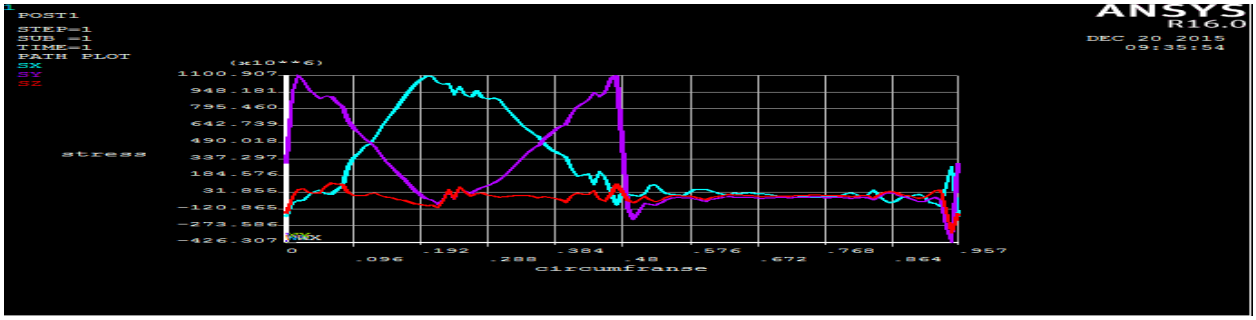


Fig 56 stress versus circumference along x,y,z axis for crack size 0.0001m

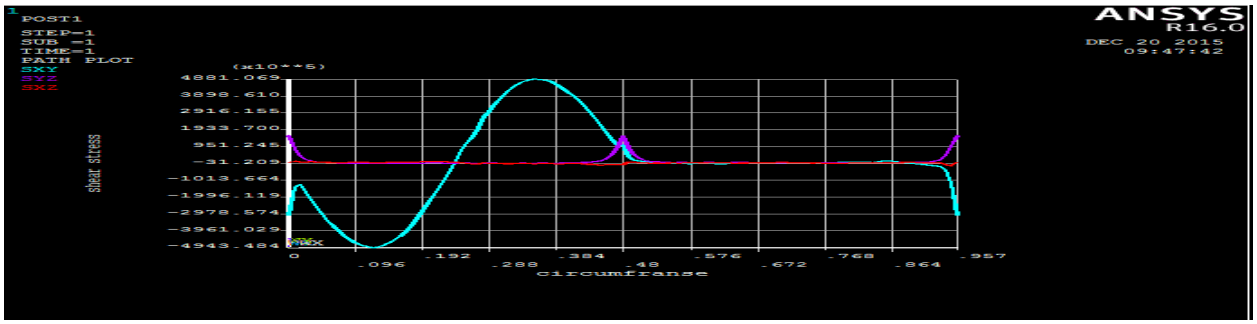


Fig 57 Shear stress along the circumference in composite pressure vessel 0.0001m.

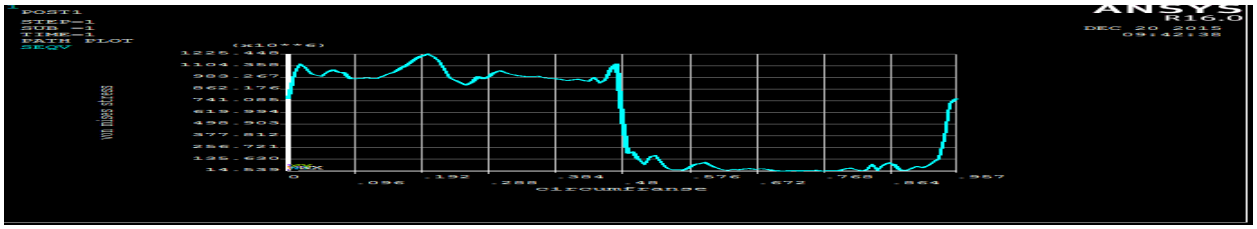


Fig 58 von mises versus circumference in composite pressure vessel for crack size 0.0001m

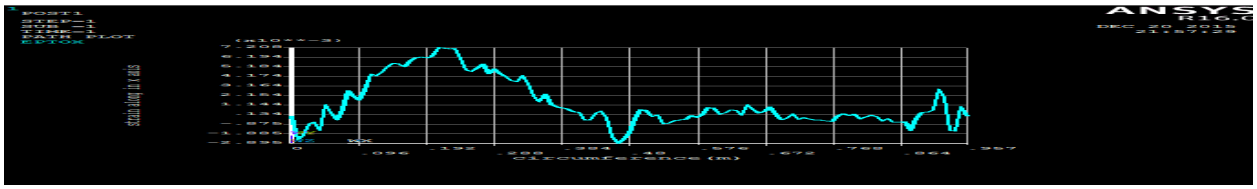


Fig 59 strain versus circumference along x axis for crack size 0.0001m

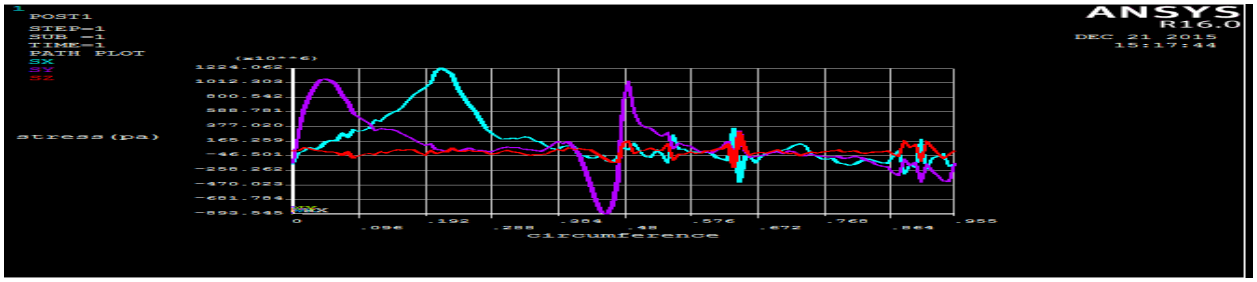


Fig 60 stress versus circumference in the composite pressure vessel for crack size 0.0005m.

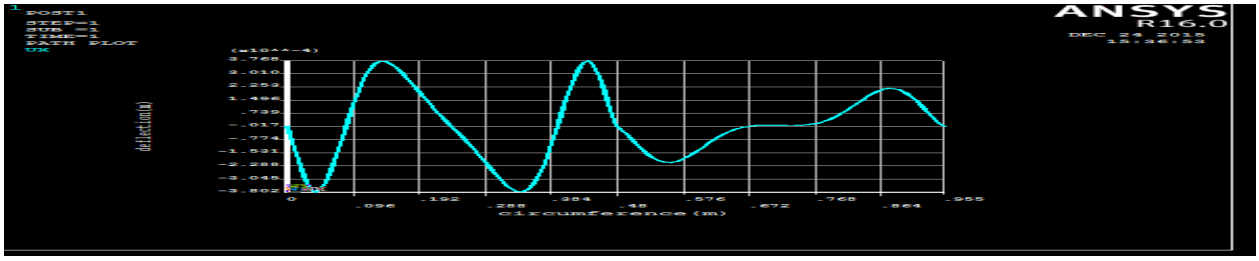


Fig 61 Displacement along x axis "$u_x$" versus circumference for crack size 0.0005m

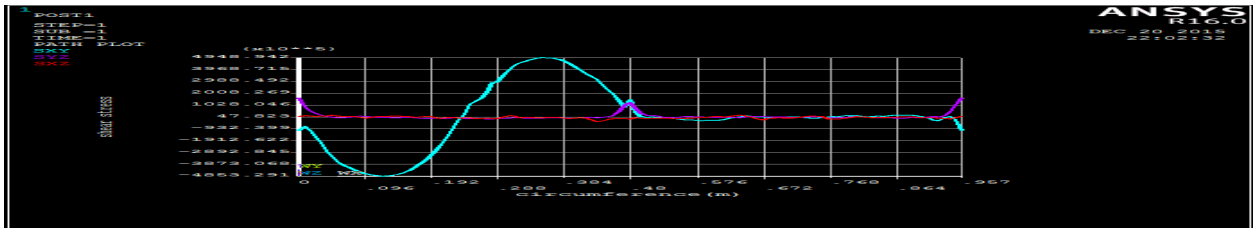


Fig 63 shear stress versus circumference in the composite pressure vessel for rack size 0.0005m.

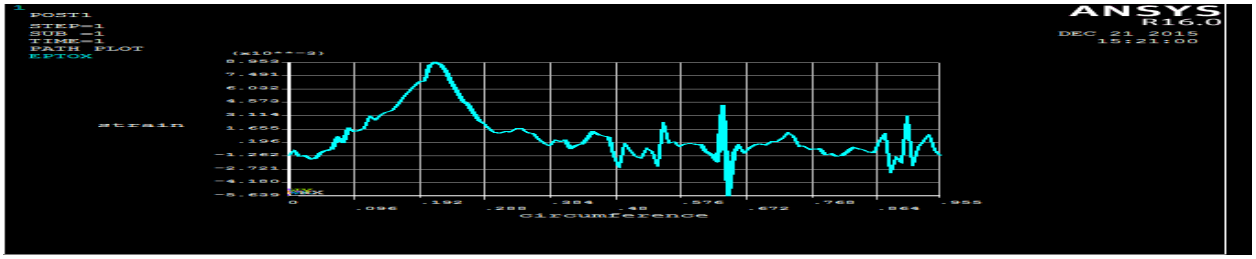


Fig 64 strain versus circumference along x axis for crack size 0.0005m

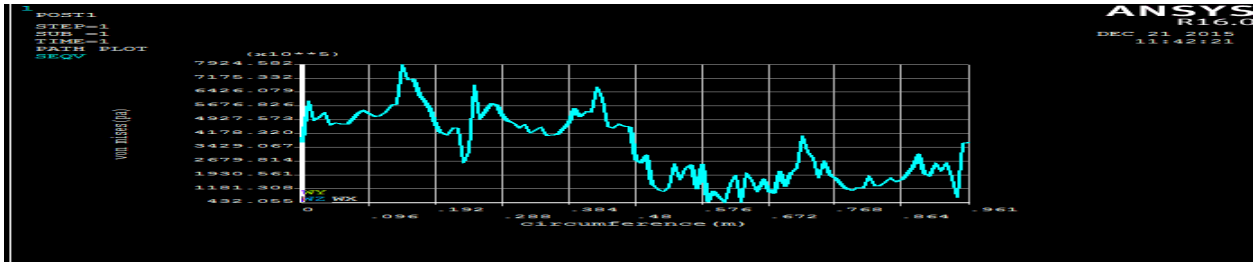


Fig 65 von misses stress versus circumference for crack size 0.0005m.

The developed surface crack is found around circumference of the “copv” and located a specific area which is clock wise direction at pi/2 times radius of the cylinder or it located around counter clock wise direction at 1.5pi times radius of the cylinder. Those points which surface crack is formed will be creating maximum stress and maximum deflection. As the graph shows that along the circumference of the “copv” at point 0.14m, there will be maximum stress and displacement. As it change different crack size in “copv” there will be different value of stress distribution and displacement along with a given x,y,z, axis. And the stress distribution through the circumference is increase as increasing the crack size from lower to higher value respectively. Due to the maximum hoop stress tangential in the direction of x axis there will be maximum average stress distribution along x axis and its deflection. From the experimental result done burn of test [27] fracture stress in different surface crack size, clearly show that effect of surface crack on stress distribution in “copv. The purpose of experimental result is to compare the analysis of stress distribution due to developed surface crack on mathematical result and FEM.

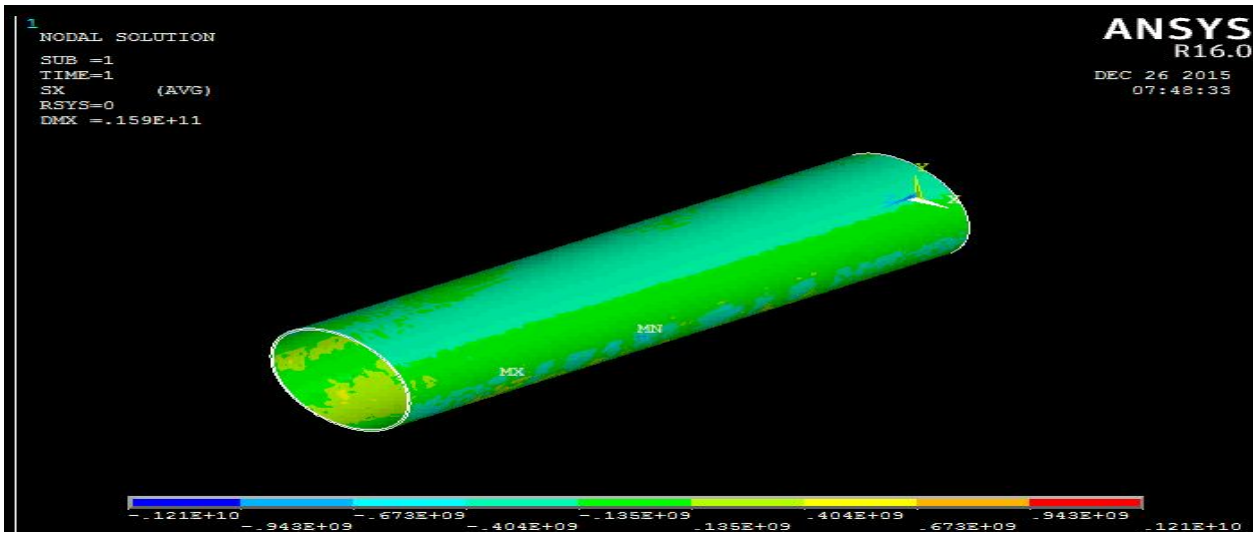


**Fig 66 Stress Distribution Along X Axis Animation**

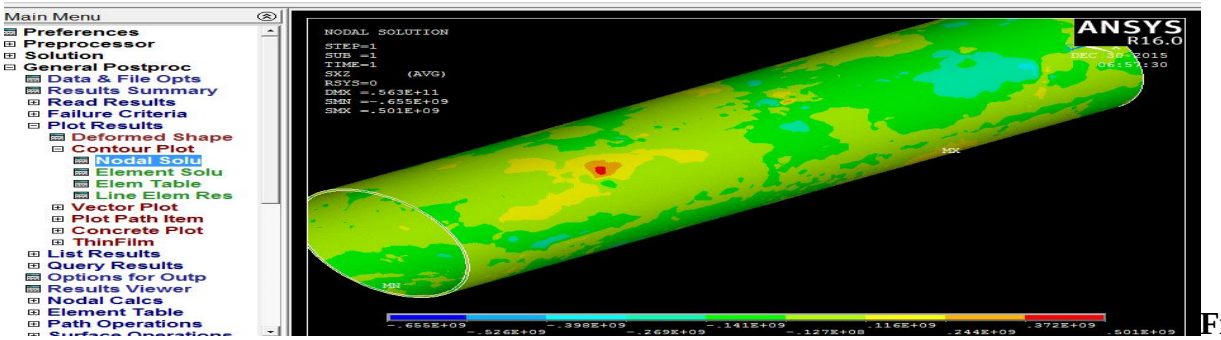


**Fig 67 Shear Stress Distribution along Xz Plain Axis Animation**

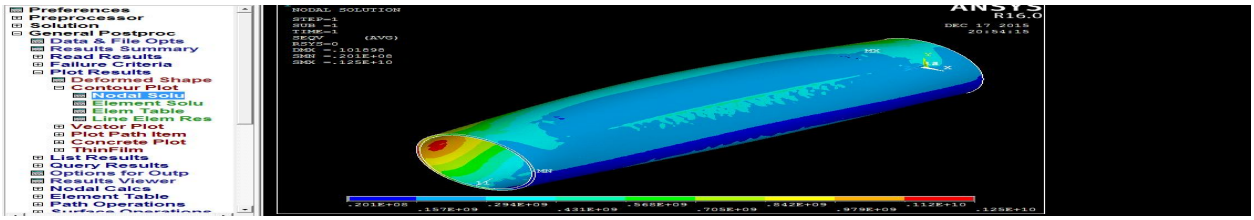


**fig 68 van miss stress distribution along xz plain axis animation**

### 4.1 comparing result of mathematical modeling, Ansys modeling and experimental

#### 4.1.1 Strength of filament wound In Composite Pressure Vessel with Surface Crack

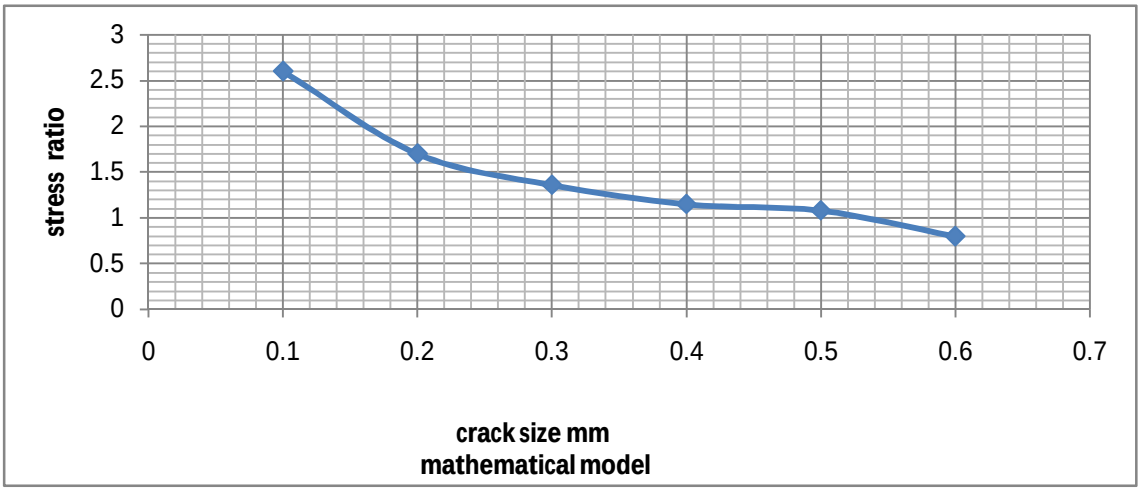


Fig 69 The Mathematical values of the fracture strength have been Normalized by maximum fracture strength vs crack size

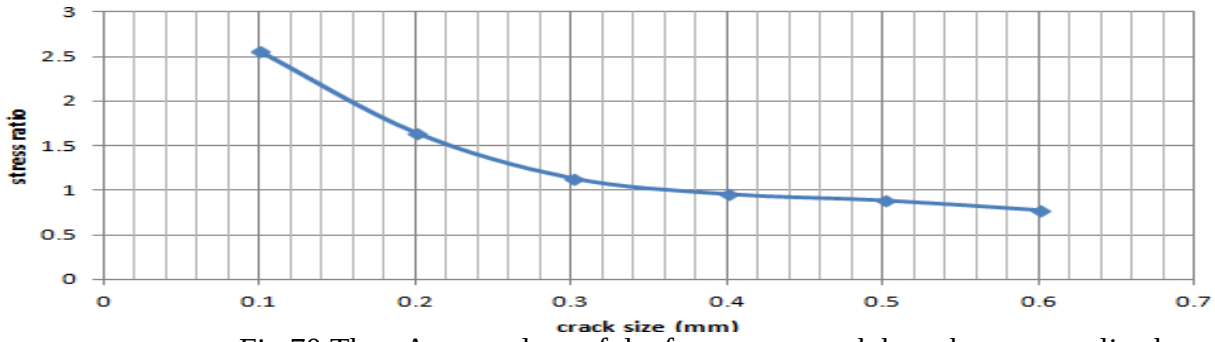


Fig 70 The Ansys values of the fracture strength have been normalize by Maximum fracture strength vs crack size.

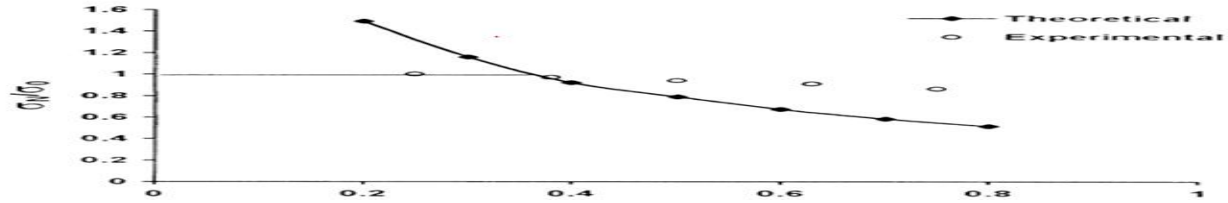


Fig 71 the experimental values of the fracture strength have been normalized by maximum fracture strength vs crack size for $55^0$ fiber orientation.

# CHAPTER FIVE

## CONCLUSION, RECOMMENDATION AND FUTURE DIRECTION

### 5.1. Conclusion

In this thesis, the main objective is to find parameters that can be used for analyzing stress and deflection on a cracked composite overwrapped pressure vessel. The parameters are determining weather the composite overwrapped pressure vessel under crack tolerable value or not.

This research first focused on mathematical and numerical relation which, represent the governing equation of composite material winding on in a pressure vessel. For modeling different crack size in the composite overwrapped pressure vessel fracture theories applied. Previously, they were studied maximum pressure cheeked without the presence of crack in composite overwrapped pressure vessel. And, they observe that the composite overwrapped pressure vessel is not burst with a given value of maximum pressure "16Mpa". But, here considering crack develops inside in a composite overwrapped pressure vessel and simulate the effect of stress and deflection in its strength.

Mathematical model and finite element analysis "ANSYS" software model vs16 is used for analysis on geometric model that simulate physical situation of composite overwrapped pressure vessel with different crack size. And, also taking experimental result what has been found literatures. The results which I got from those relations are related but, there is slight error.

From the theory what we have seen before, fracture stress is related to the average maximum stress developed around crack area. Means, if fracture stress less than average maximum stress the developed and propagate crack size will be near to critical crack size. These phenomena will be starting crack propagate at the surface.

From the existing situation I took different crack size starting from 0.1mm up to 0.6mm and relate stress fracture to average stress at each crack size and it is safe up to 0.5mm. In addition, as the surface crack size increase, there will be a variation of deflection or displacement. Because, from the above 0.5mm, there will be stress fracture is less than average maximum stress ($\sigma_f < \sigma_m$) Therefore, from the result it concludes that at crack 0.5mm there will be a beginning of surface crack propagation.

Finally in this method design is based on the modeling of crack sizes in Carbone fiber, rather than use on allowable stress as is often currently used. The method has the advantage of more accuracy. Offering greater certainty in design, it showed how crack size design fits within the more general framework of limit state design.

### 5.2. Recommendation

Now days the Finite element method is widely used for mechanical analysis. Using FEM for internal pressure of vessel develops crack size analysis fracture toughness: get the solution with reasonable accuracy; requires a short period of time for analysis and less cost as compared to the experimental method. However proper high computational facility is required to get a better result and do the analysis in a more reasonable time.

### 5.3. Future work

In this work, only internal pressure developed crack size was studied. Other loads such that variation in temperature, external pressure and their combinations are possible.

Crack arrest in Fatigue analysis is also extremely important, since typically 15000-20000 cycles are the involved in qualification tests requisite for commercial service approvals.

The effect of hybrid ratio and orientation are considering in its strength and fracture on composite pressure vessel.

## Reference

[1] Alexis A. Krikanov., "Composite pressure vessels with higher stiffeness" 1999 Elsevier Science Ltd. Composite structures, vol-48, pp 119-127 (2000).

[2] Andhra Pradesh, India , Composite Pressure Vessel Dec-2012.

[3] S.Adali, E.B. Summers & V.E. Verijenko., "Optimization of Laminat Cylindrical pressurenvessels under strength criterion", Composite Structures, vol-25, pp 305-312 (1993), University of national Durban 4001, South Africa.

[4] Danai Abhijeet, M.C.Swami, Parmeshwar Patil A Review On Study Of Composit Materials In Presence Of Cracks. Feb-2015.

[5] Ramesh Talreja and Chandra veer Singh"Damage and Failure of Composite materials.

[6] Robert M.Jones, mechanics of composite material blackburg virigine april 1908.

[7] Gay Daniel, composite material design and Applications

[8] Lei ZU.Design and Optimization Of Filament Wound Composite Pressure Vessels. februari 2012.

[9] S Borazjani and S H Tang**,** Finite element analysis of filament-wound composite pressure vessel under internal pressure, (2013).

[10] Barboza Neto E, Chludzinski M, Roese P, Fonseca J, Amico S, & Ferreira C 2011 Experimental and numerical analysis of a LLDPE/HDPE liner for a composite pressure Vessel Polymer Testing.

[11] G.Bao, S.Ho And Z.Suo, B.Fan, The Role Of Material Orthotropy In Fracture Speecimens For Composies , Augest 1991.

[12] David S, Dawicke1. Fracture Test Methods for Plastically Responding COPV Liners

[13] Bryan C. Lung, a Structural Health Monitoring System for Composite Pressure Vessels, March 2005.

[14] Stephen W. Tsai, Theory Of Composites Design, Summer 2008.

[15] Ben C. Odegard, Jr. and George J. Thomas Testing Of High Pressure Hydrogen Composite Tanks.

[16] Aziz Önder, First Failure Pressure of Composite Pressure Vessels, February, 2007.

[17] Hyun-Sup Jee And Jong-O Lee,Acoustic Emission Of Composite Vessel, 2012.

[18] R.A Smith, Composite Defecties And Thire Detection.

[19] Pat B. Mclaughlan, P.E.Composite Overwarreped Pressure Vessels As A Primer, March 2011.

[20] MacMaster, F.J., Chan, K.S., Bergsma, S.C., Kassner, M.E. Aluminum alloy 6069 part II: Fracture toughness of 6061 T6 and 6069 T6. Materials Science and Engineering A. 289 (2000) 54.

[21] Debecker A., van der Jagt O. and Koppert J.J.M., "Fiber-reinforced pressure vessel and method of manufacturing fiber-reinforced pressure vessels Patent WO 01/57429 A1, 2001.

[22] W. K. Ahmed1, A-H. I. Mourad2 Using Fiber Reinforced Polymer to Restore Deteriorated Structural Members. 2012.

[23] Medhavi Sinha , Dr. S. N. Pandit, Design And Burst Pressures Analysis Of CFRP Composite Pressure Vessel For Various Fiber Orientations Angles.

[24] Danai Abhijeet R, M.C.Swami, Parmeshwar Patil , A Review On Study Of Composite Materials In Presence Of Cracks, Volume: 04 Issue: 02 Feb-2015.

[25] Nestor Perez, Fracture Mechanics 2004.

[26] M.P.F studffe and N.A flack 1993 effect of geometry on compressive failure of notched composites.

[27] N. Tarakc¸ioglu, A. Akdemir, A. Avci Strength of filament wound FRP pipes with surface crack,7 September 2000.

[28] Arthur P . Richard.J Schmidt, Advance Mechanics of Material Fith Edition October 1992.

[29] Christopher Bonn, Estimation of Crack Opening Displacement and Leak Rates through a Through-Flaw in Aerospace Pressure Vessels, December 2008

# APPENDIX I

## 1. THEORETICAL STRENGTH

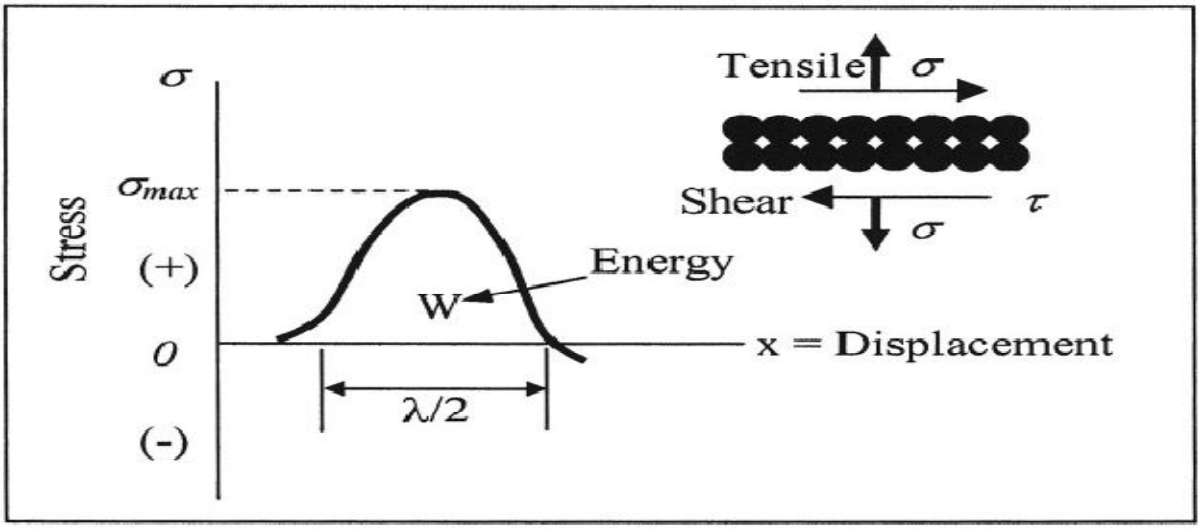


Fig 1 Sinusoidal Stress vs. Displacement

For an ideal crystal subjected to a tensile load and a shear load, which generates small displacements, the sinusoidal stress functions are:

$$\sigma = \sigma_{max} \sin\left(\frac{2\pi x}{\lambda}\right) \simeq \left(\frac{2\pi x}{\lambda}\right) \sigma_{max}$$

$$\tau = \tau_{max} \sin\left(\frac{2\pi x}{a_o}\right) \simeq \left(\frac{2\pi x}{a_o}\right) \tau_{max}$$

Thus, the maximum theoretical tensile stress becomes

$$\sigma_{max} = \left(\frac{\lambda}{2\pi x}\right) \sigma$$

$$\tau_{max} = \left(\frac{a_o}{2\pi x}\right) \tau$$

$$E = \frac{Tensile\ Stress}{Strain} = \frac{\sigma}{x/a_o}$$

$$G = \frac{Shear\ Stress}{Strain} = \frac{\tau}{x/a_o}$$

The potential or bonding energy and forces are defined by

$$U = -\frac{C_a}{x^n} + \frac{C_b}{x^m} = U_A + U_B$$
$$F = \frac{dU}{dx} = F_A + F_B$$

where $C_a$ = Attractive constant $C_b$ = Repulsive constant
$n, m$ = Exponents
$U_A, U_B$ = Attractive and repulsive energies
$F_A + F_B$ = Attractive and repulsive forces

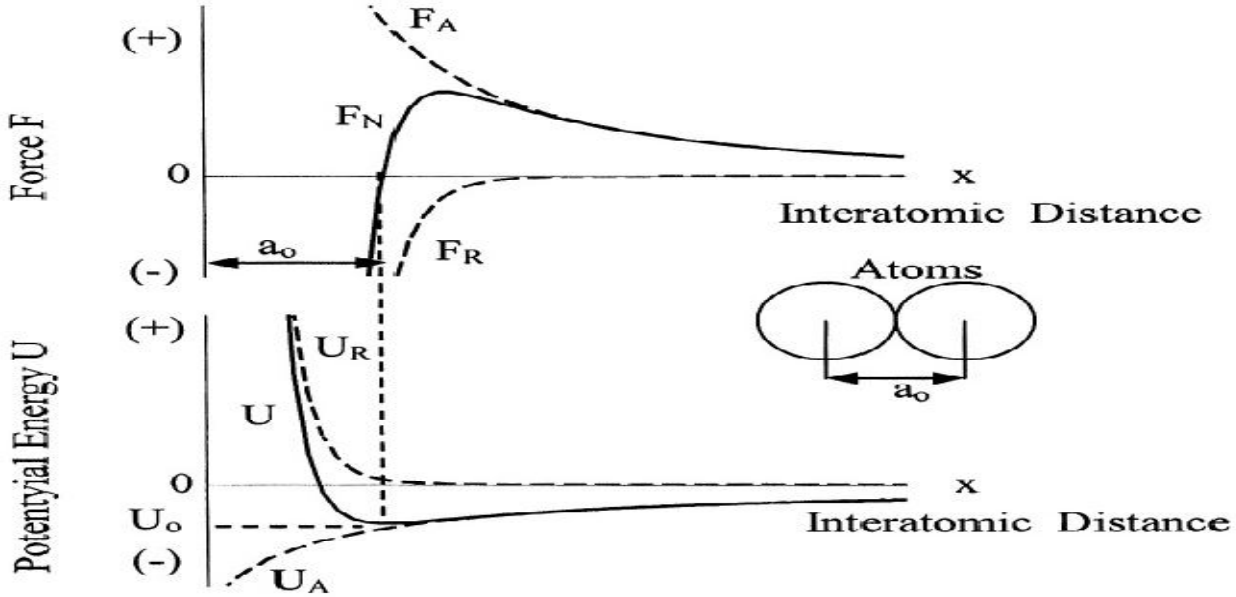


Fig 2 Schematic Variation Of Bonding Energy And Bonding Force As A Functions Of Inter Atomic Spacing.

**2. stress-Concentration Factor**

$$\frac{x^2}{a^2} + \frac{y^2}{b^2} = 1$$

$$x = c \cosh \xi \cos \beta$$
$$y = c \sinh \xi \sin \beta$$

$$\rho = \frac{b^2}{a}$$

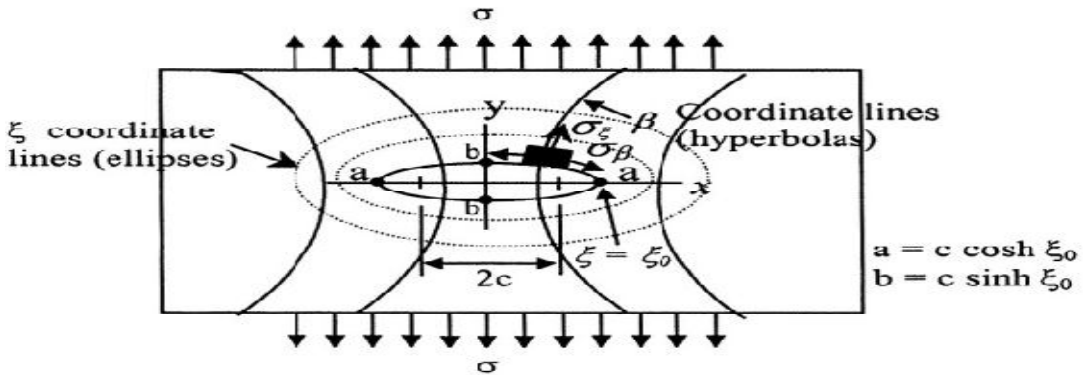


Fig 3 Elliptical coordinates in an infinite plate

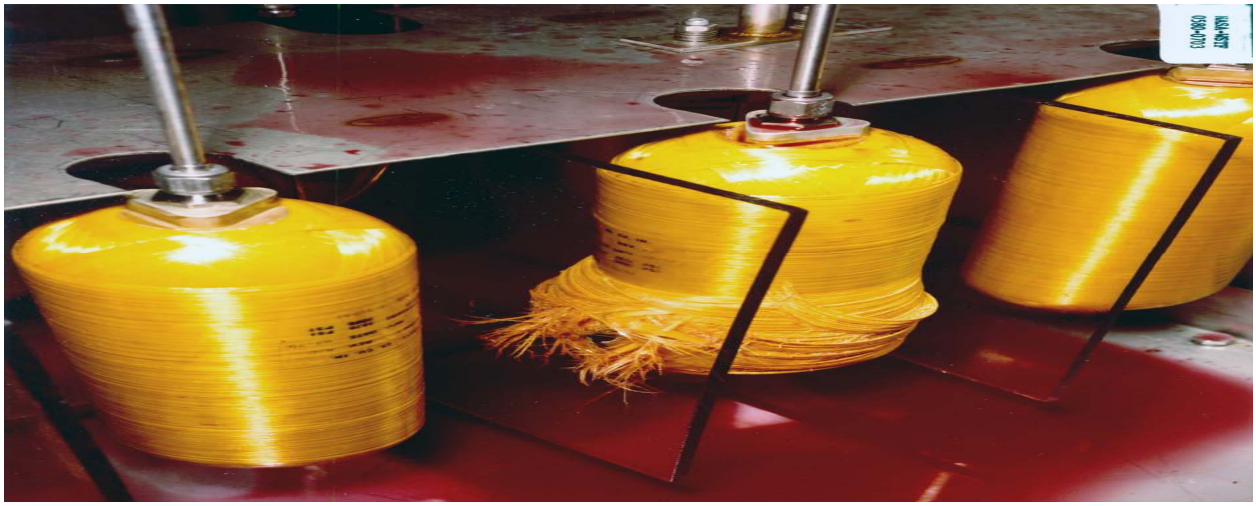

Fig 4 Stress rupture testing and a hydraulic failure

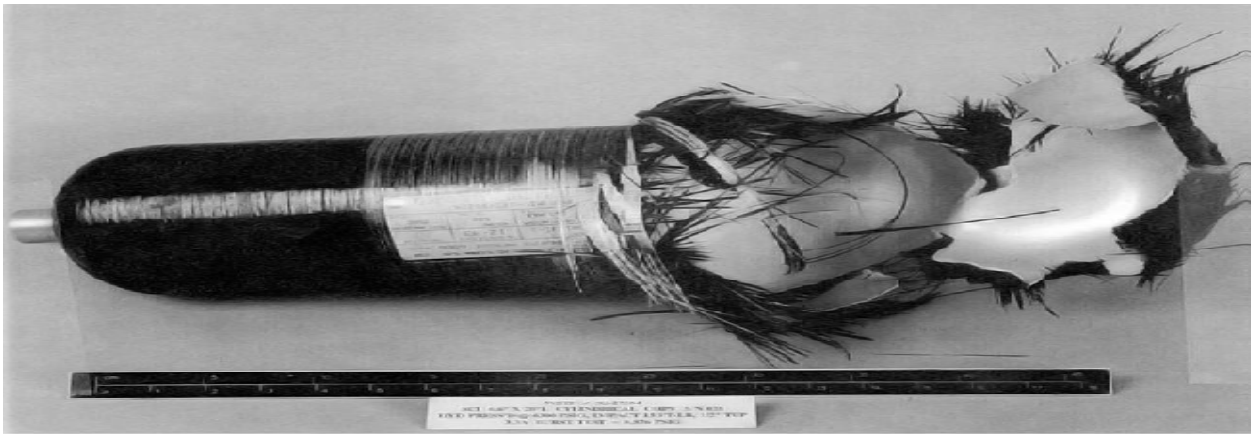

Fig 5 Hydraulic burst of a COPV

## 2. ORTHOTROPY RESCALING

Consider an orthotropic solid in a plane stress state. Plane strain deformation is treated in the Appendix. The coordinates $x$ and $y$ coincide with the principal axes 1 and 2 of the orthotropic material. Two dimensionless parameters, $\lambda$ and $\rho$, are defined in terms of the engineering elastic constants (Suo, 1990a, b):

$$\lambda = \frac{E_2}{E_1}, \quad \rho = \frac{(E_1 E_2)^{1/2}}{2G_{12}} - (\nu_{12}\nu_{21})^{1/2}. \tag{1}$$

They characterize the in-plane orthotropy: $\lambda = \rho = 1$ for isotropic materials and, $\lambda = 1$ for solids with cubic symmetry. Typical values of $\lambda$ and $\rho$ are in the range $0.05 < \lambda < 20$ and $0 < \rho < 5$.

Let $U(x, y)$ be the Airy function so that stresses at equilibrium are derived from

$$\sigma_x = \frac{\partial^2 U}{\partial y^2}, \quad \sigma_y = \frac{\partial^2 U}{\partial x^2}, \quad \tau_{xy} = -\frac{\partial^2 U}{\partial x \partial y}. \tag{2}$$

The governing equation is (Lekhnitskii, 1981):

$$\frac{\partial^4 U}{\partial x^4} + 2\lambda^{1/2}\rho \frac{\partial^4 U}{\partial x^2 \partial y^2} + \lambda \frac{\partial^4 U}{\partial y^4} = 0. \tag{3}$$

An inspection reveals that a rescaling of the $x$-axis:

$$\xi = \lambda^{1/4} x, \tag{4}$$

reduces eqn (3) to

$$\frac{\partial^4 U}{\partial \xi^4} + 2\rho \frac{\partial^4 U}{\partial \xi^2 \partial y^2} + \frac{\partial^4 U}{\partial y^4} = 0. \tag{5}$$

The equation depends on $\rho$ only. The boundary conditions for $U(\xi, y)$ are now changed to

$$\sigma_x = \frac{\partial^2 U}{\partial y^2}, \quad \lambda^{-1/2}\sigma_y = \frac{\partial^2 U}{\partial \xi^2}, \quad \lambda^{-1/4}\tau_{xy} = -\frac{\partial^2 U}{\partial \xi \partial y}. \tag{6}$$

The resultant forces on an arc are

$$T_x = \partial U/\partial y, \quad \lambda^{-1/4} T_y = -\partial U/\partial \xi. \tag{7}$$

With $\lambda$-dependence extracted explicitly, the boundary value problem, defined by eqns (5) and (6) on the $\xi$–$y$-plane, now has only one material parameter, $\rho$. Several applications of this idea can be found in Suo *et al.* (1990).

Displacements can be determined by using an auxiliary function $\chi(\xi, y)$, defined by

## Appendix II

Let the coordinate x, y and z coincide with principal material directions of an orthotropic material. For lain strain problems, the governing equation and the definition of λ and r remain unchanged, but the elastic constant need to be replaced by

$$E_1' = E_1/(1-\nu_{13}\nu_{31}), \quad \nu_{12}' = (\nu_{12}+\nu_{13}\nu_{32})/(1-\nu_{13}\nu_{31})$$
$$E_2' = E_2/(1-\nu_{23}\nu_{32}), \quad \nu_{21}' = (\nu_{21}+\nu_{23}\nu_{31})/(1-\nu_{23}\nu_{32}).$$

There is no need to change the shear modules $G_{12.}$ This replacement should be done with all the solution in the text if the plain strain condition prevails.

## Stress Strain Relation

The stress strain relation for epoxy resin/hardener specimen under tensile test is shown in Figure-3. It can be seen that the stress increases linearly with strain to the maximum value and then dropped suddenly as a brittle fracture. Figure-4 shows the photograph of matrix specimens after failure. It can be seen that the failure on the specimen is sudden and catastrophic. In addition the failure of specimen is in the gage zone and close to center.

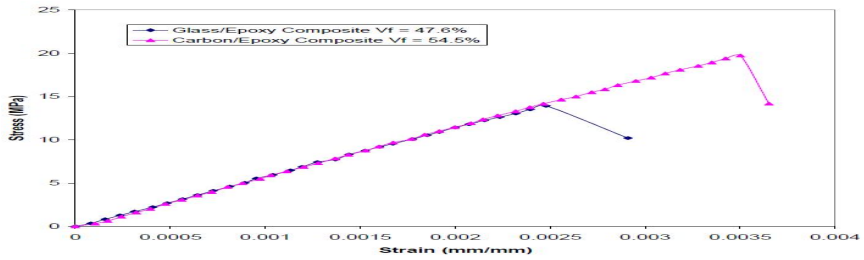


Fig 1 Tensile Stress-Strain response of a $[90^o]_4$ carbon/epoxy composite. ($v_f$ = 54.5%) and $[90^o]_4$ Glass/Epo xy Composite ($v_f$ = 47.6%)

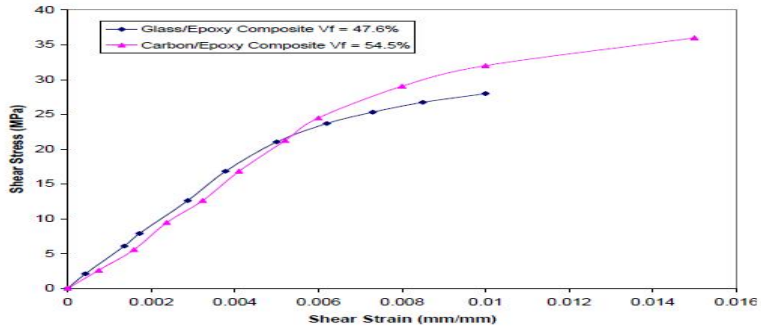


Fig 2 Shear Stress - Strain curve obtained from a tensile test of a $[45]_4$ carbons. Fiber Test Specimen, ($v_f$ = 54.5%) and $[45]_4$ Glass Fiber Test Specimen, ($v_f$ = 47.6%).

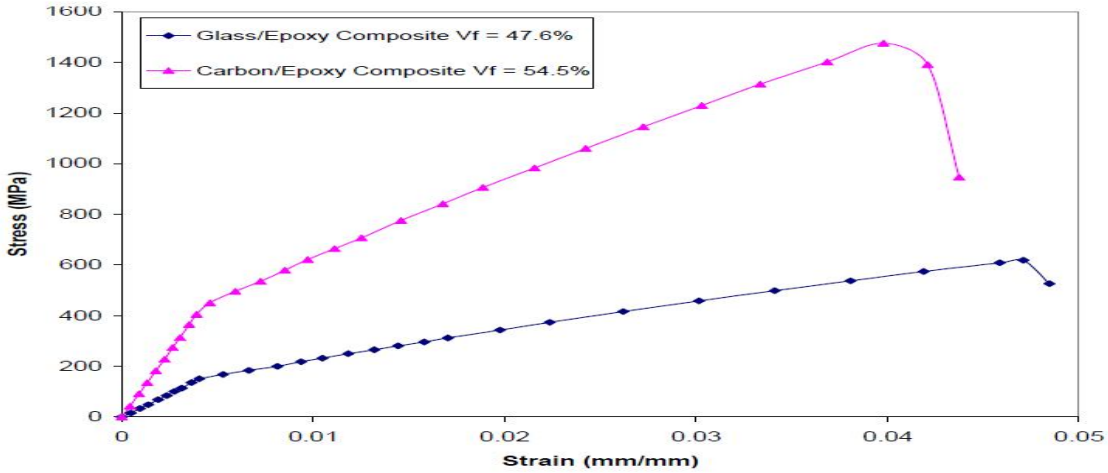


Fig 3 Tensile Stress-Strain response of a $[0^o]_4$ carbon/epoxy composite. ($v_f$ = 54.5%) and $[0^o]_4$ Glass/Epoxy Composite ($v_f$ = 47.6%)

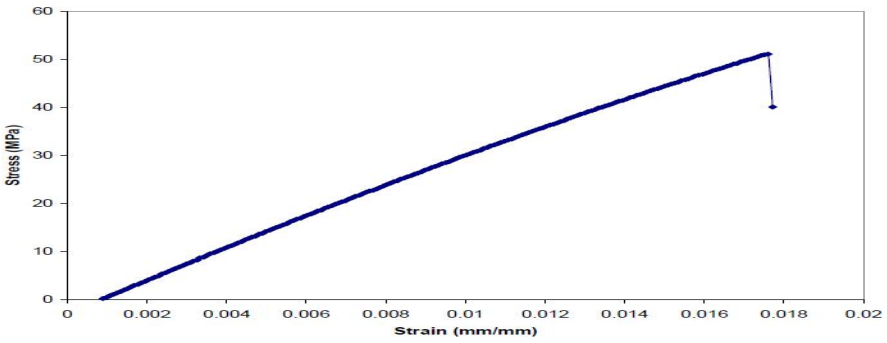


Fig 4 Stress strain relations for the Matrix

**Example of chemical bonds between carbon fiber and matrix**

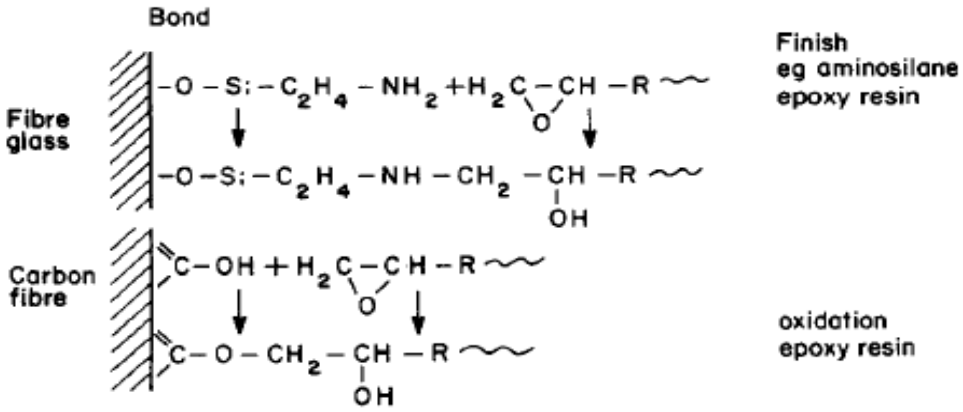


**Table 1 - Visual Acceptance/ Rejection Criteria for Composite Pressure Vessels**

| Type of Degradation or Damage | Description of Degradation or Damage | Acceptable Level of Degradation or Damage | Rejectable Level of Degradation or Damage |
|---|---|---|---|
| Abrasion | Abrasion is damage to the filaments caused by wearing or rubbing of the surface by friction | Less than 0.050 in. depth in the pressure bearing thickness. | $\geq$ 0.050 in. depth in the pressure bearing thickness |
| Cuts | Linear indications flaws caused by a impact with a sharp object | Less than 0.050 in. depth in the pressure bearing thickness. | $\geq$ 0.050 in. depth in the pressure bearing thickness |
| Impact Damage | Damage to the tank caused by striking the tank with an object or by being dropped. This may be indicated by discoloration of the composite or broken filaments and/or cracking. | Slight damage that causes a frosted appearance or hairline cracking of the resin in the impact area | Any permanent deformation of the tank or damaged filaments |
| Delamination | Lifting or separation of the filaments due to impact, a cut, or fabrication error. | Minor delamination of the exterior coating | Any loose filament ends showing on the surface. Any bulging due to interior delaminations |

| | | | |
|---|---|---|---|
| Dents | A depression in the exterior of the tank caused by impact or dropping | < 1/16 in. in depth | Any dents with a depth ≥ 1/16 in. Or with a diameter greater than 2 inches |
| Reported collision, accident, or fire | Damage to the tank caused by unanticipated excursion from normally expected operating conditions | None reported | Any indication or report of impact or heat damage |
| Environmental Damage or Weathering | Ultraviolet or other environmental attack under the exterior coating. | None | Any discoloration that can not be washed off* |
| Crazing | Hairline surface cracks only in the composite resin | Light hairline cracks only in the resin | Any damage to the filaments |
| Damage to a protective or sacrificial layer | Abrasion, cuts, chemical attack, scratches/gouges, corrosion, environmental damage, or crazing that are limited only to the protective or sacrificial layer. | The depth of any damage to the protective or sacrificial layer that does not exceed the thickness of the protective or sacrificial layer plus 0.050 inch. | The depth of any damage to the protective or sacrificial layer that exceeds the thickness of the protective or sacrificial layer plus 0.050 inch. |
| Cracks | Sharp, linear indications | None | None |
| Scratches/Gouges | Sharp, linear indications caused by mechanical damage. | Less than 0.050 in. depth in the pressure bearing thickness No structural fibers cut or broken | ≥ 0.050 in. depth in the pressure bearing thickness or structural fibers cut or broken |
| Soot | A deposit on the composite caused by thermal or environmental exposure | Soot that washes off and leaves no residue | Any permanent marking that will not wash off the surface under the exterior coating |
| Over pressurization | Excessive pressure due to operational malfunction | None reported | Any report of pressurization beyond the MAWP or any indication of distortion |
| Corrosion | Degradation of the composite due to exposure to specific corrosive environments | None visible | Any surface damage to structural identified as corrosion |

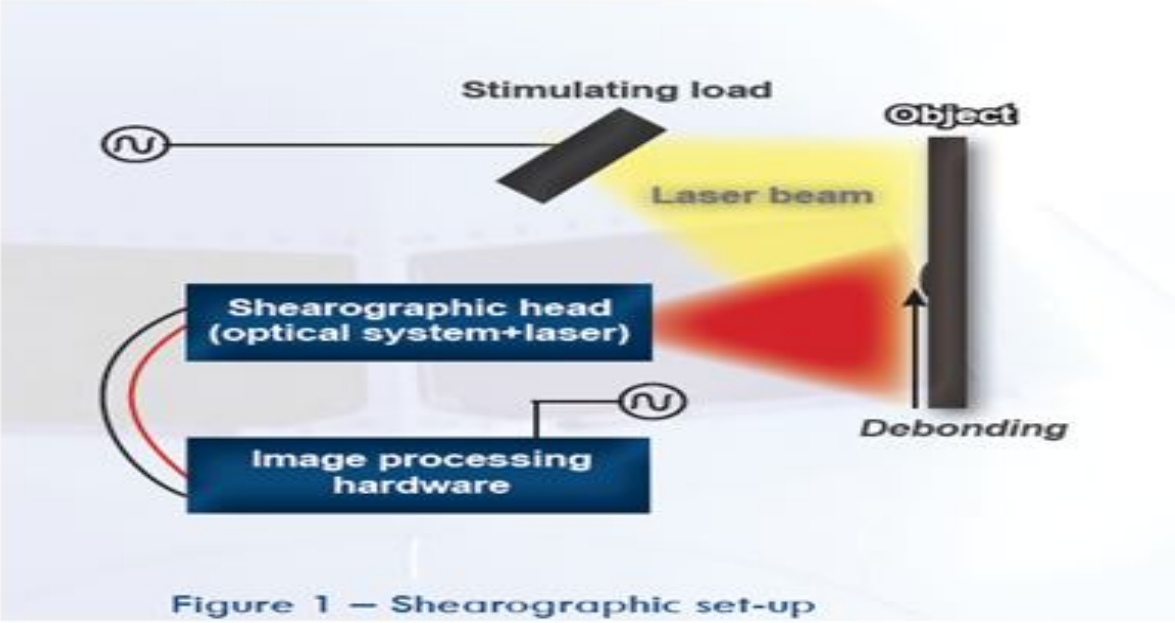


Figure 1 — Shearographic set-up